MUSCLE SPINDLE FEEDBACK AND LIMB COORDINATION DURING LOCOMOTION

by

William P. Mayer

Submitted in partial fulfilment of the requirements
for the degree of Doctor of Philosophy

at

Dalhousie University
Halifax, Nova Scotia
June 2020

This thesis is dedicated to my loved wife,
Luana Mayer, for being my continuing source of
encouragement, support, and compassion.

TABLE OF CONTENTS

LIST OF TABLES

LIST OF FIGURES

ABSTRACT

Understanding how the nervous system controls locomotion is of great importance to improve treatments of mobility disorders. The numerous muscles and joints in a limb participating in a given movement, have to feed sensory information back to the central nervous system, so that, individuals have the capacity to perform functional movements and cope with diverse environmental variables. The integration of proprioceptive feedback derived from muscle spindles and Golgi tendon organs into the central nervous system is still a fascinating topic requiring a deeper understanding. We have analyzed locomotor patterns in different behavioral conditions in mice, in which proprioceptive feedback was genetically removed or attenuated by adeno-associated virus technology. Our results showed that proprioceptive feedback from muscle spindles and Golgi tendon organs are essential for the coordination of flexor and extensor muscles necessary for functional terrestrial locomotion or swimming. Wide-spectrum muscle spindle feedback deficiency changed muscular activation patterns, generated incapability to precisely target the limbs after a stumble event during walking, and harmed the regulation of muscle activity-strength or speed-dependent EMG amplitude. Our results show that the ablation of proprioceptive feedback from an individual group of muscles, neither diminished functional locomotion nor altered muscle activation pattern. Nonetheless, the feedback from muscle spindles of the ankle extensor muscles, the triceps surae, is the main source of speed-dependent modulation of activity-strength, in contrast to the muscle spindle feedback from the knee joint which has no influence on speed-dependent amplitude modulation. We conclude that proprioceptive feedback is essential for controlling variable aspects of locomotion. The group Ia/II and Ib afferents carry the information used by the spinal cord to control muscle activity strength and regulate the onset and offset-timing of muscle activity patterns during locomotion.

LIST OF ABBREVIATIONS AND SYMBOLS USED

~	Approximately
°C	Degree Celsius
<	Less than
≤	Less than or equal to
>	Greater than
≥	Greater than or equal to
=	Equal
%	Percent
±	Plus or minus
µA	Microampere
µm	Micrometer
AAV	Adeno-associated virus
AAV9	Adeno-associated virus serotype 9
AEP	Anterior extreme position
BF	Biceps femoris
cm	Centimeter
CNS	Central nervous system
CPG	Central pattern generators
Cre	Causes recombination
ct	Control
deg	Degree
DRG	Dorsal root ganglia
DTA	Diphtheria toxin A chain
DTR	Diphtheria toxin receptor
DTX	Diphtheria toxin
dur	Duration
Egr3	Early growth response 3
Egr3$^{-/-}$	Egr3 knock-out
EMG	Electromyography
ext	Extension

FL_{PEP}	Forelimb posterior extreme position
flx	Flexion
GFP	Green fluorescent protein
GM	Gluteus maximus
Gs	Gastrocnemius
GTO	Golgi tendon organ
h	Hour
HL_{AEP}	Hindlimb anterior extreme position
HL_{PEP}	Hindlimb posterior extreme position
Hz	Hertz
IN	Interneuron
Ip	Iliopsoas
IP	Intraperitoneal
Isl2	Insulin related protein 2 (islet 2)
kg	Kilogram
m	Meter
m/s	Meter per second
mg	Milligram
mm	Millimeter
MN	Motoneuron
ms	Millisecond
MS	Muscle spindle
MTP	Metatarsophalangeal
norm	Normalized
OCT	Optimal cutting temperature compound
PBS	Phosphate buffered saline
PEP	Posterior extreme position
PFA	Paraformaldehyde
PFMS	Proprioceptive feedback from muscle spindles
Pkill	*Pv::cre;Isl2::DTA* (proprioception killed mice)
PNS	Peripheral nervous system

PTP amp	Peak-to-peak amplitude
Pv	Parvalbumin
QF	Quadriceps femoris
Rel. toe_x	Toe relative position to the hip joint in the x axis
ROM	Range of motion
ROR	Retinoid-related orphan receptor
SCR	Stumbling corrective reaction/response
Sec	Seconds
Sm	Semimembranosus
SPN	Saphenous nerve
St	Semitendinosus
st	Stance
sw	Swing
TA	Tibialis anterior
TB	Toluidine blue
TS	Triceps surae
Vglut1	Vesicular glutamate transporter 1
VL	Vastus lateralis
WT	Wild type

ACKNOWLEDGEMENTS

Firstly, I thank my supervisor Dr. Turgay Akay for all efforts and dedication supporting me to develop skills as an academic professional and researcher over the years. Your guidance has transformed my appreciation for high-quality investigation in the field of neuroscience. You accepted me in your lab as an experienced anatomist, although a naïve neuroscientist that genuinely benefited from your enthusiasm, critical thinking, knowledge, and remarkable skills. These learnings I will nurture and keep them for a lifetime.

My sincere thanks to my supervisory committee members, Dr. Kazue Semba, Dr. Victor Rafuse, and Dr. Ying Zhang for your guidance, shared experience and constructive feedback that allowed me to re-think critically over my data and explore new ways to improve my research.

I especially thank Brenda Ross for being my endless source of lab knowledge and technical support. You always have made hard work feel pleasant even in those challenging days. Thank you for your encouragement, enjoyable company and for the privilege of becoming your friend.

To my colleagues, Olivier D Laflamme, Lauren Landoni, Tyler Wells, Jacob Myles, Marwan Ibrahim, Rachel Banks and Dr. Alessandro Santuz, thank you for your support and collaborative ideas along the course of this thesis. You guys have made the lab an excellent environment to work/study and a formidable place to be.

CHAPTER 1 INTRODUCTION

1.1 MOTIVATION

The ability to adapt to changes in the environment is observed from the most primitive forms of life to complex multicellular organisms. Animals have the capability to continuously extract sensory information from the world around them, process that information, and transform it into actions towards specific goals or demands. The typical well-coordinated movement observed in functional motor behavior relies on sensorimotor transformations, and in the absence of sensory feedback the movement is uncoordinated and maladaptive (Akay, Tourtellotte, Arber, & Jessell, 2014; Woo et al., 2015).

Movements that express behavior, even in its simplest form, embodies complex neural processes. In general terms, the central nervous system (CNS) is responsible for planning movements even before any type of action is produced, consequently cortical circuits must be in place to elaborate and send commands along to subcortical regions of CNS (Rizzolatti et al., 2014). These commands participate in central processes prior to the activation of skeletal muscles with the consideration of sensory feedback from the periphery that informs the CNS about the actual position of the body (Grätsch et al., 2019). This sense of self-movement and body position, known as proprioception, is essential for body coordination as it feeds the CNS with information regarding the current position and movement during different motor behaviors (Delhaye et al., 2018). Furthermore, it is also fascinating that the executive component of the movement, meaning, what muscles are recruited under which

temporal parameters and sequence is mostly assigned by processes within the spinal cord (Romanes, 1951).

The activation of limb muscles during a single step movement requires precise temporal pattern and perfect coordination of about 50 to 60 limb muscles. Thus, circuits are in place at various levels of the spinal cord to ensure proper function of flexor and extensor muscles required to perform a functional step. For example, a precise alternating activation of flexor and extensor muscles is typical when limbs move, which is essential for performing smooth and functional locomotion; thus basic neuronal circuits as shown in Figure 1 exist in the spinal cord to ensure appropriate functionality. Considering that a single limb is composed of multiple joints that move in a well-coordinated manner, the spinal circuitry that controls limb movement is even more complex, and the level of organization of these circuits is not entirely understood.

Motoneurons are key elements in this spinal neuronal network, and without them, limited action is conveyed out of the CNS. Motoneurons engage striated muscles in activity allowing body parts to move and perform all sorts of motor acts. They mostly populate the ventral horn of the spinal cord and their prolongations, the axons, project out of the spinal cord via spinal nerves to innervate muscles with remarkable precision (Romanes, 1951). As a consequence, muscles allocated in different limb compartments, with different functions, are innervated by a specific and dedicated set (pool) of motoneurons.

Figure 1. 1 Basic spinal circuit of sensory-motor control and flexor-extensor activity. (i) Motoneuron pool to flexor muscles (light green). Motoneuron pool to extensor muscles (dark green). Flexor muscle proprioceptive sensory neuron (gray). Extensor proprioceptive sensory neuron (purple). Proprioceptive sensory neurons inform the state of contraction of individual muscles back to the spinal cord for processing sensory-motor transformation. Note that the transformation occurs with one synaptic relay similar to a monosynaptic stretch reflex where sensory neuron connects directly with motoneurons innervating the same muscle. Inhibitory interneuron (brown) that silences the antagonist muscle of the movement. Commissural interneuron (Black) responsible to send sensory information to the contralateral side of the spinal cord. (ii) EMG recording illustrating alternating pattern of activation between flexor and extensor muscles.

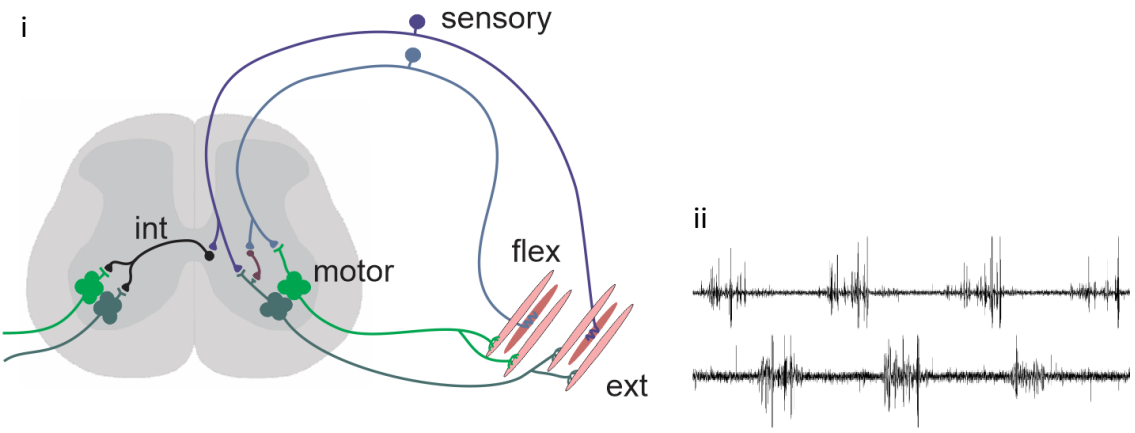

Movement-generating processes in the CNS ensure activation of motoneurons with precision, such that, muscle contraction is translated to biomechanical changes in the limbs for the purpose of any movement. Moreover, the motor act itself is constantly monitored by the CNS to certify that the required performance is being achieved and matching the behavioral needs (Prochazka, 2011). The proprioceptive sensory neurons are especially important for monitoring the state of contraction of limb muscles. Proprioceptors can respond to different aspects of muscle contraction or stretch and are, in general, classified as either tonic or phasic receptors; the first responds to a stimulus so long as the stimulus

is maintained and the latter adapts to a constant stimulus, hence stop responding after adaptation (Cabelguen, 1981).

Muscle spindles are proprioceptive sensory organs consisting of sensory and motor endings embedded among muscular fibers (Ruffini, 1898) (Figure 1.2). Each muscle spindle receives afferent innervation from a single large group Ia fibers which forms anulospiral endings in the equatorial zone of a muscle spindle. This type of sensory ending detects the dynamic phase of muscle lengthening by responding to both rapid stretch-related changes in muscle length and the velocity of length changes. Group II fibers end adjacent to the group Ia afferents and detect the tonic component of muscle stretch by sustaining action potentials in response to muscle stretch (Hulliger, 1984). Muscle spindles also receive efferent innervation from gamma motoneurons (Ellaway et al., 2002; Taylor et al., 2006). In order to maintain the responsiveness of the muscle spindles during movements, gamma motoneurons induce contraction of the intrafusal fibers which stretches the equatorial region to adjust the spindles to a functional length. In summary, changes in muscle length are detected by type Ia and II afferents as the muscles contract. The intrafusal muscle spindle fibers are adjusted by gamma motoneurons, ensuring that muscle spindles are sensitive throughout muscle contraction.

Isometric muscle contractions produce varying degrees of tension in tendons, hence encapsulated nerve endings in the vicinity of the myotendinous junctions, known as Golgi tendon organs (GTO), convey this information back to the central nervous system. GTOs are sensitive to minor changes in tendon tension and relay that information to the spinal cord via group Ib afferent fibers (Houk & Henneman, 1967). Each GTO is innervated by a

single group Ib afferents, thus the tension produced by muscle contractions excite only those fibers in the organs. In summary, GTOs signal forces produced by muscular activity or by a passive stretch applied in muscular tendons.

Figure 1. 2 Diagram of muscle spindle and Golgi tendon organ. Muscle spindle primary ending encircles the central portion (equatorial zone) of intrafusal fibers. Group Ia afferent fibers transmit sensory signals to the spinal cord regarding changes in spindle length. Muscle spindle secondary endings (group II) are adjacent to the equatorial zone and transmit signals to the spinal cord related to tonic stretch. The Golgi tendon organs are located on the myotendinous junction, are sensitive to muscle tension, and receive innervation from group Ib afferent fibers. Gamma motoneurons innervate contractile parts of intrafusal fibers to avoid loss of tension in the spindles. Alpha motoneurons innervate large extrafusal fibers via the endplates of a motor unit.

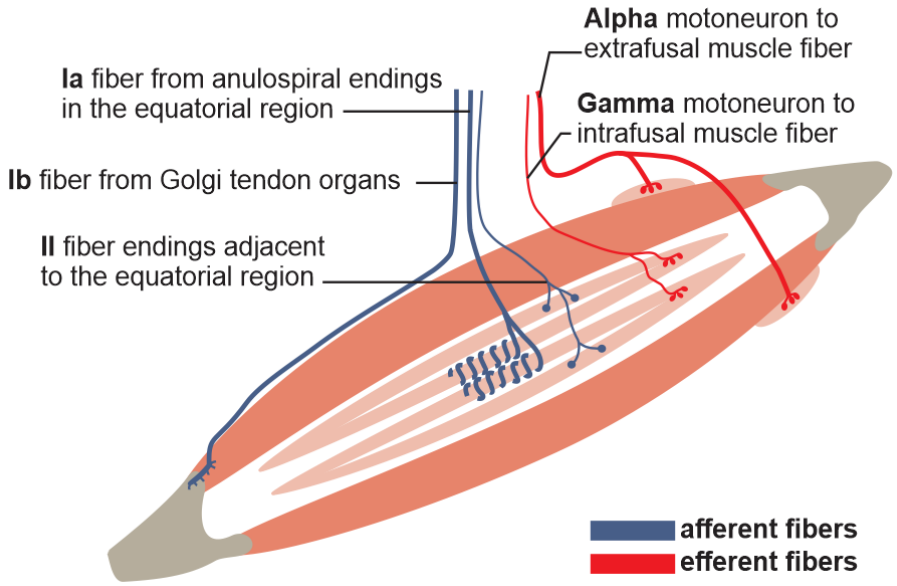

Circuits in the CNS have to accommodate for diverse motor tasks such as reaching a determined goal (Azim & Alstermark, 2015) or skilled manipulation of objects (Rizzolatti et al., 2014), and they must be able to cope with unpredictable situations while performing such tasks. For example, sensory integration and sensory-motor transformation is necessary

for overcoming complications during locomotion and keep the pace fluent (Santuz et al., 2019). It is, therefore reasonable to think that sensory feedback is of extreme importance in such a scenario. Motor actions throughout our daily life may go unnoticed due to our ability to perform them with ease, but behind simple effortless movement lies a multi-layered and complex neural process that is still to be understood.

We believe that finding answers to those poorly understood and intricate mechanisms of neural sensorimotor transformations would pave the road for better clinical applications. Numerous neurodegenerative diseases affect ones walking capabilities, and knowing how the nervous system controls locomotion may be of key importance to help health professionals develop treatments focused on regaining the ability to walk. The goal of this thesis is to improve our understanding of how proprioceptive feedback interacts with the neuronal circuits in the central nervous system that control locomotion.

1.2 Locomotion

Locomotion is defined as the individuals' ability to move around their habitat by their own means (Prochazka, Gosgnach, Capaday, & Geyer, 2017). Locomotion is necessary for animal survival and, if compromised in humans, affects the quality of life. Numerous medical conditions affect the human walk, and gait analysis has been presented as a powerful tool for diagnosing neurodegenerative diseases (Fiander et al., 2017; Radovanović et al., 2014; Strata et al., 2004).

The control of locomotion depends on the temporal coordination of multiple flexors and extensor muscle contractions acting on the hip, knee and ankle joints (Engberg & Lundberg, 1969; Grillner, 2011; Rossignol, 2011). At the spinal level, these motor programs are thought to emerge via the integrated actions of local interneuronal circuits functioning as central pattern generators (CPGs), and potentially via segmental sensory feedback mediated by cutaneous and proprioceptive inputs (Pearson, 2004; Rossignol, Dubuc, & Gossard, 2006). Despite research on these topics, core questions remain unanswered regarding the contributions of sensory feedback systems in the CPG and coordination of mammalian locomotion. These questions have remained unanswered because of our inability to manipulate the activity of a defined population of sensory afferents with anatomical precision under conditions in which locomotion *in vivo* can be evaluated.

Traditionally, kinematic and EMG analysis of the walking step cycle with particular focus on the cat hindlimb (Engberg & Lundberg, 1969; Stuart & Hultborn, 2008; Grillner, 2011; Rossignol, 2011) has provided fundamental insights into the neural control of locomotion. These studies showed that individual extensor and flexor muscles controlling the hip, knee, and ankle display distinct onset and offset timing, as well as a pronounced alternation in flexor-extensor phasing that accompanies the biomechanical transition of the hindlimb from stance to swing or swing to stance (Engberg & Lundberg, 1969; Grillner, 2011; Rossignol, 2011).

There is convincing evidence that the core aspects of locomotion are commanded through a local spinal CPG. The spinal cord itself can preserve elements of the locomotor pattern even after transection or manipulation of the descending neural pathways (Jordan, Pratt, &

Menzies, 1979; Grillner, 2011). Nonetheless, other studies suggest that sensory feedback may modify locomotor output to accommodate for changes in terrain or during specific required tasks (Duysens & Pearson, 1980; Grillner & Rossignol, 1978; Hiebert, Whelan, Prochazka, & Pearson, 1996; Lam & Pearson, 2001; Lam & Pearson, 2002; McVea, Donelan, Tachibana, & Pearson, 2005). Although proprioceptive feedback has been proved to participate in locomotion, the degree to which proprioceptors are necessary for generating a functional locomotor pattern is still obscure.

Contemporary literature proposes two models for the collaboration between proprioceptor systems and motor pattern output. The first claims that the locomotor pattern can be achieved by the CPG in the absence of the sensory feedback, implying that the locomotor pattern in an animal would be preserved following ablation of sensory feedback (Grillner & Zangger, 1984). The second model suggests that, in the absence of proprioceptive feedback, the CPG would only generate a flexor-extensor alternation where all flexor and extensor motoneuron (MN) pools would be active during the flexor or extensor phases respectively (Lundberg, 1981). This second model therefore implies that the locomotor pattern observed in an intact animal may be the result of interaction between proprioceptive feedback and the CPG. How these two models explain the generation of the CPG in an intact terrestrial mammal performing locomotion still debatable.

Differentiation between these two models requires recordings of the locomotor pattern in absence of proprioceptive feedback in freely behaving animals. Most of the available data come from experiments in which sensory input was eliminated either by acute and intensive surgical manipulations (Grillner & Zangger, 1979; Hiebert & Pearson, 1999) or by blocking

movements with drug injections (Jordan et al., 1979; Pearson & Rossignol, 1991). An alternative approach towards the elimination of proprioceptive come from work that large fiber afferents, which includes the Group Ia and Ib's from the muscle spindle and GTOs were silenced by pyridoxine over dosage (Pearson & Rossignol, 1991; Helgren et al., 1997), however, the drawback in this method is that it does not eliminate all large fiber primary afferents (Helgren et al., 1997). Mouse models offer wide range of applicable physiological techniques and the potential for genetic manipulation of the neural circuits underlying locomotion. Hence we believe that mice are a key animal model to understand sensory control of locomotion.

Previously, the main physiological approach used in investigating the spinal locomotor networks was the *in vitro* preparation in which the spinal cord from neonatal mice is isolated and kept alive in a dish (Kiehn, 2006). However, this valuable preparation has few limitations, including the lack of important elements crucial to locomotion, such as sensory feedback, and the fact that the neuronal network underlying locomotion in neonates is still under maturation. As technology has progressed, *in vivo* methods of recording the locomotor pattern have been improved (Pearson et al., 2005; Akay, Acharya, Fouad, & Pearson, 2006), new ways of stimulating peripheral nerves have been documented (Carp, Tennissen, Chen, & Wolpaw, 2006a, 2006b; Akay, 2014; Mayer & Akay, 2018), and different approaches to measuring kinematic parameters of limb movement during free walking in adult mice have been presented (Akay et al., 2014; Fiander et al., 2017; Santuz et al., 2019). Modern *in vivo* methodology to assess locomotion in mice has the potential to provide new insight into the sensory control of locomotion.

1.3 THESIS ORGANIZATION

Chapter 2 describes the role of proprioceptive feedback in controlling the locomotor pattern. It demonstrates that functional walking or swimming is not accomplished in a total lack of proprioceptive feedback. It also presents a novel methodology that allowed us to investigate the role of muscle spindle feedback from a single joint of the hindlimb. Using this new methodology, we discuss the importance of muscle spindle feedback from the hip, knee and ankle joints.

Chapter 3 outlines features of how muscle spindle feedback ensures precise foot placement during locomotion. It unveils a methodology to trigger stumbling corrective reaction in freely-behaving mice as an investigative tool and demonstrates that proprioceptive feedback from muscle spindles is important in targeting the hindlimb during normal locomotion or in skilled locomotion where precise foot placement is task-required.

Chapter 4 delineates the role of muscle spindle feedback in regulating muscle activity strength. It shows that proprioceptive feedback plays a major role in the regulation of muscle activity strength during walking and suggests that muscle spindle feedback is necessary for both, the increased walking speed and speed-dependent amplitude modulation. Finally, it supports the view that muscle spindle feedback from ankle extensors is required to modulate and regulate muscle activity strength locally.

Chapter 5 summarizes, discusses and concludes the major findings reached in our work, as well as postulates future directions motivated by this thesis.

CHAPTER 2 PROPRIOCEPTIVE FEEDBACK CONTROLLING THE LOCOMOTOR PATTERN

2.1 INTRODUCTION

The patterned contractions of multiple muscles working in agonism, antagonism, and synergies produce rhythmic and well-coordinated limb movements (Engberg & Lundberg, 1969; Grillner, 2011; Prochazka, Trend, Hulliger, & Vincent, 1989; Santuz, Ekizos, Eckardt, Kibele, & Arampatzis, 2018). In general, flexor and extensor muscles responsible for moving the hip, knee and ankle joints must be coordinated to achieve functional locomotion. Dedicated motoneuron pools within the spinal cord innervate different muscles and provide command for the patterned contractions during locomotion (locomotor pattern), thereby body movements are achieved in a coordinated manner. The patterned activation of motoneuron pools is driven by the collaboration between local interneuronal circuitry participating in central pattern generators (CPGs) processes and sensory feedback (Brown, 1911; Duysens & Van de Crommert, 1998; Grillner & Jessell, 2009).

Scientists have provided insights into the neural control of locomotion by analyzing kinematic and electromyographic (EMG) parameters of the step cycle (Engberg & Lundberg, 1969; Stuart & Hultborn, 2008; Grillner, 2011; Rossignol, 2011). Studies have shown that the activity of flexor and extensor muscles controlling the hip, knee, and ankle joint, display distinct onset and offset timing with remarkable alternation in flexor and extensor phasing during movements of the hindlimb (Grillner, 2011; Rossignol, 2011). Nevertheless, after surgical manipulation of descending neural pathways or total spinal

cord transection, animals preserve the basic features of locomotion, which is persuasive evidence that a localized spinal circuitry is sufficient to generate locomotion (Grillner & Zangger, 1979; Jordan et al., 1979; Grillner, 2011).

Several studies, using stimulation and perturbation of single joints or the entire limb, suggest that sensory feedback modifies the locomotor pattern in a terrain- or task-dependent manner (Grillner & Rossignol, 1978; Duysens & Pearson, 1980; Hiebert, Whelan, Prochazka, & Pearson, 1996; Lam & Pearson, 2001; Lam & Pearson, 2002; McVea, Donelan, Tachibana, & Pearson, 2005). Although these approaches were successful in describing the role of different aspects of proprioception in locomotion, they did not show how proprioceptive feedback control core elements of the mammalian locomotor pattern. Published data come from experiments in which either sensory feedback was eradicated by acute and severe surgical approaches (Grillner & Zangger, 1979, 1984; Hiebert & Pearson, 1999), or motor output was blocked and proprioceptive feedback was silenced by drug administration (Jordan et al., 1979; Pearson & Rossignol, 1991; Helgren et al., 1997; Pearson, Misiaszek, & Hulliger, 2003). However, the question of how the spinal CPGs convert feedback information to its functions in an intact and freely behaving animal has not been resolved.

The mouse is becoming an important animal model for addressing the role of proprioception in locomotion since their neural circuits can be genetically manipulated for studies (Kiehn, 2006). Advances in genetics have made it possible to modify neuronal networks and manipulate the proprioceptive neurons in intact animals (Tourtellotte & Milbrandt, 1998; de Nooij, Doobar, & Jessell, 2013; de Nooij et al., 2015; Bourane et al.,

2015; Mayer et al., 2018). Hence, in this chapter, we discuss our combination of mouse genetics, virus technology, and *in vivo* recording techniques (Akay, 2014; Akay et al., 2014) to selective eliminate proprioceptive sensory feedback, and characterize changes in locomotor pattern.

In the following, we will present a series of experiments that corroborate with the hypothesis that proprioceptive feedback is necessary for the establishment of functional locomotor patterns in intact animals. We also consider the mechanisms by which proprioceptive feedback interacts with CPGs to generate locomotor patterns and how proprioceptive feedback from an individual or a particular group of muscles affects the coordinated activity of multiple muscles moving different joints.

2.2 METHODS

2.2.1 Animals

The experiments in this chapter were conducted on adult mice of either sex and ages ranging from 60 days to 90 days. None of the mice were trained prior to the experiments. All procedures were in accordance with the Canadian Council on Animal Care and approved by the University Committee on Laboratory Animals at Dalhousie University.

2.2.2 Total Removal of Proprioceptive Feedback

To remove proprioceptive feedback from both muscle spindles and GTOs, we have used a mutant mouse line which is an offspring of an intersectional breeding of *Pv::cre* (Pv, parvalbumin) (Hippenmeyer et al., 2005) and *Isl2::DTA* (X. Yang et al., 2001) mice. In the *Pv::cre* mouse, the cre recombinase is expressed under the control of the *Parvalbumin* promoter, which is expressed selectively in all proprioceptors. In *Isl2::DTA* line, a gene encoding conditionally activatable diphtheria toxin A chain (DTA) is introduced into the Isl2 locus. Since *Isl2* is expressed in all sensory neurons in the dorsal root ganglia, this strategy would induce the eradication of sensory proprioceptive neurons. The resulting mouse line (*Pv::cre;Isl2::DTA* or here so named *Pkill* mice) lack all proprioceptive neurons from both muscle spindle and GTOs (Vrieseling & Arber, 2006).

2.2.3 Complete Removal of Muscle Spindle Feedback

To remove proprioceptive feedback from the muscle spindles we utilized the *Egr3* knock-out mice (*Egr3*$^{-/-}$). In this line, the proprioceptive system is intact at birth, however, muscle spindles progressively degenerate over the first two weeks of age (Tourtellotte & Milbrandt, 1998). In contrast, the group Ib afferent feedback from the GTOs are preserved (Chen et al., 2002). Thus, the *Egr3*$^{-/-}$ provide an opportunity to access the impact of the selective loss of proprioceptive feedback from muscle spindles.

2.2.4 Selective Attenuation of Muscle Spindle Feedback from Specific Muscles

To acutely eliminate muscle spindle feedback from a subset of muscles, we used the *Pv::cre* mice in combination with gene delivery through adeno-associated virus (AVV). To conditionally and selectively ablate proprioceptors we used AAV serotype 9 to deliver a gene encoding the diphtheria toxin receptor (DTR) fused with green fluorescent protein (GFP) in a Flex-switch (AAV9-*DTR*-*GFP*) (Azim et al., 2014).

Injection of the AAV9 into selected muscles caused infection off all motoneurons and the proprioceptive afferents from that particular muscle. Since only proprioceptive afferents but not the motoneurons express the parvalbumin, the expression of the DTR-GFP only occurs in the Pv^{+} proprioceptive sensory neurons. The injections of the AAV9 were conducted while the mice were 7-10 days old as the Pv expression diminished after the second week following birth. This injection made proprioceptive afferents from muscle spindles from the injected muscle to selectively express the DTR. After these AAV9 injections, mice were kept until adulthood when they underwent to EMG electrode implantation surgeries (see 2.2.5) and control recordings of locomotion (see 2.2.6). Finally, the acute elimination of muscle spindle afferents was performed by intraperitoneal injection of diphtheria toxin (DTX, 400mg dissolved in sterile phosphate buffer). In these experiments, since only the afferent neurons from muscle spindles of the muscles injected with the AAV9 will express the receptor, these afferents will selectively be affected by DTX (detailed information results 2.3.4 and Figure 2.8).

2.2.5 Electrode Implantation Surgeries

Each wild type, *Pv::cre;Isl2::DTA*, *Egr3*$^{-/-}$, or *Pv::cre* mouse injected with AAV9-*DTR-GFP*, received an electrode implantation surgery as previously described (Pearson et al., 2005; Akay et al., 2006; Akay et al., 2014). Briefly, the animals were anesthetized with isoflurane, ophthalmic eye ointment was applied to the eyes, and the skin of the mice was sterilized with three-part skin scrub using hibitane, alcohol, and povidone-iodine. A set of six bipolar EMG electrodes was implanted in all experimental mice as follows: the neck region and the right hindlimb were shaved. Small incisions were made in the neck region and in the hindlimb just above the aimed muscles. The electrodes were drawn subcutaneously from the neck incision to the limb incisions and the headpiece connector was stitched to the skin around the neck incision.

The EMG recording electrodes were implanted into hip flexor (iliopsoas, Ip) and extensor (anterior biceps femoris, BF), knee flexor (semitendinosus, St) and extensor (vastus lateralis, VL), and ankle flexor (tibialis anterior, TA) and extensor (gastrocnemius, Gs). The incisions were closed, and buprenorphine (0.03 mg/kg) and ketoprofen (5 mg/kg) were injected subcutaneously as analgesics and anti-inflammatory drugs. Additional buprenorphine injections were performed in 12-hour intervals for 48 hours. The anesthetic was discontinued and mice placed in a heated cage for 3 days and finally returned to their regular mouse rack. Food mash and hydrogel was provided for the first 3 days after the surgery. Handling of the mice was avoided until they were fully recovered and the first recording session started no earlier than ten days after electrode implantation surgeries.

2.2.6 Behavioral Recording Sessions

Following the full recovery from electrode implantation surgeries, the behavioral recordings were performed as shown in Figure 2.1 and previously described (Akay et al., 2006; Pearson et al., 2005). Under brief anesthesia with isoflurane, custom made cone-shaped reflective markers (1-2 mm diameter) were attached to the skin at the level of the anterior tip of the iliac crest, hip, knee, ankle, the metatarsophalangeal joint (MTP), and the tip of the fourth digit (toe).

The anesthesia was discontinued and the mouse placed on the mouse treadmill (model 802; custom built in the workshop of the Zoological Institute, University of Cologne, Germany). The electrodes were connected to the amplifier (model 102, custom-built in the workshop of the Zoological Institute, University of Cologne, Germany). We waited at least five minutes before the session started to allow the mice to fully recover from anesthesia. The mice started walking on the treadmill when the treadmill was turned on. The speed of the treadmill was changed starting from 0.2 m/s and increased up to the 0.6 m/s a speed at which all wild type mice could walk.

The walking mouse was filmed from the sagittal plane with a high-speed video camera (IL3, Fastec Imaging) at 250 frames per second, and video files stored in the computer for later motion analysis. The EMG data were stored separately on the computer by using the Digitizer (Power 1401, Cambridge Electronic Design, UK) combined with Spike 2 software (Version 8, Cambridge Electronic Design, UK). Only walking sequences where the mouse would walk stationary without drifting forward or backward indicating equal walking speed

and treadmill speed were considered for data analysis. These recordings were performed once with each wild type and *Egr3*$^{-/-}$ mouse. In the experiments with the *Pv::cre* mice that received AAV9 injection, recordings at different days were performed before and after DTX injections. As the *Pv::cre;Isl2::DTA* mice were not able to perform functional walk, the recordings took place in a walkway instead of a treadmill. After walking trials, all mice were placed in a longitudinal water tank with controlled temperature at 24°C. The swimming EMG activity was recorded for approximately 2 minutes.

Figure 2. 1 Kinematic and EMG recording procedures to measure locomotor pattern. **A**: investigation of two different locomotor behaviors. **Ai** walking on a treadmill and **Aii** swimming in longitudinal tank. **B**: EMG recordings from multiple muscles in the hindlimb. **Bi**: electrodes chronically implanted in six muscles of the hindlimb. **Bii**: representation of EMG recordings of the exact same muscles performed over different conditions and behaviors. **C**: kinematic data obtained by digital reconstruction of the hindlimb. **Ci**: markers attached to the skin over bony parts and joints in the hindlimb to detect coordinates. **Cii**: by connecting the coordinates provided by markers, the hindlimb is reconstructed. **Ciii**: frame-by-frame reconstruction of the hindlimb allowing investigation of spatial dislocation during movements. (adapted with permission from Akay et al., 2014).

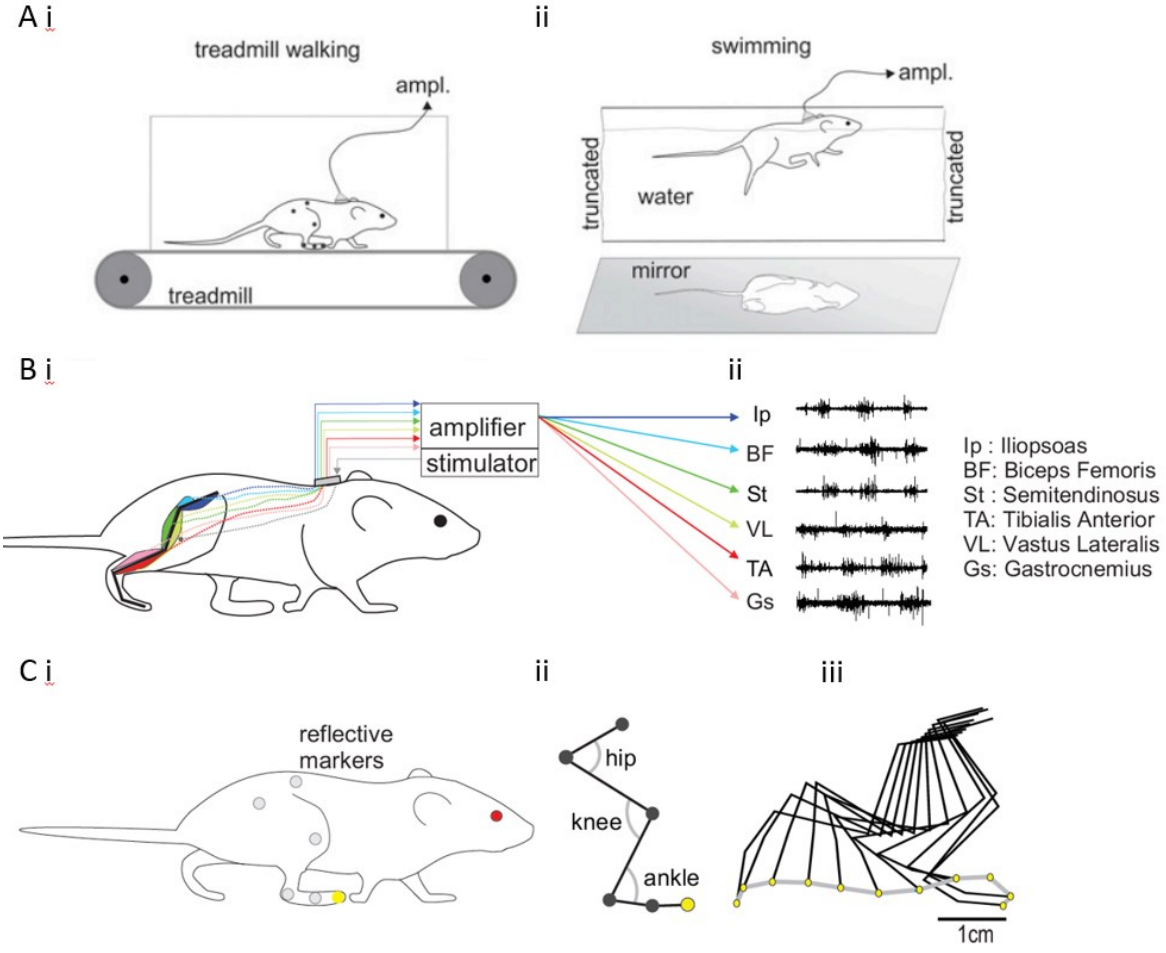

2.2.7 Data Analysis

The kinematic parameters of walking were obtained from the video files using a custom made software written by Dr. Nicolas Stifani with ImageJ (KinemaJ) and R (KinemaR) (Bui et al., 2016; Fiander et al., 2017). The coordinates and the angular joint movements were then imported into the Spike2 files containing the EMG data using a custom-written Spike2 script to analyze the kinematic and EMG data.

All plots were created with the Excel 2016 software and statistical analysis with the data analysis package for Excel: the statistiXL (version 1.8). Student's *t*-test was used to compare data between wild type and *Egr3*$^{-/-}$ mice, and the walking at 0.2 m/s and 0.4 m/s in wild type mice. Moreover, *t*-test for paired data comparing data before and after DTX injection in *Pv::cre* mice injected with AAV9 were used. The changes were considered statistically significant if $P < 0.05$.

2.3 RESULTS

2.3.1 Describing the Mice Locomotor Pattern

Locomotion involves the repetitive rhythmic movements of multiple appendages. In mice the hindlimbs produce well-coordinated movements among the hip, knee and ankle joints. In this thesis, the coordinated movement of one hindlimb was measured while mice walked forward on a treadmill at 0.2, 0.4, and 0.6 m/s. During the stance phase, while the foot was on the ground and the limb was supporting the body's weight, the foot moved in a caudal

direction from the anterior extreme position (AEP) towards the posterior extreme position (PEP) (Figure 2.2Ai). At the end of the stance phase, when the limb was extended, the foot reached the PEP and the swing movement began. During the swing phase, the mice lifted the foot off the surface and moved it forward in a smooth trajectory, returning back to the treadmill belt at the AEP (Figure 2.2Aii). As the foot progressed from the PEP to AEP, it crossed the level of the hip joint at the horizontal axis (rel. toe_x) and landed, on average, 15 mm ± 2 standard deviation (SD) in front of the hip joint at the AEP. The step cycle was defined as one swing phase with the following stance phase.

The coordinated movement of three limb joints during a step cycle is controlled by the patterned contraction of multiple flexor and extensor muscles. Angular movement of the hip, knee, and ankle joints, synchronized with electromyogram (EMG) activity of six muscles throughout four swing phases (shaded background) and three stance phases (white background) are illustrated in Figure 2.2B. The hip joint was flexed during the swing phase, whereas the knee and ankle joints were initially flexed and then extended. At early swing, the transition from flexion to extension occurred first in the knee joint than it was followed by the ankle joint (Figure 2.2B). The angular movement of the joints was well reflected in the EMG activity pattern of the hip, knee, and ankle joint flexor and extensor muscles. That is, the hip flexor, iliopsoas (Ip), was active during swing phase and the hip extensor, biceps femoris (BF) during stance phase. For movements performed in the knee and ankle, the muscle activity switches from flexor, semitendinosus (St), to extensor, vastus lateralis (VL), moving the knee followed by flexor, tibialis anterior (TA), to extensor, gastrocnemius (Gs), transition in ankle joint. Details of the activation pattern of flexor and extensor muscles are given in Table 2.1.

Figure 2. 2 Kinematics and EMG pattern of stepping in mice. **A**: stick reconstruction of one stance (i) and one swing phase (ii). Toe trajectory is indicated by the red line and the direction of the foot movement is indicated by the green arrows. PEP, posterior extreme position (white circle); AEP, anterior extreme position (yellow circle). **B**: joint angles, toe position on the horizontal axis relative to hip (rel. toe_x; dotted horizontal line indicates the hip position), toe height, and raw EMG data from flexor and extensor muscles during a stepping sequence that includes four swing phases (shaded background, a, b, c, d) and three stance phases (white background). Ip, iliopsoas (hip flexor); BF, anterior head of biceps femoris (hip extensor); St, semitendinosus (knee flexor); VL, vastus lateralis (knee extensor); TA, tibialis anterior (ankle flexor); Gs, gastrocnemius (ankle extensor). As in A, PEP and AEP are indicated by white and yellow circles, respectively. The stick diagram at the bottom of the figure represents swing phases of a, b, c, and d. (adapted with permission Mayer & Akay, 2018)

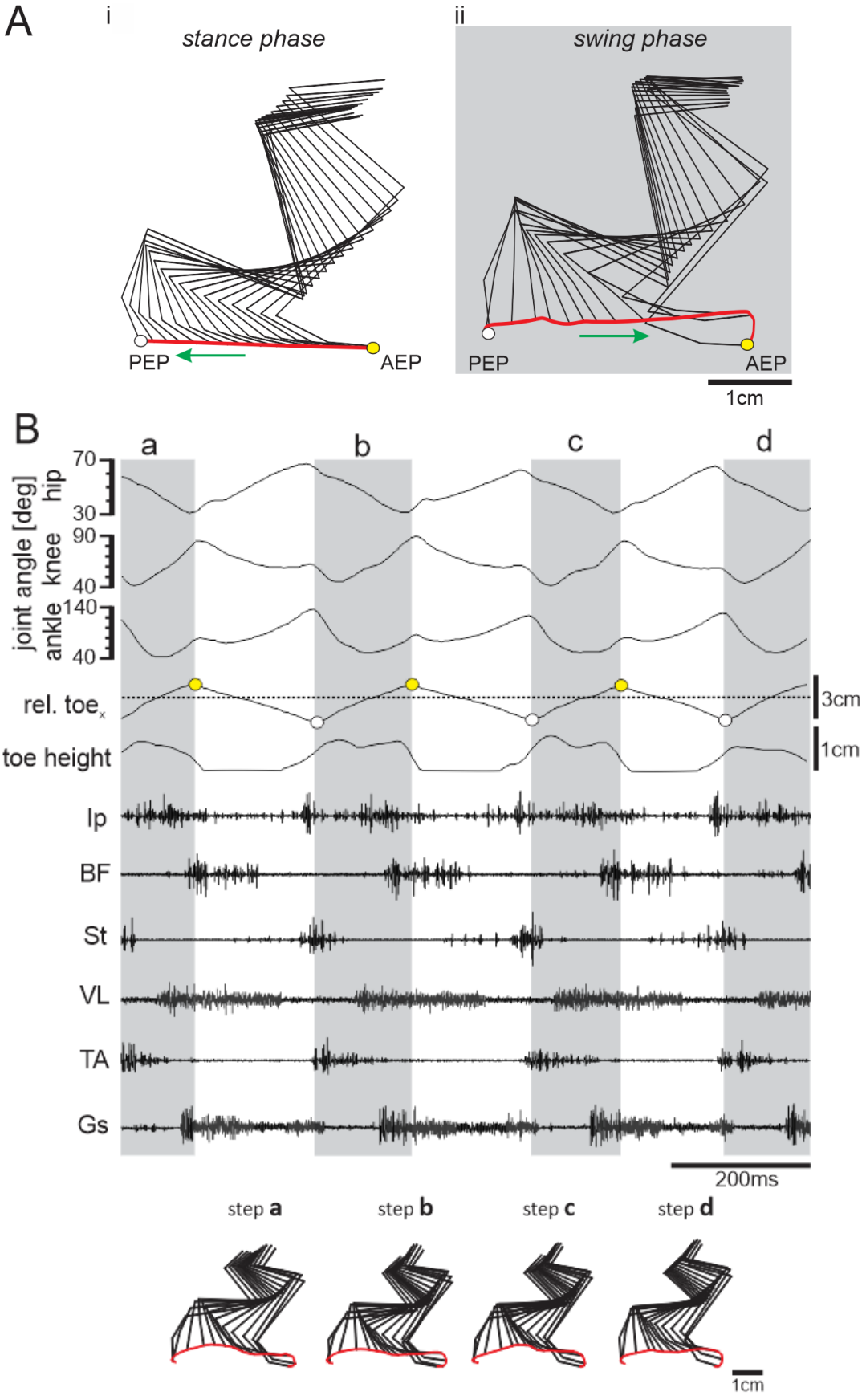
A
i
stance phase
PEP
AEP
ii
swing phase
PEP
AEP
1cm
B
a
b
c
d
joint angle [deg]
hip
70
30
knee
90
40
ankle
140
40
rel. toe$_x$
3cm
toe height
1cm
Ip
BF
St
VL
TA
Gs
200ms
step a
step b
step c
step d
1cm

Table 2. 1 Baseline muscle activity during the step cycle. Percentage values of onset and offset of EMG activity in flexor and extensor muscles related to completion of the swing or stance phase. Mean values of seven wild type animals walking at 0.2 m/s.

		ONSET THROUGH STEP CYCLE	OFFSET THROUGH STEP CYCLE
Flexor muscles	**Ip**	80.7% (stance-phase)	91.8% (swing-phase)
	St	89.5% (stance-phase)	28.6% (swing-phase)
	TA	94.4% (stance-phase)	60.2% (swing-phase)
Extensor muscles	**BF**	95.9% (swing-phase)	96.4% (stance-phase)
	VL	65.7% (swing-phase)	82.6% (stance-phase)
	Gs	79.2% (swing-phase)	99.2% (stance-phase)

This set of data illustrate the temporal sequence of muscle activity from flexor and extensor muscles moving the hip, knee, and ankle joints during walking in wild type mice.

2.3.2 Functional Locomotion Relies on Proprioceptive Feedback

The locomotor pattern as observed in the wild type mice was severely disrupted in the absence of proprioceptive feedback. The same features of locomotion were studied in *Pkill* mice in which the proprioceptive afferents (group Ia/Ib/II) were abolished during early development.

In the *Pkill* mice, traces of the joint angles became unstable. The distal joints (knee and ankle) exhibited inconsistent kinematic recordings while the hip joint described more organized traces (Figure 2.3). The toe landing after the swing phase was measured relative to the hip position (rel. toe_x) and recorded an average of 7 mm (± 9 mm SD). The large

variability of the rel. toe_x indicates that foot placement was either in front of or behind the hip joint. Inconsistent spatial dynamics of the foot were also observed with the toe heights and with the stick diagram reconstruction of four swing phases. Every step (step a, b, c, d Figure 2.4) had a different hindlimb displacement and lacked regular intralimb coordination and pattern in the absence of proprioceptive feedback.

Figure 2. 3 Kinematics and EMG pattern of *Pkill* walking mice. Joint angles, toe position on the horizontal axis relative to hip (rel. toe_x; dotted horizontal line indicates the hip position), toe height, and raw EMG data from flexor and extensor muscles during a stepping sequence that includes four swing phases (shaded background, a, b, c, d) and three stance phases (white background). Ip, iliopsoas (hip flexor); GM, gluteus maximus (hip flexor); St, semitendinosus (knee flexor); VL, vastus lateralis (knee extensor); TA, tibialis anterior (ankle flexor); Gs, gastrocnemius (ankle extensor). PEP and AEP are indicated by white and yellow circles, respectively. The stick diagram at the bottom of the figure represents swing phases of a, b, c, and d. Note the flexor and extensor muscles activated during the swing phase and inconsistent limb coordination during the swing phase represented by stick diagrams.

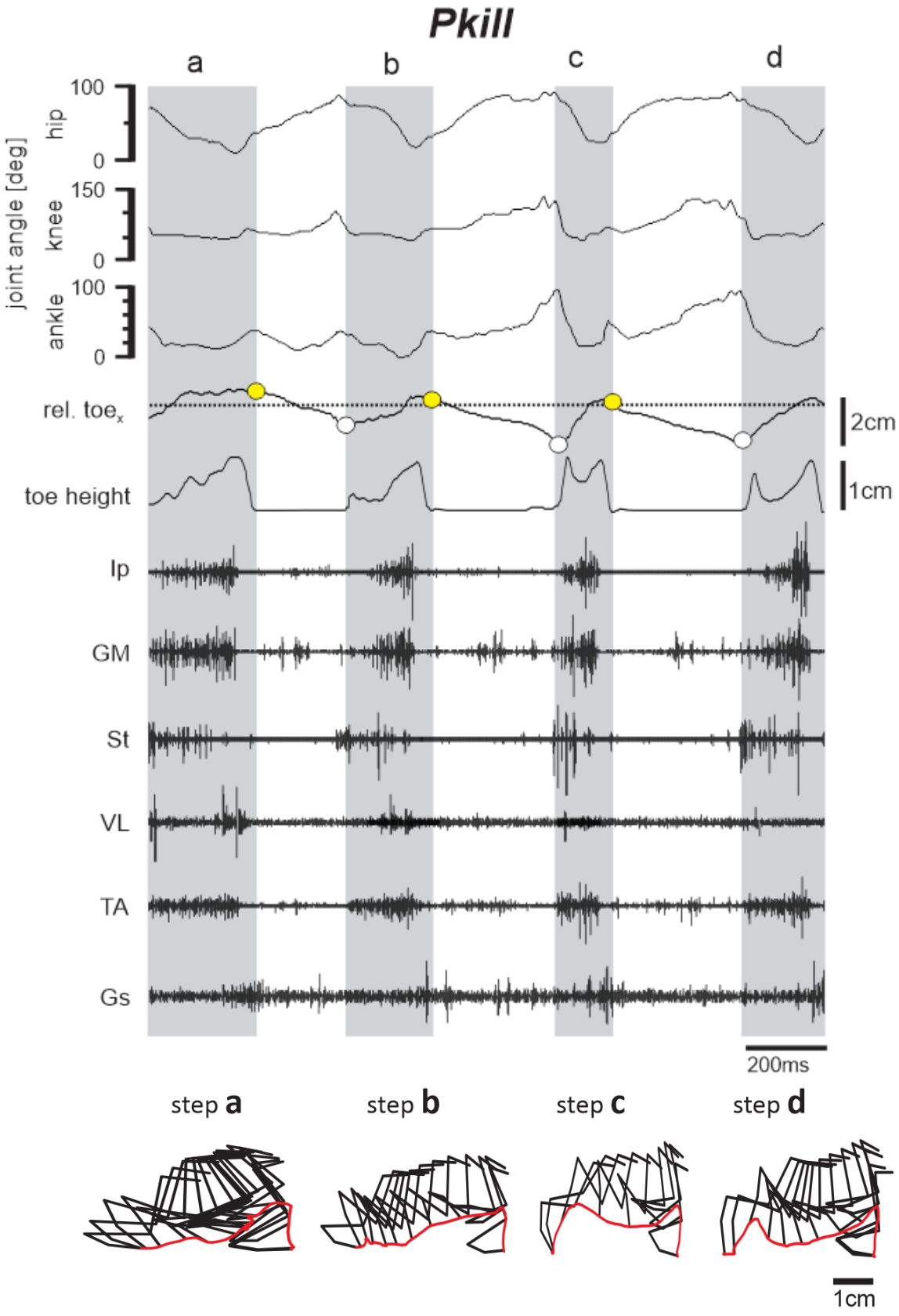
Pkill
a
b
c
d
joint angle [deg]
hip
100
0
knee
150
0
ankle
100
0
rel. toe$_x$
2cm
toe height
1cm
Ip
GM
St
VL
TA
Gs
200ms
step a
step b
step c
step d
1cm

The typical sequence of activation of flexor and extensor muscles moving the hip, knee and ankle joints (Figure 2.2B and 2.4Ai) was drastically changed to synchronous activity of all recorded muscle during the swing phase (shaded background Figure 2.3 and 2.4Aii). Each *Pkill* mouse had adopted a different strategy for weight-bearing during the stance phase. In each animal, a different extensor was activated during the stance phase while the other extensor muscles were activated alongside the flexor muscles during the swing phase (Figure 2.4Aii). Although all recorded flexor muscles were activated during the swing phase, the temporal structure of the activity pattern showed remarkable variability. These data suggest that a well-coordinated locomotor pattern requires proprioceptive feedback from muscle spindles and GTOs.

Some other afferents are likely to be compromised in *Pkill* mice as well, since 10-15% of the Pv^+ cells in the DRG are not from muscle spindles or GTOs but from Meissner or Pacinian corpuscles (de Nooij et al., 2013; Ernfors et al., 1994). Therefore, the missing non-proprioceptive Pv^+ positive sensory neurons might have influenced the locomotor pattern especially while the limbs were in contact with the ground. To better understand the neuronal network and the firing pattern of the motoneurons, we reasoned that swimming the *Pkill* mice would eliminate the interference of weight-bearing and cutaneous feedback on the locomotor pattern.

The Figure 2.4Bi shows that the wild type mice expressed a well-coordinated activity pattern of flexor (black bars and EMG traces) and extensor muscles (grey bars and EMG traces) during swimming that is clearly distinct from the pattern expressed during walking. On the other hand, changing the cutaneous and proprioceptive feedback (*Pkill* swimming)

led to an activity pattern where all muscles were active simultaneously (Figure 2.4Bii) and these mice were not able to swim. The on- and offsets of muscular activity during walking and swimming in wild types and *Pkill* mice are shown in Table 2.2. These data suggest that sensory feedback is necessary to generate a well-coordinated and functional locomotor pattern.

Figure 2. 4 Degradation of locomotor pattern in total absence of proprioceptive feedback from muscle spindles and Golgi tendon organs. **Ai**: treadmill locomotion at 0.2 m/s in wild type mice including two complete swing phases (blue background) and one complete stance phase (white background). Averaged EMG activities are represented by black bars for flexor muscles, and gray bars for extensor muscles (N = 6 wild type mice, 64 bursts for Ip, 64 for BF, 55 for St, 55 for VL, 64 for TA, and 55 for Gs). **Aii**: individualized averaged locomotor pattern of four *Pkill* mice during free walking. Note that the flexor muscles are likely to fire within the swing phase while a chaotic organization of extensor muscle activities. The difference in the scale bar indicates that the step cycles are longer in *Pkill* mice (N = 4 *Pkill* mice, 27 bursts for Ip, 27 for GM, 27 for St, 18 for VL, 27 for TA, and 14 for Gs). **Bi** (*left*): bar diagram illustrating the average EMG activity pattern during wild type swimming. The white rectangle indicates a swimming cycle. **Bi** (*right*): Average EMG activity during swimming in wild type mice. EMG recordings for flexor muscles are in black and extensor muscles are in grey. Ip onset as a reference for swimming cycle (vertical dashed line). Note the antagonism of flexor and extensor muscles (N = 6 wild type mice, 70 bursts for Ip, 70 for BF, 59 for St, 70 for VL, 60 for TA, and 55 for Gs). **Bii** (*left*): bar diagram illustrating EMG activity pattern of swimming *Pkill* mice lacking muscular antagonism. **Bii** (*right*): the average EMG activity shows co-activation of all muscles in reduced gravitational conditions in the swimming tank. Note that Gs activation is likely to be delayed among the recorded muscles (N = 4 *Pkill* mice, 80 bursts for Ip, 80 for GM, 80 for St, 80 for VL, 80 for TA, and 52 for Gs).

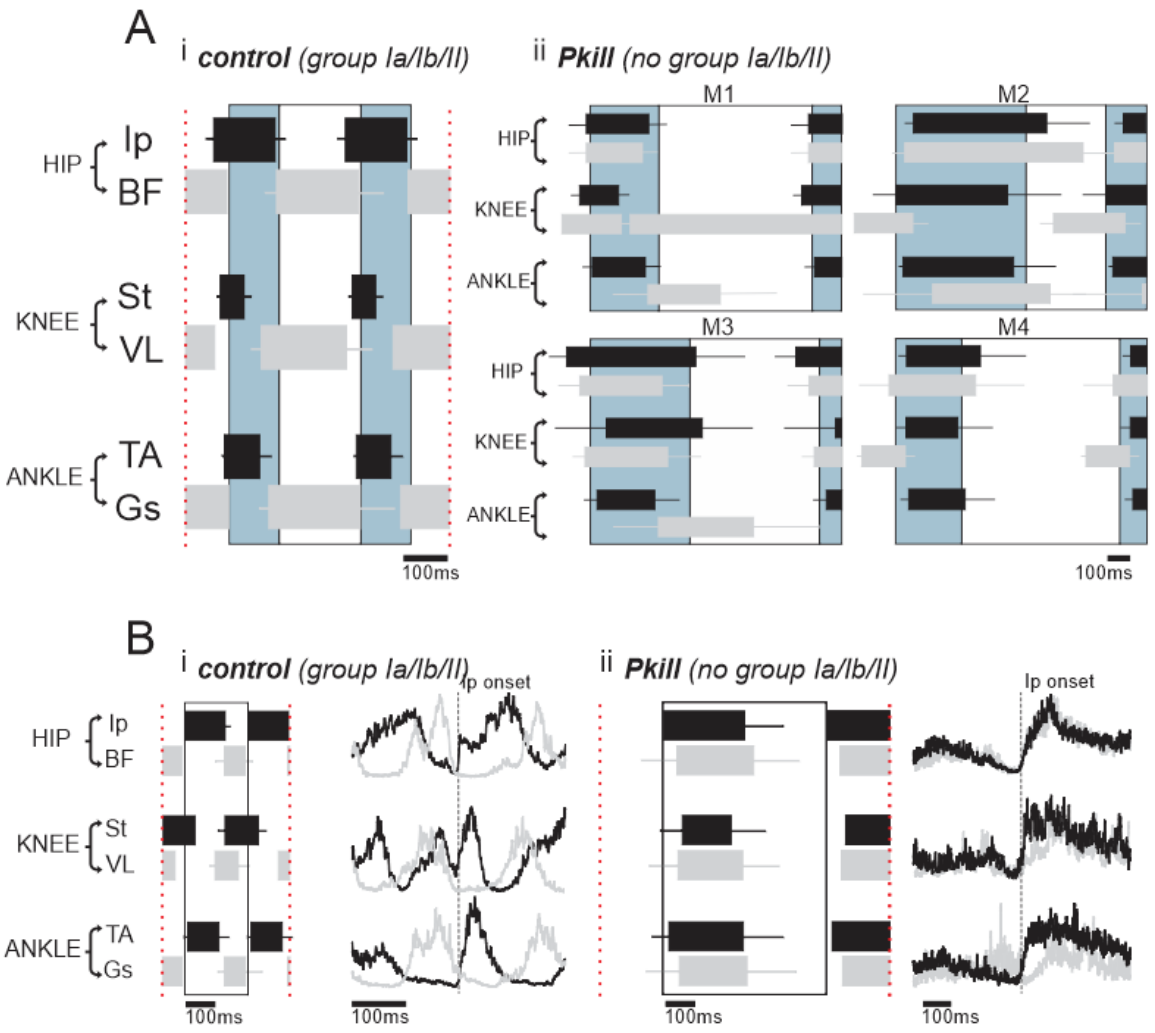
A
i control (group Ia/Ib/II)
ii Pkill (no group Ia/Ib/II)
HIP
Ip
BF
KNEE
St
VL
ANKLE
TA
Gs
M1
M2
M3
M4
100ms
B
i control (group Ia/Ib/II)
ii Pkill (no group Ia/Ib/II)
Ip onset
100ms

Table 2. 2 Muscle activity during the step and swimming cycle (wild type x *Pkill* mice). Percentage values represent the onset and offset of EMG activity in flexor and extensor muscles through phases. Mean values of seven wild types walking at 0.2 m/s and four *Pkill* mice free walking.

wild type X *Pkill* walking

		ONSET THROUGH STEP CYCLE		OFFSET THROUGH STEP CYCLE	
		WT	*Pkill*	WT	*Pkill*
Flexor Muscles	**Ip**	80.7% (stance-phase)	98.8% (stance-phase)	91.8% (swing-phase)	4.5% (next stance-phase)
	St	89.5% (stance-phase)	97.4% (stance-phase)	28.6% (swing-phase)	69.4% (swing-phase)
	TA	94.4% (stance-phase)	2.5% (swing-phase)	60.2% (swing-phase)	93.9% (swing-phase)
Extensor muscles	**BF/GM**	95.9% (swing-phase)	97.2% (stance-phase)	96.4% (stance-phase)	95.2% (swing-phase)
	VL	65.7% (swing-phase)	88.9% (swing-phase)	82.6% (stance-phase)	69.3% (next swing-phase)
	Gs	79.2% (swing-phase)	56.4% (swing-phase)	99.2% (stance-phase)	93.4% (stance-phase)

wild type X *Pkill* swimming

		ONSET THROUGH SWIMMING CYCLE		OFFSET THROUGH SWIMMING CYCLE	
		WT	*Pkill*	WT	*Pkill*
Flexor muscles	**Ip**	0% (flexor-phase)	0% (flexor-phase)	100% (flexor-phase)	100% (flexor-phase)
	St	99.3% (flexor-phase)	22.3% (flexor-phase)	26% (flexor-phase)	83.3% (flexor-phase)
	TA	7.2% (flexor-phase)	6.2% (flexor-phase)	83.7% (flexor-phase)	99.3% (flexor-phase)
Extensor muscles	**BF/GM**	91.6% (flexor-phase)	16.2% (flexor-phase)	86.2% (extensor-phase)	4.3% (extensor-phase)
	VL	70.9% (flexor-phase)	17.9% (flexor-phase)	58% (extensor-phase)	98.1% (flexor-phase)
	Gs	90.9% (flexor-phase)	19.2% (flexor-phase)	89.5% (extensor-phase)	1.2% (extensor-phase)

These data demonstrate that, in freely behaving mice, spinal circuits are not able to generate typical and functional walking or swimming patterns in the absence of proprioceptive feedback.

2.3.3 Locomotion in Absence of Muscle Spindle Feedback

To address the role of proprioceptive sensory feedback, specifically from the muscle spindles during walking, we directed our attention to another mouse model in which muscle spindles degenerate but GTOs are intact, the *Egr3*$^{-/-}$ mice (see methods 2.2.3). The kinematic parameters in *Egr3*$^{-/-}$ mice were similar to those findings by Akay et al (2014). Hip joint angle traces were like wild type mice, although assuming a more overall flexed position. Similarly, the knee joint was qualitatively more flexed than the wild types during the entire swing phase. As previously described (Akay et al 2014), an exaggerated flexion of the ankle joint during the swing phase was detected. In accordance with this over-flexion of the ankle joint, a prolonged TA activity during swing was also apparent (green arrows Figure 2.5). These data provide evidence that proprioceptive sensory feedback from muscle spindles is necessary for the locomotor pattern that underlies normal angular joint movement in wild type animals.

The angular changes detected in the hindlimb joints were accompanied by significant changes in toe trajectories during walking. The movement of the limb and the toe traces for a walking sequence including five swing phases is illustrated in Figure 2.5. A typical high stepping behavior was observed among the seven *Egr3*$^{-/-}$ mice as a result of delayed TA and St offset activity. The relative toe_x (yellow circles Figure 2.5) was statistically shorter in *Egr3*$^{-/-}$ mice (10 ± 3 mm) compared to the wild type (15 ± 2 mm; $P < 0.001$ after *t*-test). This suggest that proprioceptive feedback from the muscle spindles is necessary for maintaining the typical toe trajectory during walking.

Figure 2. 5 Kinematics and EMG pattern of *Egr3*$^{-/-}$ mouse walking at 0.2 m/s. Joint angles, toe position on the horizontal axis relative to hip (rel. toe_x; dotted horizontal line indicates the hip position), toe height, and raw EMG data from flexor and extensor muscles during a stepping sequence that includes five swing phases (shaded background, a, b, c, d, e) and four stance phases (white background). Ip, iliopsoas (hip flexor); BF, anterior head of biceps femoris (hip extensor); St, semitendinosus (knee flexor); VL, vastus lateralis (knee extensor); TA, tibialis anterior (ankle flexor); Gs, gastrocnemius (ankle extensor). The PEP and AEP are indicated by white and yellow circles, respectively. The stick diagram at the bottom of the figure represents swing phases of a, b, c, d, and e. Note that the AEP (yellow circles) are positioned close to the hip joint (dashed line) and the prolonged activation (green arrows) of the TA muscle resulting in high step behavior. Functional locomotion is achieved without disrupting the overall intralimb coordination (stick diagrams in the bottom).

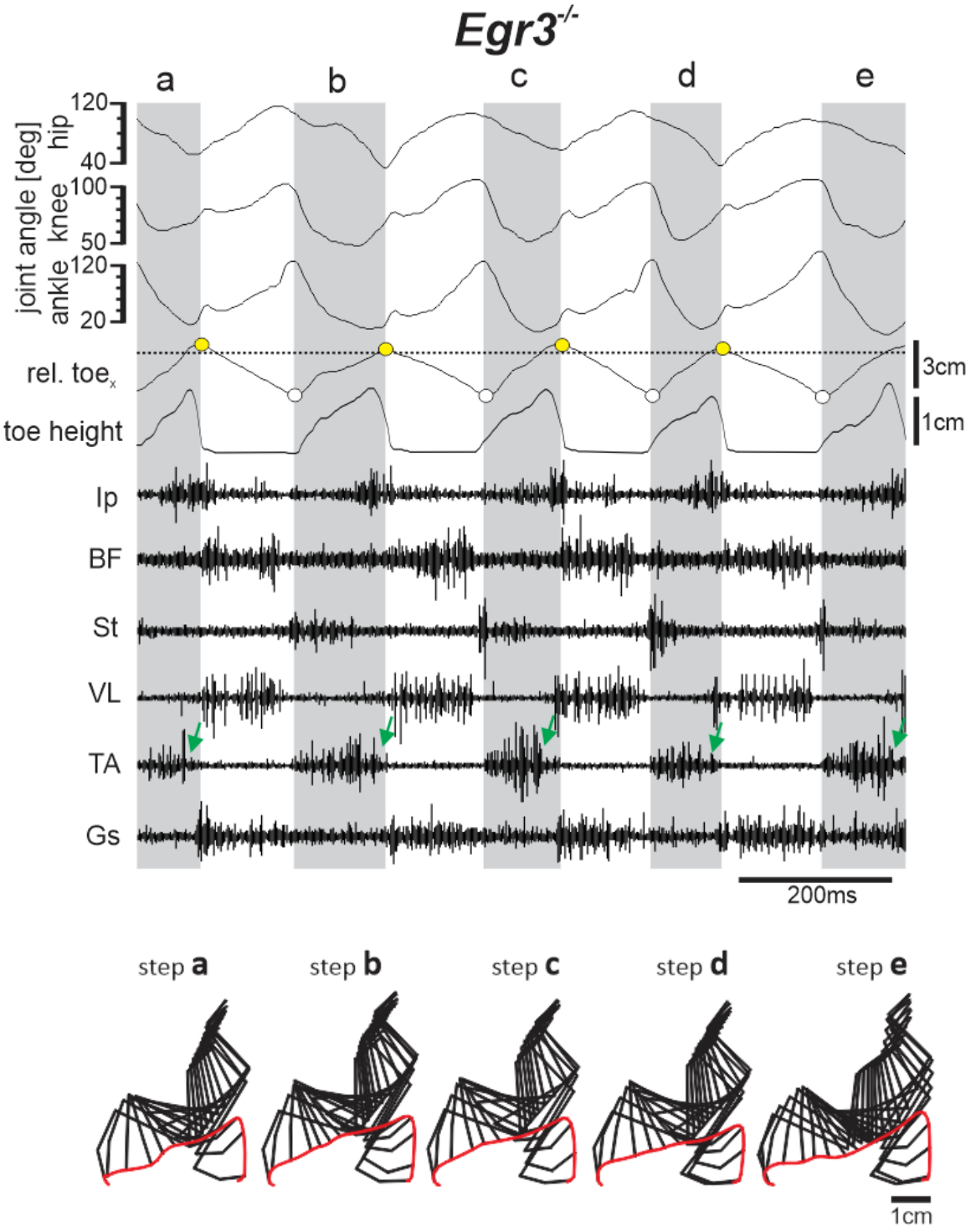
Egr3-/-
a
b
c
d
e
joint angle [deg]
hip
120
40
knee
100
50
ankle
120
20
rel. toe$_x$
toe height
3cm
1cm
Ip
BF
St
VL
TA
Gs
200ms
step a
step b
step c
step d
step e
1cm

Removing the muscle spindles also effected the temporal parameters of stepping movements (Figure 2.6). During walking at 0.2 m/s, the average step cycle was statistically shorter in *Egr3*$^{-/-}$ mice (0.28 ± 0.03s) than in the wild types (0.30 ± 0.06; $P < 0.01$ after *t*-test). All of the wild types managed to walk at 0.4 m/s, however, two out of seven *Egr3*$^{-/-}$ mice could not walk at that speed. The step cycle was also statistically shorter in *Egr3*$^{-/-}$ mice walking at 0.4 m/s (0.17 ± 0.02s) than in the wild type*s* (0.19 ± 0.03; $P < 0.001$ after *t*-test, Figure 2.6A). The swing duration was statistically shorter in *Egr3*$^{-/-}$ mice (0.10 ± 0.02s) than in the wild types (0.11 ± 0.02; $P < 0.001$ after *t*-test) while walking at 0.2m/s. During walking at 0.4 m/s, the swing duration was also statistically shorter in *Egr3*$^{-/-}$ mice (0.07 ± 0.01s) than in the wild type*s* (0.08 ± 0.03 $P < 0.001$ after *t*-test, Figure 2.6A). Stance duration, however, was not significantly different in *Egr3*$^{-/-}$ mice (0.18 ± 0.03s) compared to wild types (0.19 ± 0.04s). One possible explanation for the altered swing phase with minor changes in stance phase is that the lack of muscle spindle feedback may be compensated by GTO signaling during stance. The decrease in the step cycle period was largely the result of a decrease in the swing phase and lesser to changes in stance duration (Figure 2.6A).

The spatial parameters of locomotion exhibited changes after abolishing muscle spindle feedback. During treadmill walking at 0.2m/s, the swing amplitude was statistically shorter in *Egr3*$^{-/-}$ mice (2.9 ± 0.5cm) than in the wild type*s* (3.2 ± 0.6; $P < 0.01$ after *t*-test). While walking at 0.4m/s, swing amplitude remained statistically shorter in *Egr3*$^{-/-}$ mice (3.06 ± 0.3cm) compared to wild type*s* (3.4 ± 0.4; $P < 0.001$ after *t*-test). Thus, these data suggest that muscle spindle feedback likely plays a role in regulating swing amplitude.

Next, we were interested in how this shortening of the swing movement in *Egr3*$^{-/-}$ mice was achieved. Figure 2.6Bii shows that the swing onset position was more distant from the hip joint in the *Egr3*$^{-/-}$ mice walking in both speeds (at 0.2m/s wild type: -1.64cm ±0.60; *Egr3*$^{-/-}$: -1.90cm ± 0.44; $P < 0.05$ and at 0.4m/s wild type: -2.02cm ± 0.35; *Egr3*$^{-/-}$: -2.37cm ± 0.35; $P < 0.001$). As for the swing offset position, there was little difference across speeds in wild type mice (1.56cm ± 0.23 at 2.0m/s and 1.37cm ± 0.21 at 0.4m/s). The swing offset position was significantly closer to the hip joint in the *Egr3*$^{-/-}$ mice (1.04cm ± 0.38 at 2.0m/s and 0.66cm ± 0.41 at 0.4m/s; $P < 0.001$ in both speeds). These data suggest that in absence of feedback from muscle spindles, not only the swing amplitude decrease, but also the entire step shift posteriorly relative to the hip position.

Figure 2. 6 Step cycle and spatial parameters in the absence of muscle spindle feedback. **A**: box plots showing cycle period, swing duration and stance duration. At 0.2 and 0.4 m/s the cycle period and swing durations are consistently lower in *Egr3*$^{-/-}$ mice (red boxes). **Bi**: swing amplitude in the absence of muscle spindle feedback is shorter during 0.2 and 0.4 m/s walking. **Bii**: hindlimb positioning at the beginning (sw onset position) and end (sw offset position) of the swing phase. *Egr3*$^{-/-}$ mice started the swing phase with the leg positioned more distant from the hip joint compared to wild types, and ended the swing phase with the leg positioned closer. Seven wild types were able to walk at 0.2 and 0.4 m/s, seven *Egr3*$^{-/-}$ mice walked at 0.2 m/s and only five mice reach 0.4 m/s. Two-tailed *t*-test $^{**}P < 0.01$, $^{***}P < 0.001$.

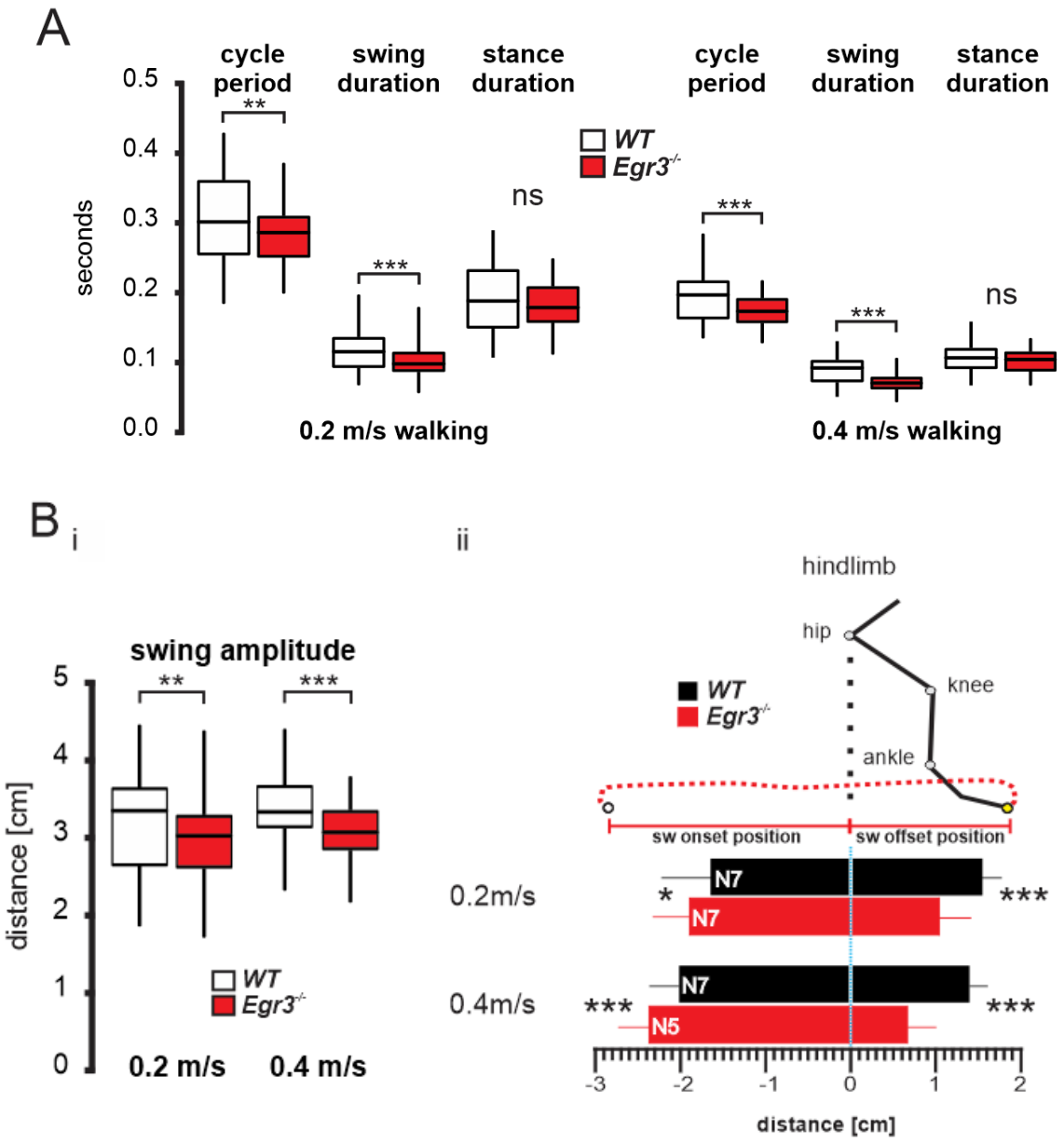

We also investigated the quantitative changes in the locomotor pattern in the absence of proprioceptive feedback from the muscle spindles by comparing EMG activity patterns of wild type and *Egr3*$^{-/-}$ walking and swimming. In wild type mice walking, muscle activation underwent a sequential propagation from the proximal muscles to the distal muscles (Figure 2.7Ai). The hip flexor (Ip) onset occurred first at the end of stance, followed by knee flexor (St) onset, and finally the onset of ankle flexor (TA), all of these events occurred prior the start of the swing phase. The offsets of the flexor muscles followed a different sequence: St-TA-Ip during swing, where Ip offset occurred at the end of the swing. All the recorded extensor muscles were active during the stance phase with onsets of the knee and ankle extensors (VL and GS respectively) occurring at mid-swing phase. These data provide baseline parameters and establish the typical locomotor pattern in animals with intact proprioceptive system.

Elimination of proprioceptive sensory feedback from muscle spindles led to selective and consistent modifications in the activation-deactivation pattern of the flexor muscles. To illustrate this, we timed the on- and offset of the muscle activities adopting the swing onset as time 0. Negative numbers represented events before the swing onset whereas positive values occurred after the swing onset. The hip flexor (Ip) onset was delayed in average 17 milliseconds (wild type: -37ms ± 18 and *Egr3*$^{-/-}$: -20ms ± 12; $P < 0.001$ - Ip white hatched area Figure 2.7Aii), whereas early onset of the knee flexor (St) was observed (wild type: -20ms ± 08 and *Egr3*$^{-/-}$: -36ms ± 17; $P < 0.001$) with prolonged activity (st offset wild type: 33ms ± 18; *Egr3*$^{-/-}$: 42ms ± 24; $P < 0.001$) as shown the St red hatched area in Figure 2.7Aii. Delayed offset leading to prolonged activity of the ankle flexor (TA) were also observed (wild type: 70ms ± 27 and *Egr3*$^{-/-}$: 88ms ± 24; $P < 0.001$) as shown the TA yellow hatched

area in Figure 2.7Aii. Changes in the extensor muscles' activation/deactivation times were not consistent. We reasoned that compensatory action of proprioceptive feedback from the GTOs could explain this lack of consistent change.

During the swimming task, afferent input from the GTO's is considered low due to the lack of gravitational influence (Akay et al., 2006; Gruner & Altman, 1980). The lack of weight-bearing due to the buoyancy of the water significantly reduces the input from the Ib afferents. Because kinematics was not measured during swimming, the swimming cycles were defined from the onset to the next onset of the iliopsoas muscle activity. The averaged EMG recordings showed in the Figure 2.7Bi demonstrate that wild type mice performed a swimming pattern in which the extensor muscles BF, VL, and Gs produced overlapping activity and two distinct periods of activations for the flexor muscles. In a first moment co-activation of Ip and TA muscle followed by activation of St muscle. Particularly, all wild type mice also showed perfect alternation, with minor overlapping activity, between flexor and extensor muscles moving a single joint.

The locomotor pattern found in wild type mice was not observed in the *Egr3*$^{-/-}$ mice while exposed to buoyancy effects of water. Lack of afferent signals from Ia/II and reduced signaling from the Ib afferents led to remarkable synchrony of flexor and extensor muscles (Figure 2.7Bii) that resembled the walking and swimming pattern of *Pkill* mice (described in section 2.3.2). However, the activation of extensor muscles in the *Egr3*$^{-/-}$ mice appear to propagate from proximal to distal muscles, starting from BF to VL to Gs (Figure 2.7Bii), differently than wild types in which extensor muscles are activated concurrently (Figure 2.7Bi). Table 2.3 shows detailed onset-offset timing for flexor-extensor of muscles in wild

types and *Egr3*$^{-/-}$ mice. These data suggest that proprioceptive feedback from muscle spindles and GTO are necessary for functional locomotion, supporting the conclusions reached with the *Pkill* mice in section 2.3.2.

Figure 2. 7 Degradation of locomotor pattern in absence of proprioceptive feedback from muscle spindles. **Ai**: treadmill locomotion at 0.2 m/s in wild type mice including two complete swing phases (blue background), and one complete stance phase (white background). Averaged EMG activities are represented by black bars for flexor muscles and gray bars for extensor muscles (N = 6 wild type mice, 64 bursts for Ip, 64 for BF, 55 for St, 55 for VL, 64 for TA, and 55 for Gs). **Aii**: averaged locomotor pattern of seven *Egr3*$^{-/-}$ mice during 0.2 m/s walking. Note that the flexor muscles display a dashed area indicating changes in onset-offset of the muscles. The white dashed area is the delayed onset activity of the Ip muscle in of *Egr3*$^{-/-}$ mice compared with wild type after Student's *t*-test ($P < 0.001$). The red dashed areas indicate differences in earlier St onset ($P < 0.001$) and delayed onset ($P < 0.01$) in *Egr3* $^{-/-}$mice compared with wild types. The yellow dashed areas indicate that the TA offset is delayed when compared with wild types ($P < 0.001$). N = 7 *Egr3*$^{-/-}$ mice, 88 bursts for Ip, 35 for BF, 88 for St, 48 for VL, 88 for TA, and 67 for Gs). **Bi**: (*left*) bar diagram illustrates the average timing of EMG activities during wild-type swimming. The white rectangle indicates a swimming cycle. **Bi**: (*right*) averaged EMG recording during wild-type swimming. EMG activities of flexor muscles are indicated by black lines, whereas the gray lines illustrate the average EMG activities of extensor muscles. Ip onset was taken as a reference for the swimming cycle (vertical dashed line). Note the antagonism of flexor and extensor muscles (N = 6 wild type mice, 70 bursts for Ip, 70 for BF, 59 for St, 70 for VL, 60 for TA, and 55 for Gs). **Bii**: (*left and right*) as in Bi but for *Egr3*$^{-/-}$ mice. Notice that during *Egr3*$^{-/-}$ swimming (Bii, *right*) the averaged EMG activity shows co-activation of all muscles under reduced gravitational conditions in the swimming tank. Note that GS activation is likely to be delayed among the recorded muscles (N = 7 *Egr3* $^{-/-}$ mice, 69 bursts for Ip, 48 for BF, 62 for St, 62 for VL, 69 for TA, and 48 for Gs).

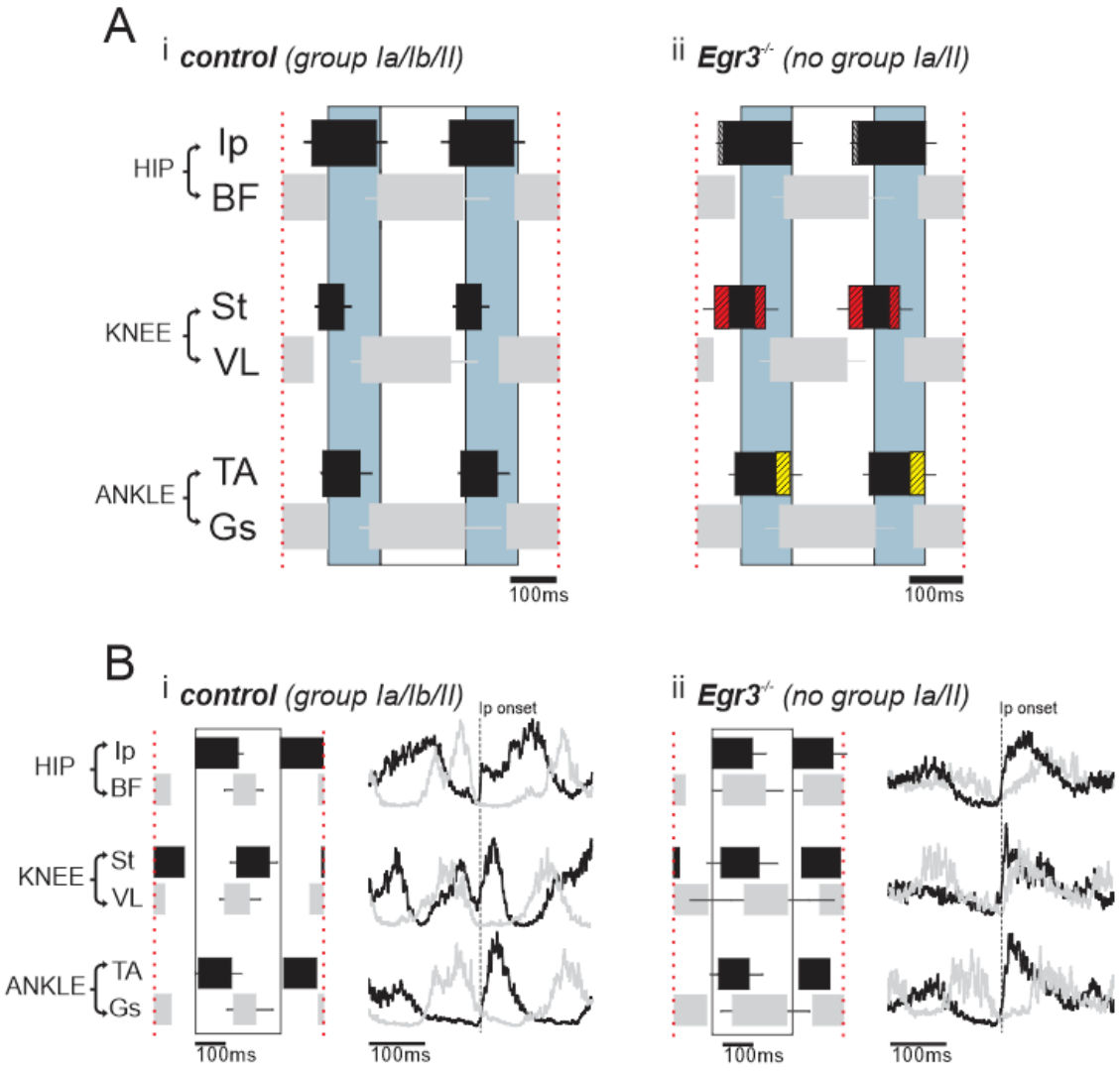
A
i control (group Ia/Ib/II)
ii Egr3-/- (no group Ia/II)
HIP
Ip
BF
KNEE
St
VL
ANKLE
TA
Gs
100ms
100ms
B
i control (group Ia/Ib/II)
ii Egr3-/- (no group Ia/II)
Ip onset
Ip onset
HIP
Ip
BF
KNEE
St
VL
ANKLE
TA
Gs
100ms
100ms
100ms
100ms

Table 2. 3 Muscle activity during the stepping and swimming cycles of wild type and Egr3$^{-/-}$ mice. Percent values represent the onset and offset of EMG activity in flexor and extensor muscles during the phases. Mean values of seven wild types walking and seven *Egr3*$^{-/-}$ mice walking at 0.2 m/s.

wild type X *Egr3*$^{-/-}$ 0.2 m/s walking

		ONSET THROUGH STEP CYCLE		OFFSET THROUGH STEP CYCLE	
		WT	*Egr3*$^{-/-}$	WT	*Egr3*$^{-/-}$
Flexor muscles	**Ip**	80.7% (stance-phase)	88.9% (stance-phase)	91.8% (swing-phase)	97.8% (swing-phase)
	St	89.5% (stance-phase)	80% (stance-phase)	28.6% (swing-phase)	41.5% (swing-phase)
	TA	94.4% (stance-phase)	94.8% (stance-phase)	60.2% (swing-phase)	86.5% (swing-phase)
Extensor muscles	**BF**	95.9% (swing-phase)	81.7% (swing-phase)	96.4% (stance-phase)	93.7% (stance-phase)
	VL	65.7% (swing-phase)	62.4% (swing-phase)	82.6% (stance-phase)	70.7% (stance-phase)
	Gs	79.2% (swing-phase)	86.2% (swing-phase)	99.2% (stance-phase)	100% (stance-phase)

wild type X *Egr3*$^{-/-}$ swimming

		ONSET THROUGH SWIMMING CYCLE		OFFSET THROUGH SWIMMING CYCLE	
		WT	*Egr3*$^{-/-}$	WT	*Egr3*$^{-/-}$
Flexor muscles	**Ip**	0% (flexor-phase)	0% (flexor-phase)	100% (flexor-phase)	100% (flexor-phase)
	St	99.3% (flexor-phase)	23.2% (flexor-phase)	26% (flexor-phase)	17% (extensor-phase)
	TA	7.2% (flexor-phase)	17% (flexor-phase)	83.7% (flexor-phase)	90.4% (flexor-phase)
Extensor muscles	**BF**	91.6% (flexor-phase)	26% (flexor-phase)	86.2% (extensor-phase)	35.5% (extensor-phase)
	VL	70.9% (flexor-phase)	82.6% (flexor-phase)	58% (extensor-phase)	95.3% (extensor-phase)
	Gs	90.9% (flexor-phase)	50.4% (flexor-phase)	89.5% (extensor-phase)	86.9% (extensor-phase)

2.3.4 Role of Muscle Spindle Feedback from Specific Joints in Locomotion

How is proprioceptive information from the muscle spindle processed by the central nervous system to generate the temporal aspect of muscle activity pattern that coordinated

limb movement during locomotion? Our previous experiments showed that the locomotor pattern during walking is subtly changed when inputs from GTOs are intact and muscle spindle feedback is eliminated. On the other hand, attenuating proprioceptive feedback from both the muscle spindles and GTOs, as shown in the studies with the *Pkill* mice or during the swimming task for the *Egr3*$^{-/-}$ mice, drastically changes the locomotor pattern to a point that no longer resembles typical locomotion. Here we were interested to address the question of whether muscle spindle feedback signaling angular displacement of a particular joint has a specific role in pattern generation or whether proprioceptive information from all joints is equally important.

If the muscle spindle feedback from the hip, knee, and ankle joints are equally important for locomotor pattern generation, attenuation of muscle spindle feedback from one of the joints should have similar but slight effects. In contrast, if muscle spindle feedback from a specific joint is more important than the others, attenuation from that particular joint should have a larger effect on the locomotor pattern. To differentiate between these possibilities, we acutely eliminated amounts of muscle spindles from only one of the hip, knee, and ankle joints in a single leg and analyzed differences in the locomotor pattern before and after experimental procedures.

To acutely attenuate muscle spindle feedback from a subset of muscles (Figure 2.8 and methods 2.2.4), we used the *Pv::cre* mice in combination with AAV9 as described above. When injected into the muscle of *Pv::cre* animals at p10, AAV9 infects sensory and motoneurons innervating that particular muscle. Since Pv is only expressed in proprioceptive afferents during the first two postnatal weeks, the DTR-GFP is expressed

only in Pv^+ proprioceptors due to the Flex-switch (Figure 2.8Ai). Noteworthy is that AAV9 is incapable of jumping synapses, therefore Pv^+ interneurons that synapse onto motoneurons (such as the Ia inhibitory interneurons) are not infected. Expression of DTR makes proprioceptive afferents susceptible to diphtheria toxin (DTX) by which mice are normally not affected. After the AAV9 injections, *Pv::cre* mice were kept until adulthood when they underwent EMG implantation (methods 2.2.5). Figure 2.8Aii shows that muscle spindle morphology was unaltered after AAV9 administration. Next, EMG and kinematic data recordings were performed before (Figure 2.8Aii) and 5-15 days after intraperitoneal diphtheria toxin (DTX) injection when the muscle spindle afferents were destroyed (Figure 2.8Aiii).

Although parvalbumin is expressed in all proprioceptive sensory neurons in the dorsal root ganglia (de Nooij et al., 2015), the AAV9 injected in the center of the muscular belly is possibly avoiding the infection of the group Ib afferents due to its anatomical location at the myotendinous junctions (Figure 2.8Bi) further away from the injection site. This method eliminates 55% to 73% of the muscle spindles in infected muscles (Mayer et al., 2018) while the GTO morphology remains unaltered (Figure 2.8Bii). Although Pv is expressed in some muscle fibers (Celio & Heizmann, 1982) and AAV9 is known to also infect extrafusal muscle fibers (Katwal et al., 2013), we performed experiments with histological assessments to show that DTX injection did not affect extrafusal muscle fibers (Chapter 4 and Mayer et al., 2018).

Figure 2. 8 Acute elimination of proprioceptive afferents from specific muscles. Adeno-associated virus (AAV9) was used to deliver a cre-conditional (flexed) gene encoding a diphtheria toxin receptor (DTX) into targeted muscles of *Pv::cre* mice, where parvalbumin (Pv) was selectively expressed in proprioceptive afferents and some interneurons. **Ai**: dorsal root ganglia of a *Pv::cre* mouse's gastrocnemius injected with AAV9 at p10. Axons and bodies of proprioceptive neurons were labeled with GFP. Motoneurons do not express Pv, therefore the diphtheria toxin receptor (DTR) gene was only expressed in proprioceptive afferents. **Aii**: muscle spindle labeling of a mouse at p50 showing that the AAV9 does not alter morphological characteristics of spindle afferents. Electromyogram electrodes were implanted during this stage for control recordings. **Aiii**: muscle spindle afferent removal. Notice that the typical anulospiral structures degraded to punctuated structures in the experimental leg after DTX injection. Post-DTX recordings were done 5–15 days after intraperitoneal DTX injection. **Bi**: schematic representing the site of muscular injection, Ib afferents are likely preserved due to their anatomical location within the myotendinous junction. **Bii**: histological images of proprioceptive afferents innervating Golgi tendon organs from a Gs muscle. Afferent fibers were labeled with antibody staining against VGluT1 (green) and UV light (blue) reflecting the tendinous structure. The pre-DTX image is from a muscle that received only AAV9 injection, and the post-DTX image shows a muscle after AAV9 and DTX injection. Note that the GTOs appear normal in both cases. Scale bars, 50 μm.

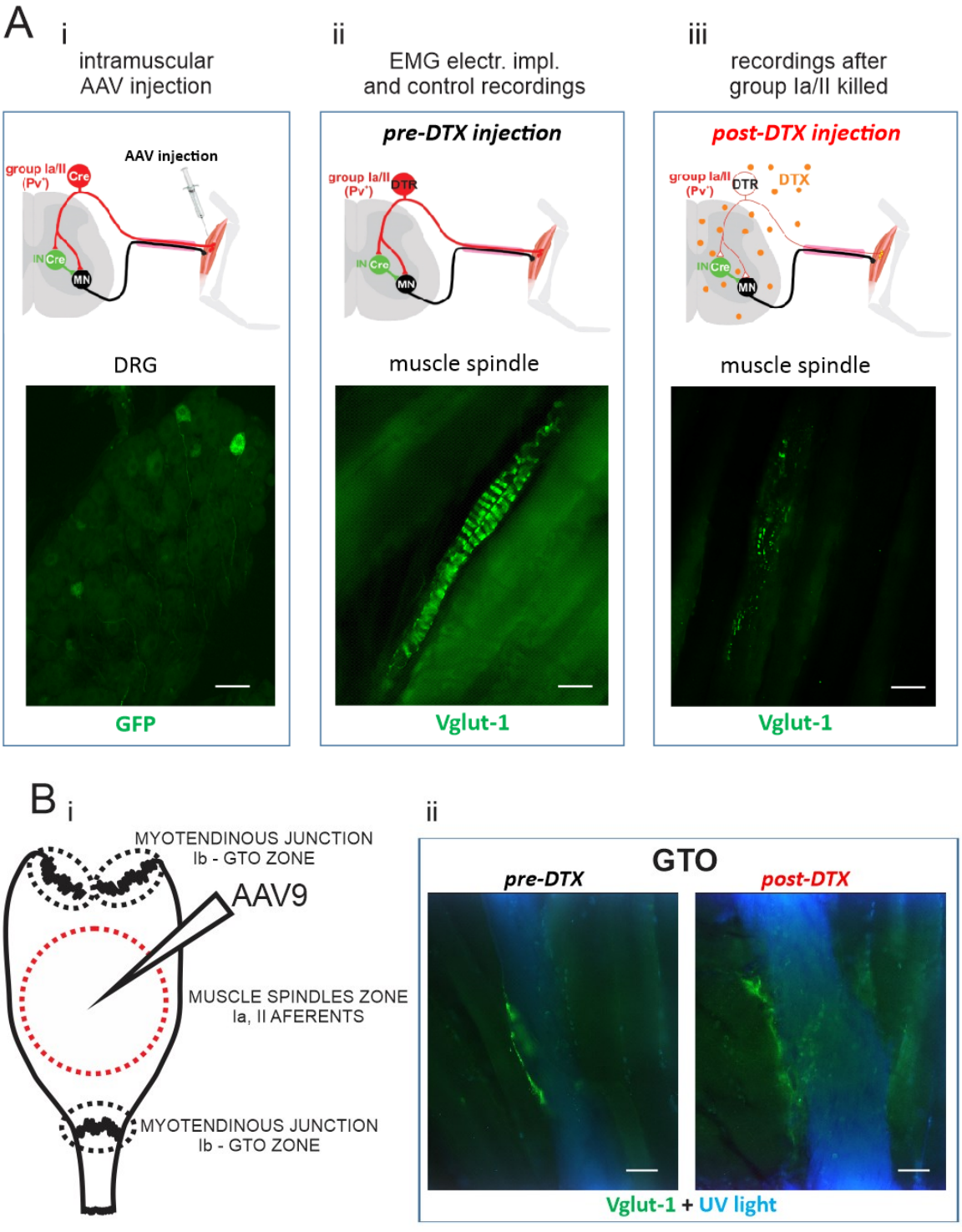
A
i
intramuscular
AAV injection
ii
EMG electr. impl.
and control recordings
iii
recordings after
group Ia/II killed
pre-DTX injection
post-DTX injection
AAV injection
group Ia/II (Pv+)
Cre
IN
MN
DTR
DTX
DRG
muscle spindle
muscle spindle
GFP
Vglut-1
Vglut-1
B
i
ii
MYOTENDINOUS JUNCTION
Ib - GTO ZONE
AAV9
MUSCLE SPINDLES ZONE
Ia, II AFERENTS
MYOTENDINOUS JUNCTION
Ib - GTO ZONE
GTO
pre-DTX
post-DTX
Vglut-1 + UV light

Two wild type mice received DTX injections to serve as treated controls. Since those animals were not genetically manipulated, we confirmed that the diphtheria toxin injections by themselves were not enough to induce kinematic variations (Figure 2.9A) or temporal changes in the step cycle parameters (Figure 2.9B). Measurements in the mean motion and range of motion (ROM) in those treated control mice were performed throughout their step cycles, and the results are shown in Table 2.4. These results demonstrate that the DTX injections, without the selective expression of DTR, have no qualitative effect on locomotion parameters.

Figure 2. 9 Joint kinematics and gait temporal parameters of DTX-treated controls. Intraperitoneal DTX injections in wild-type mice did not alter the functional aspects of walking behavior. **A**: kinematics of hip, knee and ankle joints pre-injection (black traces) and post-injection (red traces). Bold traces denote average motion and thinner traces denote the 95% confidence interval. The pink shadowed area represents the 95% confidence overlapping in pre- and post-DTX recordings. **B**: the average duration of step cycles, swing phases and stance phases did not change in treated control animals (N = 2 wild type mice, 26 steps pre-DTX and 21 steps post-DTX at 0.2 m/s, 19 steps pre-DTX and 18 steps post-DTX at 0.4 m/s, 16 steps pre-DTX and 19 steps post-DTX at 0.6 m/s).

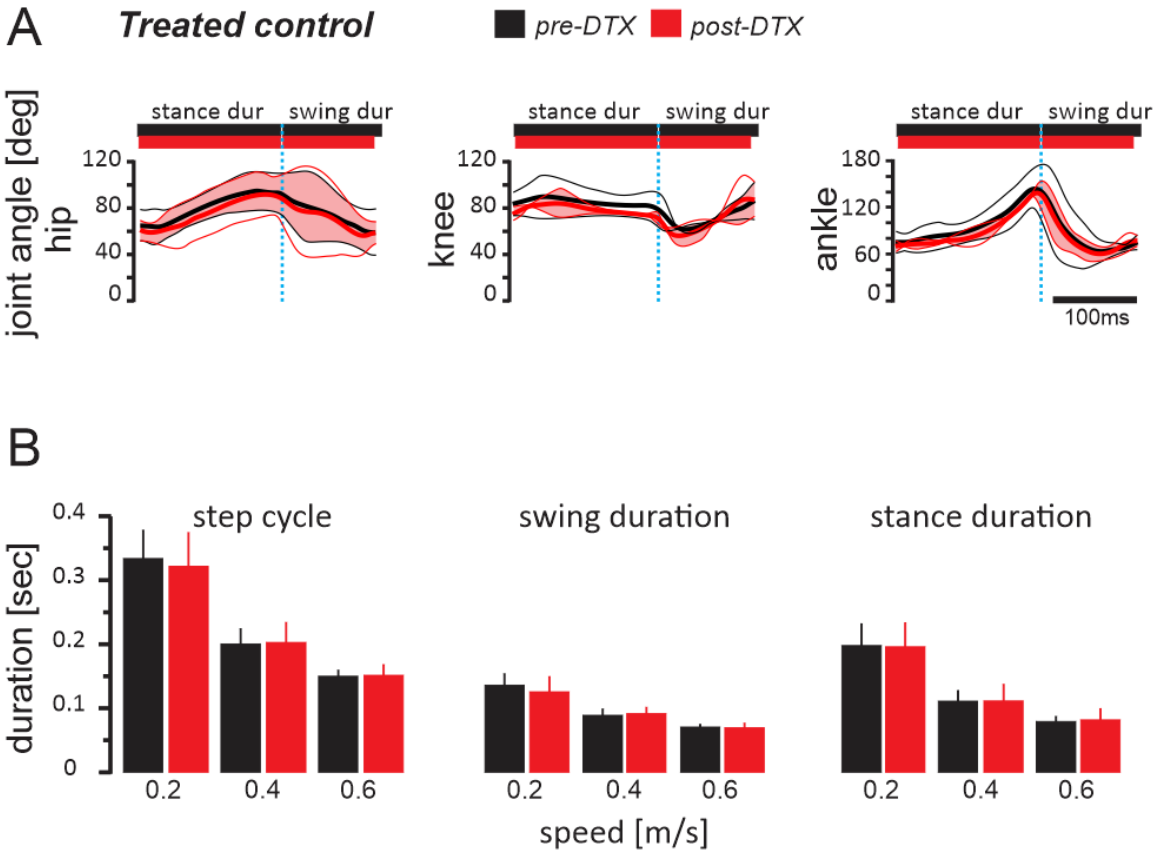

Table 2. 4 Motion parameters during the step cycles of treated control mice. The mean motion (average joint position during walking) and range of motion (amount of joint excursion from its maximum flexed position to its maximum extended position) are shown for pre-DTX and post-DTX experiments in wild type animals.

		Mean Motion			Range of Motion		
	Joint	*pre-DTX*	*post-DTX*	outcome %	*pre-DTX*	*post-DTX*	outcome %
Treated Control	Hip	77.8˚ (±10.8)	73.2˚ (±13)	5.8 flx	34.9˚ (±1.5)	35.6˚ (±1.8)	+ 1.9
	Knee	79.1˚ (±5.8)	74.8˚ (±1.7)	5.3 flx	28.2˚ (±13)	32.9˚ (±16)	+ 16.4
	Ankle	97.0˚ (±13.7)	91.2˚ (±2.3)	5.9 flx	85.7˚ (±8.3)	83.5˚ (±0.2)	- 2.6

These data demonstrate that we have a reliable method to target and reduce muscle spindle feedback from a specific group of muscles in the hindlimb. Also, we have shown that the diphtheria toxin injection in non-genetically modified mice does not induce kinematic disorders or temporal changes in the step parameters. Therefore, the results obtained in this section provide a scientific background for the following experiments described in this thesis.

2.3.5 Reducing Muscle Spindle Feedback from Hip Muscles

We next did a set of experiments in which we recorded the locomotor pattern during walking and swimming both before and after the attenuation of the muscle spindle feedback signaling hip joint angles. To assess the functional group of hip flexors and extensor, the iliopsoas muscle (Ip) and the muscular mass inserted in the vicinity of ischial tuberosity (Charles et al., 2016) represented by the semimembranosus (Sm), semitendinosus (st) and biceps femoris (BF), were infected with AAV9. The Ip and BF muscles received EMG electrode implants to monitor the activity of hip flexors and extensor respectively. We first

measured the average angular movement and the range of motion of each joint before and then after DTX injection to obtain a full description of the angular movement characteristics of the joints.

The attenuation of muscle spindles in hip muscles evoked by the DTX injections decreased hip angle average (Figure 2.10A). During the step cycle, animals have adopted a 27% more flexed hip angle compared to their baseline (pre-DTX) recordings (Table 2.5), however, no statistically significant ($P = 0.061$ paired t-test), although this flexed outcome was achieved in the hip joint in three out of four mice. No remarkable changes were observed in the knee (6% more flexed post-DTX, $P = 0.273$) and ankle (3.5% more extended, $P = 0.557$) joints regarding mean motion. The range of motion (ROM) in post-DTX recordings had a tendency to decrease in the hip (22%, $P = 0.054$), however, milder changes were observed in the knee, which has ROM increased (6.9% $P = 0.305$), and ankle recording ROM decrease (10.2% $P = 0.492$) after attenuation of muscle spindles in the hip joint. The 95% confidence interval between pre- and post-DTX (shaded pink, Figure 2.10Ai) shown that the mean motion is distinguished from non-overlapping areas of the hip joint, while knee and ankle main motion tend to be performed within the 95% confidence interval. Figure 2.10Aii illustrates the mean motion and ROM performances of individual mice.

Next, we investigated whether the role of proprioceptive feedback would be more or less perceptible when locomotor speeds increase to 0.4 or 0.6 m/s. We asked if the changes observed at 0.2 m/s would become more obvious, or could even disappear while increasing the treadmill speed. Our results confirmed that the more flexed movement of the hip joint after removal of muscle spindles from the hip joint muscles was maintained regardless of

the speed of locomotion. Similar to walking at 0.2 m/s, angular movement of knee and ankle joints did not change after muscle spindle removal from the hip joint at 0.4 or 0.6 m/s (Figure 2.10Ai). As a consequence of the more flexed hip joint, we have observed that the posterior and anterior positioning of the foot at the beginning and end of the swing was shifted anteriorly (Figure 2.10B). Only in one out of four mice, the foot position at the beginning of swing shifted posteriorly. Interestingly, the landing position which is represented by the swing-offset position has shifted more anteriorly (Figure 2.10B). These data suggest that muscle spindle feedback signaling hip angular displacement may selectively control the movement of the hip joint. Nevertheless, without statistical significance presumably due to the small number of experiments.

Figure 2. 10 Joint kinematics and paw positioning parameters after attenuating the muscle spindle feedback of hip flexor and extensor muscles. **Ai**: kinematics of hip, knee and ankle joints in pre-DTX (black traces) and post-DTX (red traces) injections (N = 4 *Pv::cre* mice, average from ~10 step cycles from each animal pre- and post-DTX in all given speeds). Bold lines represent average motion and thin lines the 95% confidence interval. The pink shadowed area represents the overlapping motion within the confidence interval pre- and post-DTX recordings. **Aii**: mean motion and range of motion (R.O.M.) scores of individual animals. **B**: hindlimb positioning at the beginning (sw-onset position) and ending (sw-offset position) of the swing phase. After DTX injections, three out of four mice, placed their hindlimb at a shorter distance from the hip joint and land it further compared with basal recordings. Two-tailed pair *t*-test $*P < 0.05$, $**P < 0.01$, $***P < 0.001$).

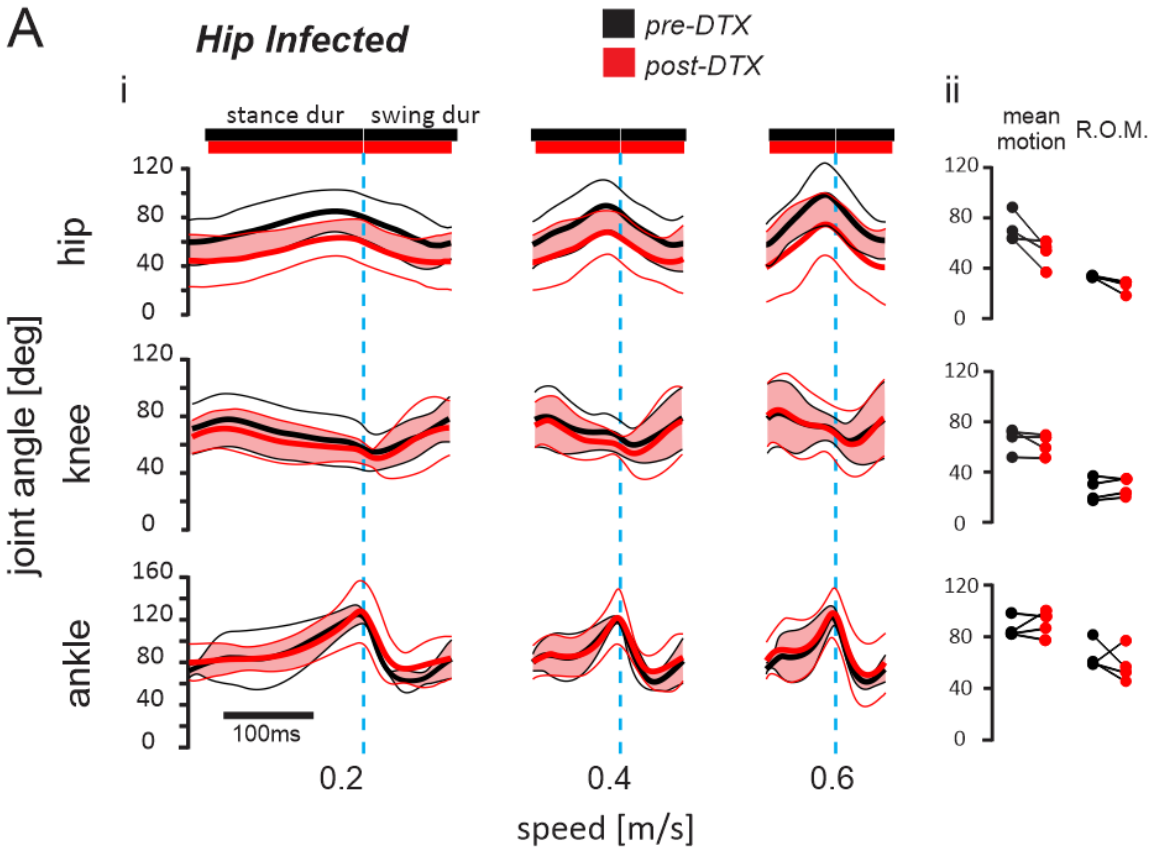
A
Hip Infected
pre-DTX
post-DTX
i
ii
stance dur
swing dur
mean motion
R.O.M.
joint angle [deg]
hip
knee
ankle
120
80
40
0
160
100ms
0.2
0.4
0.6
speed [m/s]

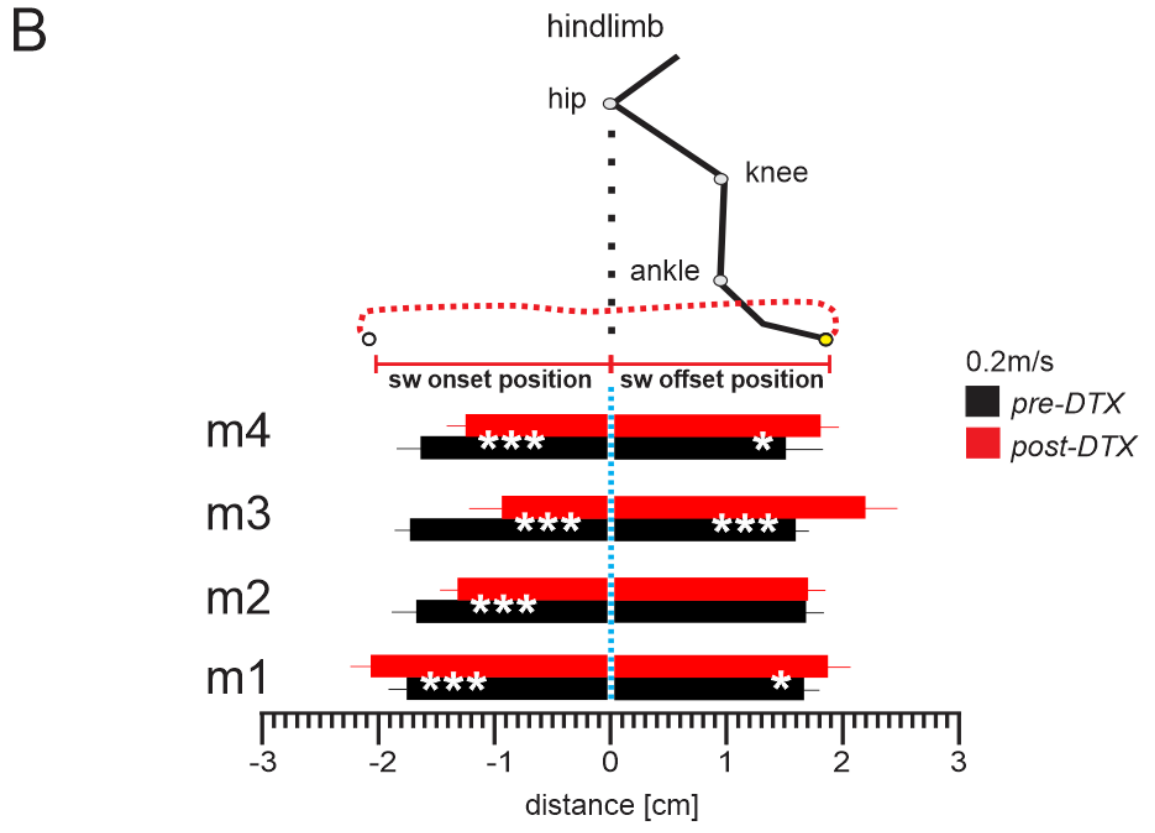
B
hindlimb
hip
knee
ankle
sw onset position
sw offset position
0.2m/s
pre-DTX
post-DTX
m4
m3
m2
m1
***
*
-3
-2
-1
0
1
2
3
distance [cm]

Table 2. 5 Motion parameters through the step cycle of hip-infected experiments. The mean motion (average joint position during walking) and range of motion (amount of joint excursion from its maximum flexed position to its maximum extended position) of pre-DTX and post-DTX infected *Pv::cre* mice are shown (Mean values and standard deviations of ~10 cycles pre- and post-DTX recordings of four *Pv::cre* mice).

		Mean Motion			Range of Motion		
	Joint	***pre-DTX***	***post-DTX***	outcome %	***pre-DTX***	***post-DTX***	outcome %
Hip Infected	Hip	71.4˚ (±11.6)	52.1˚ (±10.7)	27 flx	28.7˚ (±0.6)	22.4˚ (±4.2)	- 22
	Knee	66.2˚ (±9.9)	61.7˚ (±8.6)	6 flx	25.1˚ (±7.7)	26.9˚ (±6.2)	+ 6.9
	Ankle	86.6˚ (±7.8)	89.7˚ (±9.9)	3.5 ext	62.4˚ (±9.5)	56.3˚ (±11.9)	- 10.2

Despite the changes in hip joint angles and the anterior shifting of the foot position after removal of spindle feedback from the hip joint, the temporal characteristics of the stepping were not changed. Parameters such as step cycle, swing duration, and stance duration showed no changes after the DTX injections at any speed (Figure 2.11Ai). We reasoned that since muscle spindle feedback plays a more crucial role during the swimming (Akay et al., 2014), we decided to investigate temporal parameters for the swimming cycle as well as the flexor and extensor phases. Our results indicate that the ablation of muscle spindles only from one hip joint was not enough to generate changes in the temporal characteristics of the limb movements during swimming (Figure 2.11Aii).

To further investigate locomotor pattern generation following the ablation of hip joint muscle spindles, we examined the EMG activity patterns before and after removing hip joint muscle spindles by aligning muscle activity bursts to phases of the step or swim cycles. Muscle onset (closed circles Figure 2.11B) and offset (open circles Figure 2.11B) were studied according to the swing-onset time (vertical dashed line Figure 2.11Bi for walking)

and the Iliopsoas onset (vertical dashed line Figure 2.11Bii for swimming) serving as reference. Our results showed that all flexor muscles recorded here (Ip, St, TA) had its onset before the beginning of the swing phase, and the DTX administration has not influenced the pattern of activation of these muscles during walking (Ip-onset $P = 0.878$, St-onset $P = 0.437$, TA-onset $P = 0.381$) (Figure 2.11Bi). The activation of extensor muscles (BF, VL, Gs) occurred towards the end of swing phase, and no changes in their pattern were observed after limiting the feedback from muscle spindles of the hip joint with DTX administration (BF-onset $P = 0.154$, VL-onset $P = 0.681$, Gs-onset $P = 0.347$). Similarly, no changes in offset timings relative to the step cycle could be detected after DTX injection in flexor muscles (Ip-offset $P = 0.331$, St-offset $P = 0.509$, TA-offset $P = 0.474$) or in the extensor muscles (BF-offset $P = 0.067$, VL-offset $P = 0.659$, Gs-offset $P = 0.545$). Finally, the activation pattern remained the same during the swimming task in flexor muscles onset (St-onset $P = 0.210$, TA-onset $P = 0.073$), flexors offset (Ip-offset $P = 0.676$, St-offset $P = 0.498$, TA-offset $P = 0.120$) extensor onset (BF-onset $P = 0.360$, VL-onset $P = 0.979$, Gs-onset $P = 0.292$) or extensor offset (BF-offset $P = 0.336$, VL-offset $P = 0.903$, Gs-offset $P = 0.561$) (Figure 2.11Bii). Our data suggest that muscle spindle feedback from the unilateral hip joint muscles has no effect on the timing of the locomotor pattern during walking and swimming. It may, nonetheless, be important for selectively maintaining hip joint angular movement during walking.

Figure 2. 11 Temporal parameters of locomotion and muscle activity pattern after attenuating hip joint muscle spindle feedback. **Ai**: duration of step cycle, swing phase and stance phase were not susceptible to changes after DTX muscle spindle attenuation (N = 4 *Pv::cre* mice, average from ~10 step cycles from each animal pre- and post-DTX in all given speeds). **Aii**: swimming cycle period and extensor phase showed slightly lower values although without statistical significance (N = 4 *Pv::cre* mice, average from ~10 swimming cycles from each animal pre- and post-DTX). **Bi**: treadmill locomotion at 0.2 m/s. The swing onset time is represented by the dashed vertical line, pre-DTX recordings are shown in black, and post-DTX recordings are shown in red. Closed circles represent muscle onset and open circles represent muscle offset. Note that onset and offset timing were similar after ablating muscle spindles. **Bii**: swimming behavior. There were no detectable changes using a paired *t*-test (N = 4 *Pv::cre* mice, average from ~10 step and swimming cycles from each animal pre- and post-DTX).

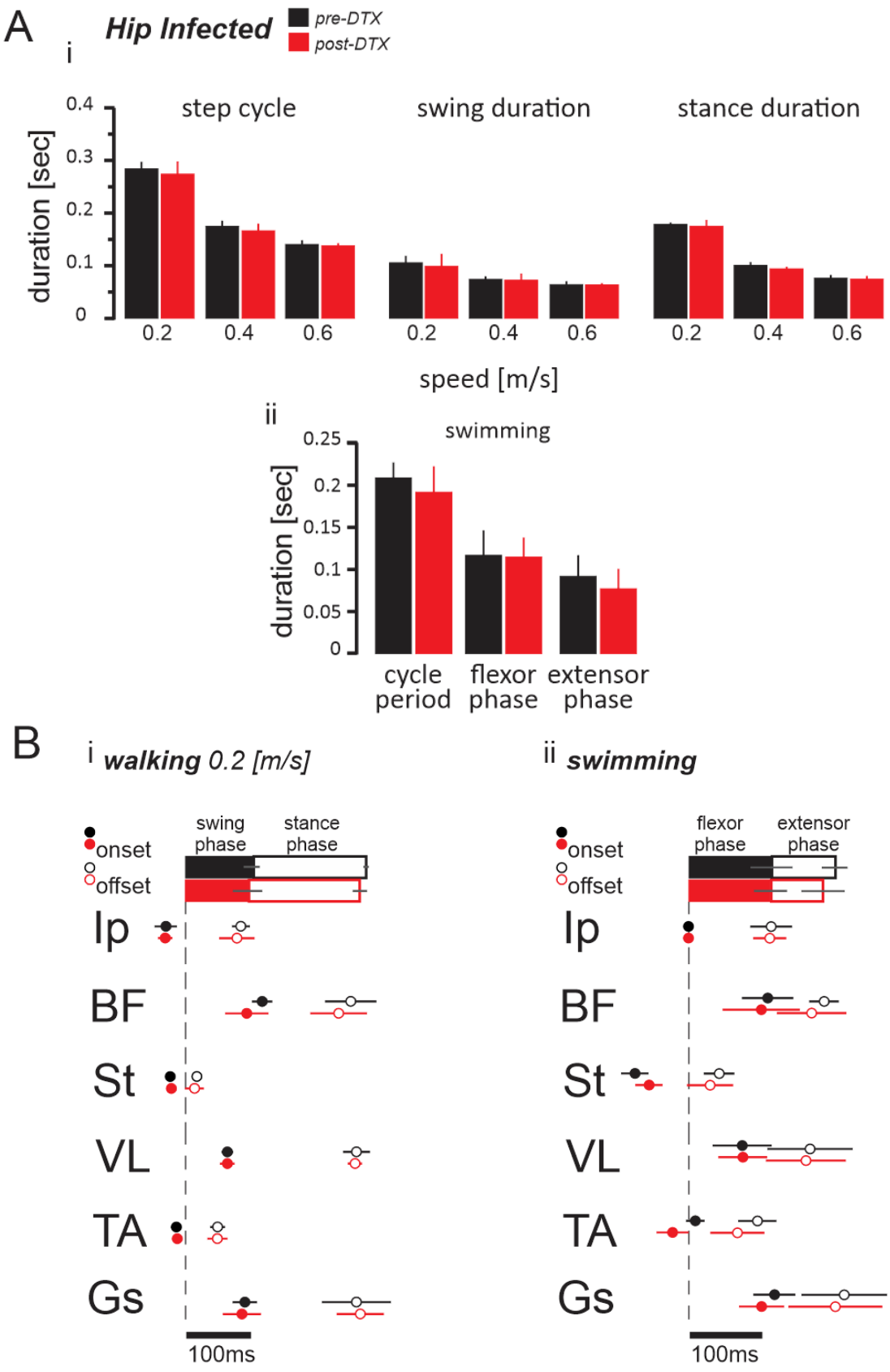
A
i
Hip Infected
pre-DTX
post-DTX
step cycle
swing duration
stance duration
duration [sec]
0.4
0.3
0.2
0.1
0
0.2
0.4
0.6
speed [m/s]
ii
swimming
0.25
0.2
0.15
0.1
0.05
cycle period
flexor phase
extensor phase
B
i walking 0.2 [m/s]
ii swimming
swing phase
stance phase
flexor phase
extensor phase
onset
offset
Ip
BF
St
VL
TA
Gs
100ms

2.3.6 Reducing Muscle Spindle Feedback from Knee Muscles

We next investigated the role of muscle spindle feedback selectively from the flexor and extensor muscles moving the knee joint. The AAV9 infections were performed in the quadriceps muscle (knee extensors) and hamstrings (knee flexors). Attenuation of the knee muscle spindles evoked by the DTX injections increased the average knee angle but not proximal (hip) and distal (ankle) joints (Figure 2.12Ai). During the step cycle, animals adopted a 12.3% more extended knee angle ($P < 0.05$) compared to their baseline (pre-DTX) recordings (Table 2.6), and this extended outcome was achieved in all four mice (Figure 2.12Aii). Although a slight increase of the mean motion was detected in the knee joint after DTX injections, we observed that the mean motion was mostly performed within the center of 95% confidence interval (thick lines and pink shaded area knee joint, Figure 2.12Ai).

Table 2. 6 Motion parameters through the step cycle of knee infected experiments. The mean motion (average joint position during walking) and range of motion (amount of joint excursion from its maximum flexed position to its maximum extended position) are shown in pre-DTX and post-DTX infection of *Pv::cre* mice (mean values and standard deviations of ~10 cycles pre- and post-DTX recordings of four *Pv::cre* mice).

		Mean Motion			**Range of Motion**		
	Joint	***pre-DTX***	***post-DTX***	outcome %	***pre-DTX***	***post-DTX***	outcome %
Knee Infected	Hip	55.2˚ (±7.3)	57.1˚ (±13.5)	3.4 ext	24.7˚ (±3.5)	23.9˚ (±3.1)	- 3.1
	Knee	47.3˚ (±9.2)	53.1˚ (±9.3)	12.3 ext	23.2˚ (±2.6)	23.6˚ (±2.2)	+ 1.7
	Ankle	79.0˚ (±5.1)	80.5˚ (±9.4)	1.8 ext	56.7˚ (±9.8)	56.8˚ (±14.3)	+ 0.2

No remarkable changes were observed in the hip (3.4% more extended post-DTX, $P = 0.662$) and ankle (1.8% more extended, $P = 0.727$) joints regarding mean motion. The 95%

confidence interval shows the overlapping performance of the hip and ankle joints as well (pink shaded area Figure 2.12Ai). The range of motion (ROM) in post-DTX recordings decreased only 3.1% (P = 0.714) in the hip, increased 1.7% (P = 0.860) in the knee and increased 0.2% (P = 0.985) in the ankle after attenuation of muscle spindles in the knee joint (Table 2.6). Individual scores for each animal are represented in Figure 2.12Aii. The slightly extended knee during walking induced different leg positioning at the end of the swing phase. The point where the foot touched the ground at the swing offset became more distant from the hip joint after the DTX injections in 3 out of 4 animals (Figure 2.12B). This suggest that muscle spindle feedback from the knee may change the positioning of the limb during locomotion despite no changes in angular joint movements could be detected.

Figure 2. 12 Joint kinematics and paw position parameters after attenuating the muscle spindles from the knee flexor and extensor muscles. **Ai**: kinematics of the hip, knee and ankle joints pre-DTX (black traces) and post-DTX (red traces) injections (N = 4 *Pv::cre* mice, average from ~10 step cycles from each animal pre- and post-DTX in all given speeds). Bold lines represent average motion and thin lines represent the 95% confidence interval. The pink shadowed area represents the overlapping motion within the confidence interval pre- and post-DTX recordings. **Aii**: mean motion and range of motion (R.O.M.) scores of individual animals. None of these were statistically different after *t*-test for paired data. **B**: hindlimb position at the beginning (sw-onset position) and end (sw-offset position) of the swing phase. Three out of the four mice placed their paws further from the hip after the knee infection when compared with basal recordings. Two-tailed paired *t*-test $*P < 0.05$, $**P < 0.01$, $***P < 0.001$).

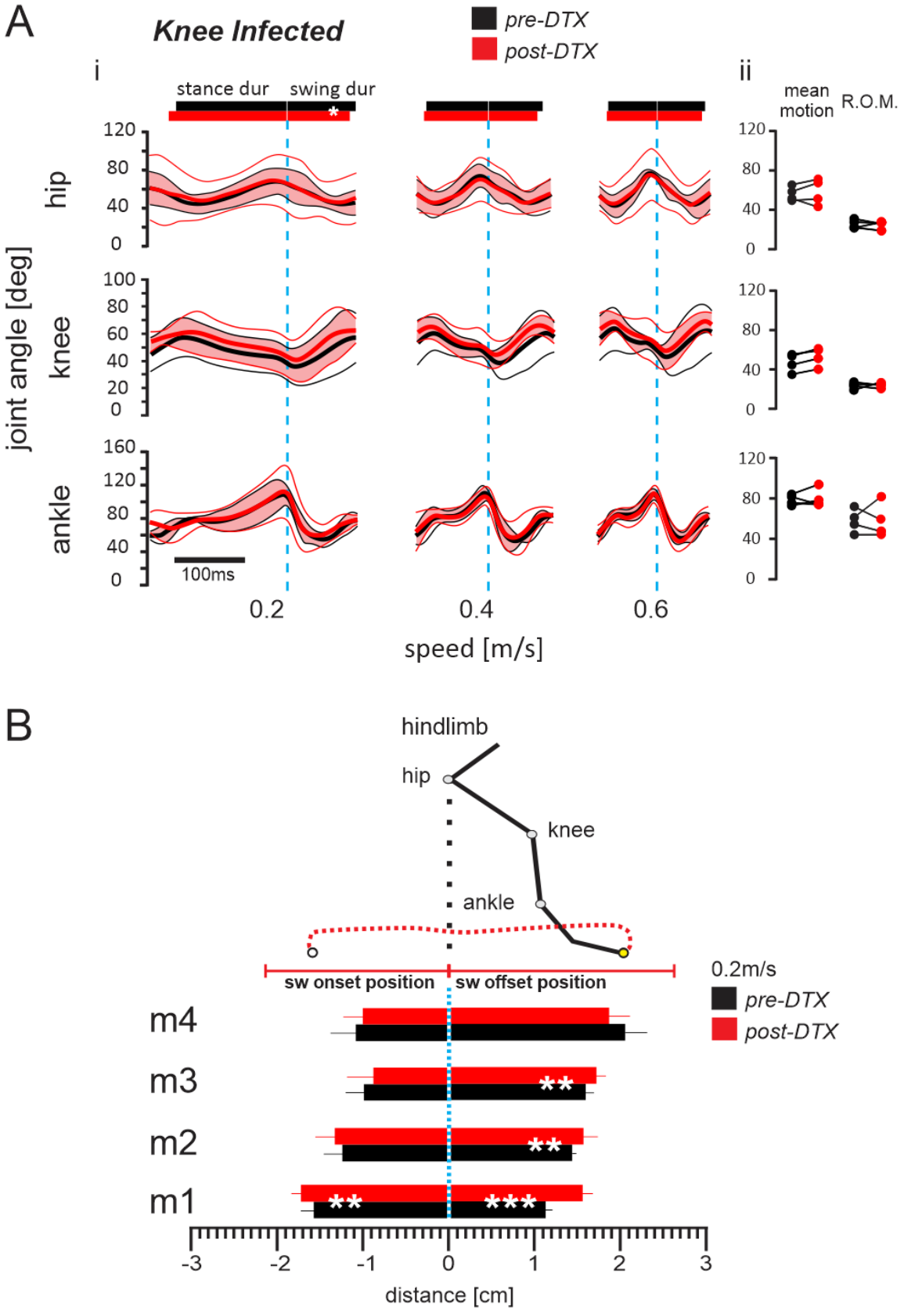
A
Knee Infected
pre-DTX
post-DTX
i
ii
stance dur
swing dur
mean motion
R.O.M.
joint angle [deg]
hip
knee
ankle
100ms
0.2
0.4
0.6
speed [m/s]
B
hindlimb
hip
knee
ankle
sw onset position
sw offset position
0.2m/s
pre-DTX
post-DTX
m4
m3
m2
m1
distance [cm]

Next, we investigated the temporal characteristics of locomotion. We found that the swing duration was shorter after the DTX injections, but only during walking at 0.2 m/s (pre-DTX= 0.10sec ±0.01, post-DTX= 0.09 ± 0.01; $P < 0.05$) (Figure 2.13Ai). No changes were detected in the temporal properties during swimming (Figure 2.13Aii).

To further investigate the effect of attenuating knee joint muscle spindles, we examined the EMG activity patterns before and after attenuation and aligned muscle activity to phases of the stepping or swimming cycles. The onset (closed circles Figure 2.13B) and offset (open circles Figure 2.13B) of the muscles were examined relative to the swing-onset time (vertical dashed line Figure 2.13Bi for walking) and the Ip onset (vertical dashed line Figure 2.13Bii for swimming) as a reference. Our results showed that all flexor muscles recorded here (Ip, St, TA) had its onset before the beginning of the swing phase, and the DTX administration has not influenced the pattern of activation of these muscles during walking (Ip-onset $P = 0.832$, St-onset $P = 0.263$, TA-onset $P = 0.867$) (Figure 2.13Bi). The activation of extensor muscles (BF, VL, Gs) occurred towards the end of the swing phase, and no changes in their pattern were observed after limiting the feedback from muscle spindles of the knee joint (BF-onset $P = 0.620$, VL-onset $P = 0.180$, Gs-onset $P = 0.222$) (Figure 2.13Bi). Similarly, no changes in offset timings relative to the step cycle could be detected in flexor muscles (Ip-offset $P = 0.068$, St-offset $P = 0.160$, TA-offset $P = 0.072$) or in extensor muscles (BF-offset $P = 0.411$, VL-offset $P = 0.946$, Gs-offset $P = 0.636$) (Figure 2.13Bi) after DTX injection. Finally, the activation pattern remained the same during the swimming task in flexor muscles onset, except for st-onset (St-onset $P < 0.05$, TA-onset $P = 0.257$), flexors offset (Ip-offset $P = 0.552$, St-offset $P = 0.079$, TA-offset $P = 0.148$) extensor onset (BF-onset $P = 0.107$, VL-onset $P = 0.242$, Gs-onset $P = 0.206$) or

extensor offset (BF-offset $P = 0.872$, VL-offset $P = 0.282$, Gs-offset $P = 0.653$) (Figure 2.13Bii).

Figure 2. 13 Temporal parameters of locomotion and muscle patterns after attenuating knee flexor and extensor muscle spindle feedback. **Ai**: The duration of the swing phase was shorter during 0.2 m/s treadmill walking after DTX spindle afferent removal (N = 4 *Pv::cre* mice, average from ~10 step cycles from each animal pre- and post-DTX in all given speeds). **Aii**: The swimming cycle period and muscle phases were similar after DTX infection (N = 4 *Pv::cre* mice, average from ~10 swimming cycles from each animal pre- and post-DTX). **Bi**: treadmill locomotion at 0.2 m/s. The sw-onset time is represented by the dashed vertical line, pre-DTX recordings are shown in black, and post-DTX recordings are shown in red. Closed circles denote muscle onset and open circles denote muscle offset. Note that the onset and offset timings were similar after attenuating the knee muscle spindles. **Bii**: recordings during swimming behavior showing detectable changes in st onset, paired *t*-test (N = 4 *Pv::cre* mice, average from ~10 step and swimming cycles from each animal pre- and post-DTX).

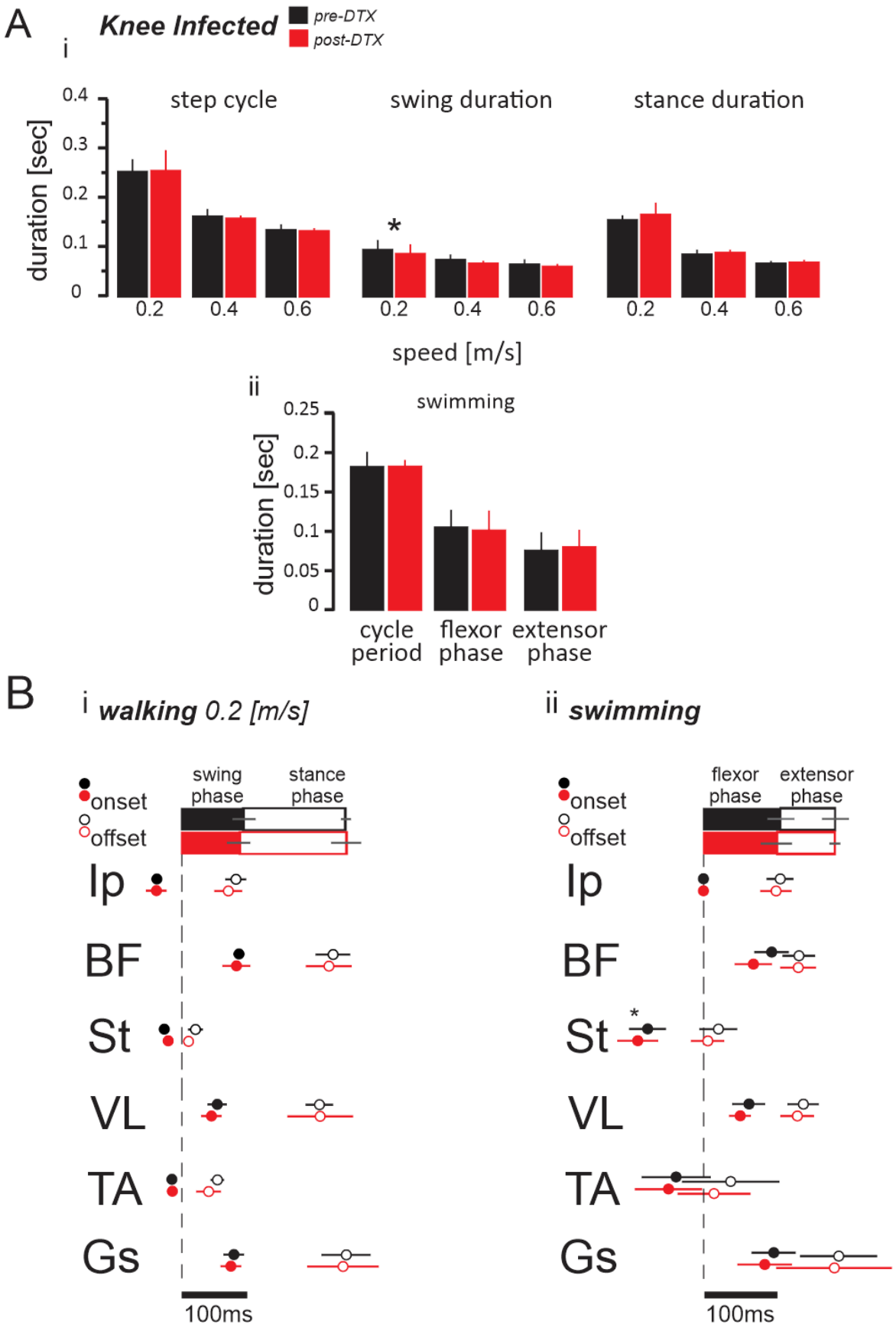
A
Knee Infected
pre-DTX
post-DTX
i
step cycle
swing duration
stance duration
duration [sec]
0.4
0.3
0.2
0.1
0
*
0.2
0.4
0.6
speed [m/s]
ii
swimming
0.25
0.15
0.05
cycle period
flexor phase
extensor phase
B
i walking 0.2 [m/s]
ii swimming
swing phase
stance phase
flexor phase
extensor phase
onset
offset
Ip
BF
St
VL
TA
Gs
100ms

Comparing the muscle activity pattern during walking and swimming revealed that muscle activation patterns were not drastically affected by the removal of muscle spindle feedback from the knee joint. These data suggest that muscle spindle feedback from the knee joint does not influence the temporal characteristics of the locomotor pattern during walking and only the st-onset timing during swimming. The data presented in this section suggest that muscle spindle feedback from the knee joint may control kinematic parameters of the knee, however without broader effects on hip and ankle joints. The attenuation of muscle spindle feedback from the knee joint does not influence severely the temporal parameters and muscular patterns of locomotion in walking or swimming.

2.3.7 Reducing Muscle Spindle Feedback from Ankle Muscles

Lastly, we investigated the effect of selectively removing muscle spindle feedback from a distal hindlimb joint, the ankle joint. The AAV9 was injected into the triceps surae muscle and the tibialis anterior. Similar to above, none of the four recorded *Pv::cre* mice had any struggle swimming or walking on the treadmill at speeds up to 0.6 m/s after DTX injection.

Average kinematic traces of the hindlimb joints revealed that ankle and hip joints became more flexed during 0.2 m/s walking after DTX injections in most of the animals and those changes diminished at higher speeds (Figure 2.14Ai). However, no statistical significance could be detected by paired *t*-test in any of the parameters. Pre- and post-DTX mean motion of the joints were performed within the overlapping range of 95% confidence interval (pink shadow Figure 2.14Ai). A persistent overlap of motion of the knee joint was recorded at all speeds. The hip and ankle joint mean motion tend not to overlap at 0.2 m/s (Table 2.7),

although this performance was achieved within overlapping range of 95% confidence interval. During the step cycle, animals have adopted a 13.1% more flexed motion in the hip joint, although not statistically significant ($P = 0.186$) compared to their baseline (pre-DTX) recordings (Table 2.7), and this flexed outcome was observed in 3 out of 4 mice (Figure 2.14Aii). Minor values were observed in the knee joint (1.1% more flexed $P = 0.871$) post-DTX and slightly higher values were achieved in the ankle joint (9.8% more flexed, $P = 0.403$) post-DTX. The range of motion (R.O.M.) in post-DTX recordings decreased 18.7% ($P = 0.143$) in the hip, reduced 14.2% ($P = 0.358$) in knee and diminished 21.6% ($P = 0.142$) in ankle after attenuation of muscle spindles in the ankle joint. Individual scores for average motion are illustrated in Figure 2.14Aii, and it shows that three out of four animals had adopted similar joint performance. The changes in the joint movements before and after DTX injection are illustrated in Table 2.7. These data suggest that muscle spindle feedback from the ankle joint may have widespread effects on the movement of all three joints, however none of these changes could be statistically verified.

Table 2. 7 Motion parameters during the step cycle of ankle infected experiments. The mean motion (average joint position during walking) and range of motion (amount of joint excursion from its maximum flexed position to its maximum extended position) are shown for pre-DTX and post-DTX recordings of *Pv::cre* mice (mean values and standard deviations of ~10 cycles pre- and post-DTX recordings of four *Pv::cre* mice).

		Mean Motion			Range of Motion		
	Joint	***pre-DTX***	***post-DTX***	outcome %	***pre-DTX***	***post-DTX***	outcome %
Ankle Infected	Hip	84.8˚ (±11.6)	73.6˚ (±7.8)	13.1 flx	34.8˚ (±6.0)	28.3˚ (±5.8)	- 18.7
	Knee	57.9˚ (±8.0)	57.2˚ (±4.7)	1.1 flx	22.2˚ (±6.9)	19.1˚ (±1.2)	- 14.2
	Ankle	82.1˚ (±16.3)	74.0˚ (±6.7)	9.8 flx	63.3˚ (±8.0)	49.6˚ (±5.9)	- 21.6

The flexed behavior on hip and ankle joints post-DTX administration, as shown in Table 2.7 and Figure 2.14A, was accompanied by an anterior shift of the foot position at the onset of the swing phase in 3 out of 4 mice (Figure 2.14B). These data suggest that muscle spindle feedback from the ankle may change the positioning of the limb during locomotion and slightly affects the movement of hip and ankle joints while walking at slower speeds.

Figure 2. 14 Joint kinematics and paw positioning parameters after attenuation of muscle spindle feedback from ankle flexor and extensor muscles. **Ai**: kinematics of hip, knee and ankle joints in pre-DTX (black traces) and post-DTX (red traces) injections (N = 4 *Pv::cre* mice, average from ~10 step cycles from each animal pre- and post-DTX in all given speeds). Bold lines represent average motion and thin lines the 95% confidence interval. The pink shadowed area represents the overlapping motion within the confidence interval pre- and post-DTX recordings. **Aii**: mean motion and range of motion (R.O.M.) scores of individual animals. **B**: hindlimb positioning at the beginning (sw-onset position) and ending (sw-offset position) of the swing phase. After DTX injections, three out of four mice placed their hindlimb closer to the hip joint at the beginning of the swing phase and two animals further at the end of the swing phase after ankle infection. Data compared with basal recordings. Two-tailed pair *t*-test $*P < 0.05$, $**P < 0.01$, $***P < 0.001$).

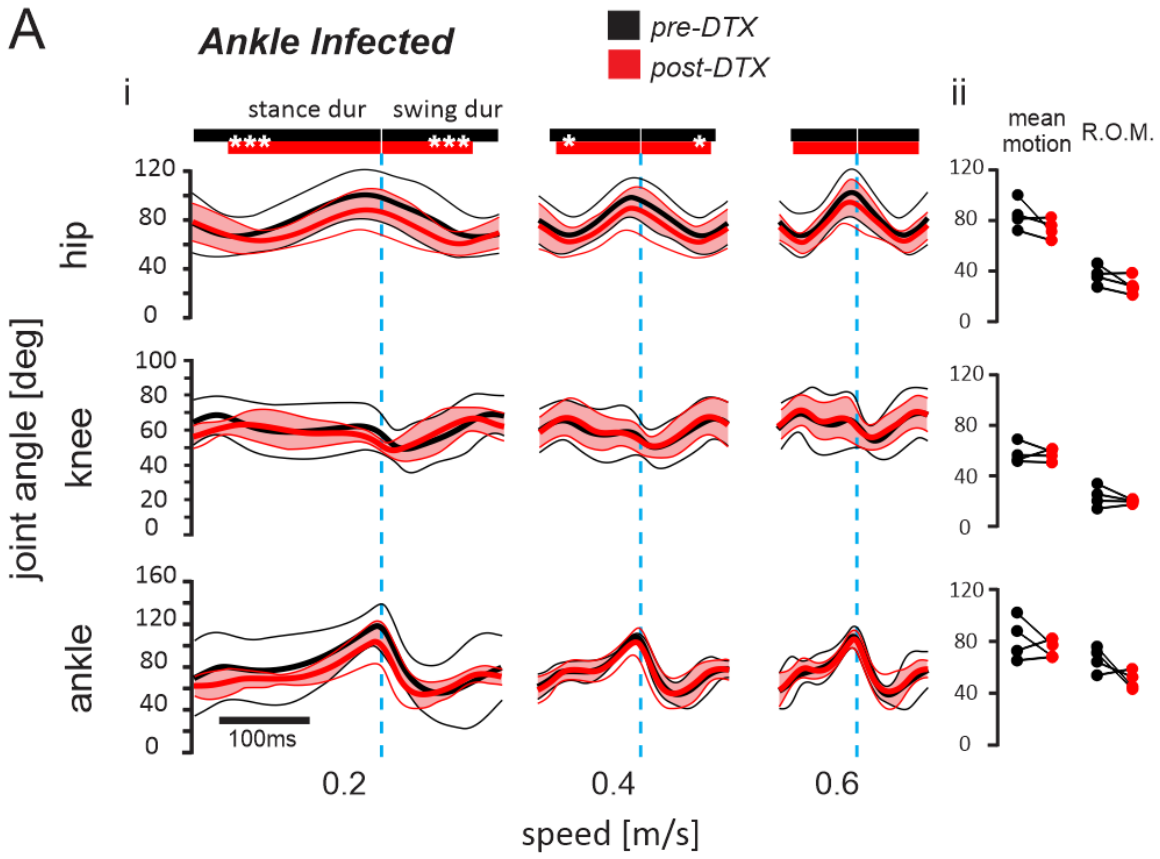
A
Ankle Infected
pre-DTX
post-DTX
i
ii
stance dur
swing dur
mean motion
R.O.M.
hip
knee
ankle
joint angle [deg]
100ms
0.2
0.4
0.6
speed [m/s]

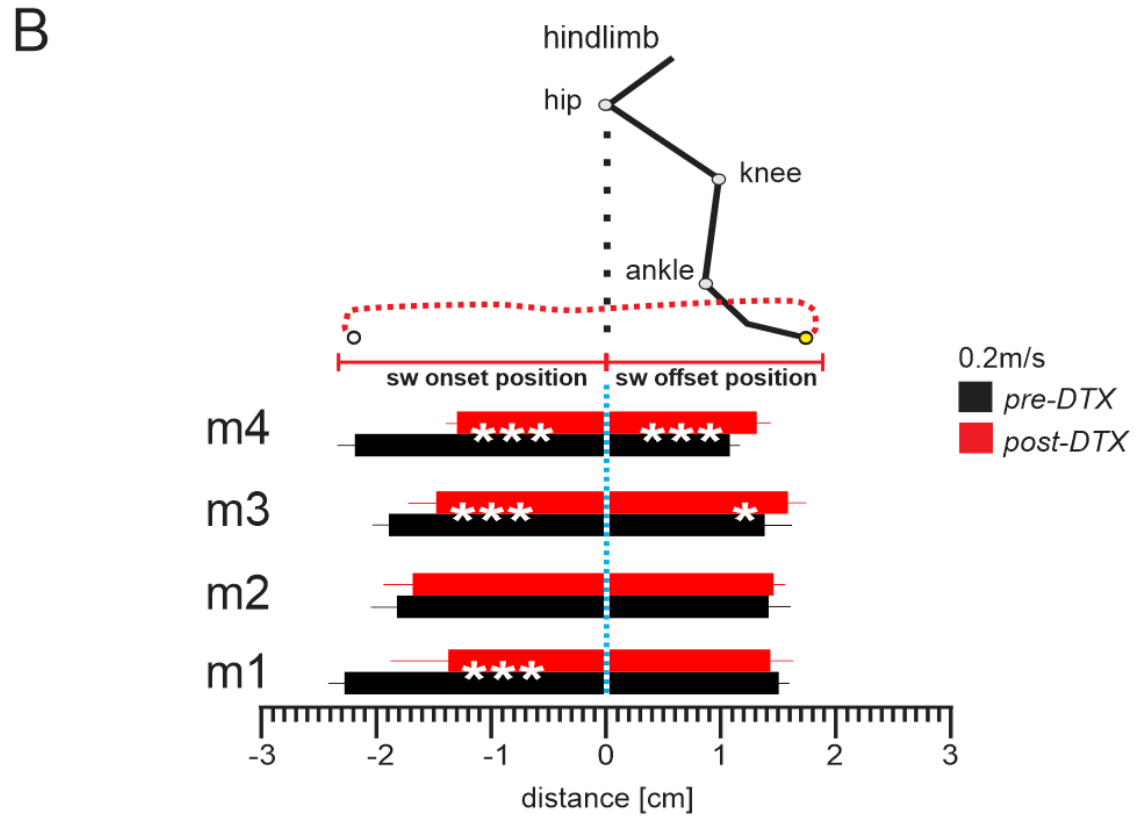
B
hindlimb
hip
knee
ankle
sw onset position
sw offset position
0.2m/s
pre-DTX
post-DTX
m4
m3
m2
m1
distance [cm]

Removal of muscle spindle feedback selectively from ankle joint caused larger changes in temporal characteristics compared when muscle spindle feedback was selectively removed from the hip or knee joints. The step cycle duration differed significantly during walking at 0.2 m/s between pre-DTX (0.328 ± 0.017 sec) and post-DTX (0.263 ± 0.023 sec) ($P < 0.001$); and at 0.4 m/s pre-DTX (0.178 ± 0.008 sec) and post-DTX (0.166 ± 0.011 sec) ($P < 0.001$). Moreover, the swing durations were significantly different in 0.2 and 0.4 m/s ($P < 0.001$ and $P < 0.005$ respectively). The average swing duration pre-DTX was 0.125 ± 0.017 sec and post-DTX 0.098 ± 0.012 sec at 0.2 m/s; and 0.080 ± 0.009 sec pre-DTX and 0.075 ± 0.005 sec post-DTX at 0.4 m/s. Stance duration was also influenced by the manipulation of muscle spindles in the ankle joint at 0.2 and 0.4 m/s treadmill walking, with more severe changes at 0.2 m/s speed. Pre-DTX recordings at 0.2 m/s score an average time of 0.202 ± 0.022 sec as post-DTX timed 0.165 ± 0.013 ($P < 0.001$); while walking at 0.4 m/s the results were pre-DTX 0.098 ± 0.004 sec and post-DTX 0.091 ± 0.006 ($P < 0.05$) (Figure 2.15Ai). However, inconsistent results were observed during the swimming task which had increased the variability and standard deviation, especially in the whole cycle period (pre-DTX= 0.182 ± 0.024s, post-DTX= 0.198 ± 0.032s) and the flexor phase (pre-DTX= 0.091 ± 0.011s, post-DTX= 0.099 ± 0.049s) (Figure 2.15Aii).

Finally, we investigated the changes in the temporal characteristics of the activities of flexor and extensor muscles during walking and swimming (Figure 2.15B). We examined the EMG activity patterns before and after muscle spindle removal from the ankle joint, aligning burst activities to phases of the step cycle or swimming cycle. The onset (closed circles Figure 2.15B) and offset (open circles Figure 2.15B) of the muscles were studied

according to the swing-onset time (vertical dashed line Figure 2.15Bi for walking) and the Iliopsoas onset (vertical dashed line Figure 2.15Bii for swimming) as a reference.

Our results showed that all flexor muscles recorded here (Ip, St, TA) had its onset before the beginning of the swing phase, and the DTX administration has not influenced the pattern of activation of these muscles during walking, except for TA (Ip-onset $P = 0.184$, St-onset $P = 0.308$, TA-onset $P = 0.021$) (Figure 2.15Bi). The activation of extensor muscles (BF, VL, Gs) occurred towards the end of swing phase, and no changes in their pattern were observed after limiting the feedback from muscle spindles of the hip joint BF-onset $P = 0.101$, VL-onset $P = 0.126$, Gs-onset $P = 0.075$) (Figure 2.15Bi). Similarly, no changes in offset timings relative to the step cycle could be detected after DTX injection in flexor muscles (Ip-offset $P = 0.112$, St-offset $P = 0.431$, TA-offset $P = 0.328$), and one of the extensor muscles, the VL, had changed its offset pattern after limiting the feedback from muscle spindles of the ankle joint (BF-offset $P = 0.071$, VL-offset $P < 0.05$, Gs-offset $P = 0.098$) (Figure 2.15Bi). No changes in these parameters in pre-DTX versus post-DTX were detected during walking at 0.6 m/s. Finally, no changes were observed in the activation pattern during the swimming task in flexor muscles onset (St-onset $P = 0.142$, TA-onset $P = 0.544$), flexors offset (Ip-offset $P = 0.773$, St-offset $P = 0.151$, TA-offset $P = 0.460$) extensor onset (BF-onset $P = 0.998$, VL-onset $P = 0.361$, Gs-onset $P = 0.934$) or extensor offset (BF-offset $P = 0.631$, VL-offset $P = 0.863$, Gs-offset $P = 0.771$) (Figure 2.15Bii). We could detect minor changes in the muscle activation pattern before and after the injection of DTX to remove muscle spindle feedback from the ankle joint. These data suggest that muscle spindle feedback from the ankle joint gently influence the timing of onset and offsets of muscle activities during walking but not while swimming.

Figure 2. 15 Locomotion temporal parameters and muscule pattern after attenuation of muscle spindle feedback from ankle flexor and extensor muscles. **Ai**: duration of step cycle, swing phase, and stance phase were shorter at 0.2 and 0.4 m/s treadmill walk after DTX spindle afferents removal (N = 4 *Pv::cre* mice, average from ~10 step cycles from each animal pre- and post-DTX in all given speeds). **Aii**: swimming cycle period, flexor and extensor phase recorded similar values after DTX infection, although exhibited higher variability (N = 4 *Pv::cre* mice, average from ~10 swimming cycles from each animal pre- and post-DTX). **Bi**: treadmill locomotion at 0.2 m/s, the sw-onset time is represented by the dashed vertical line, pre-DTX recordings in black and post-DTX recordings in red, closed circles = muscle onset activation and open circles = muscular offset activation. Note that most of the onset and offset timing were shorter after the spindle afferent removal as a consequence of shorter cycle periods, however, the muscles maintained its proportional temporal pattern within the step cycle. **Bii**: recordings during swimming behavior, no detectable changes with paired *t*-test were seen (N = 4 *Pv::cre* mice, average from ~10 step and swimming cycles from each animal pre- and post-DTX).

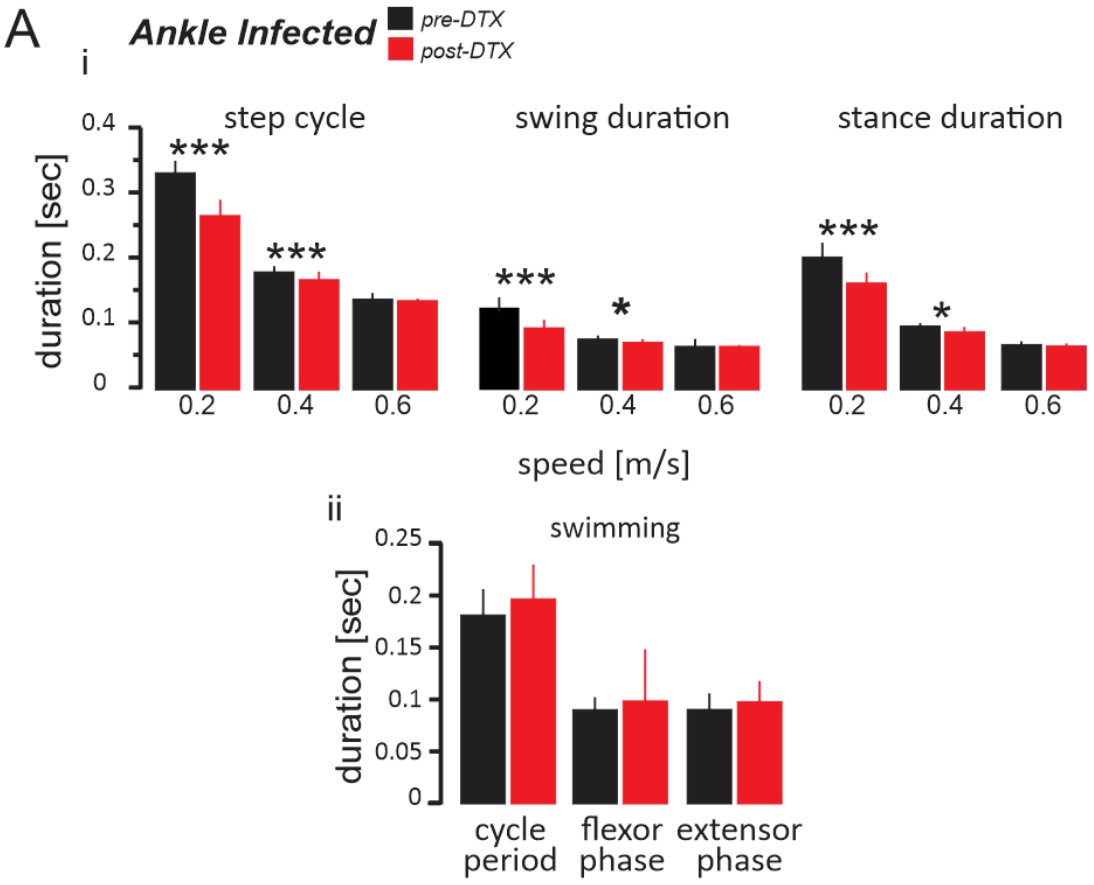
A
Ankle Infected
pre-DTX
post-DTX
i
step cycle
swing duration
stance duration
duration [sec]
0.4
0.3
0.2
0.1
0
***
***
***
*
***
*
0.2
0.4
0.6
0.2
0.4
0.6
0.2
0.4
0.6
speed [m/s]
ii
swimming
duration [sec]
0.25
0.2
0.15
0.1
0.05
0
cycle period
flexor phase
extensor phase

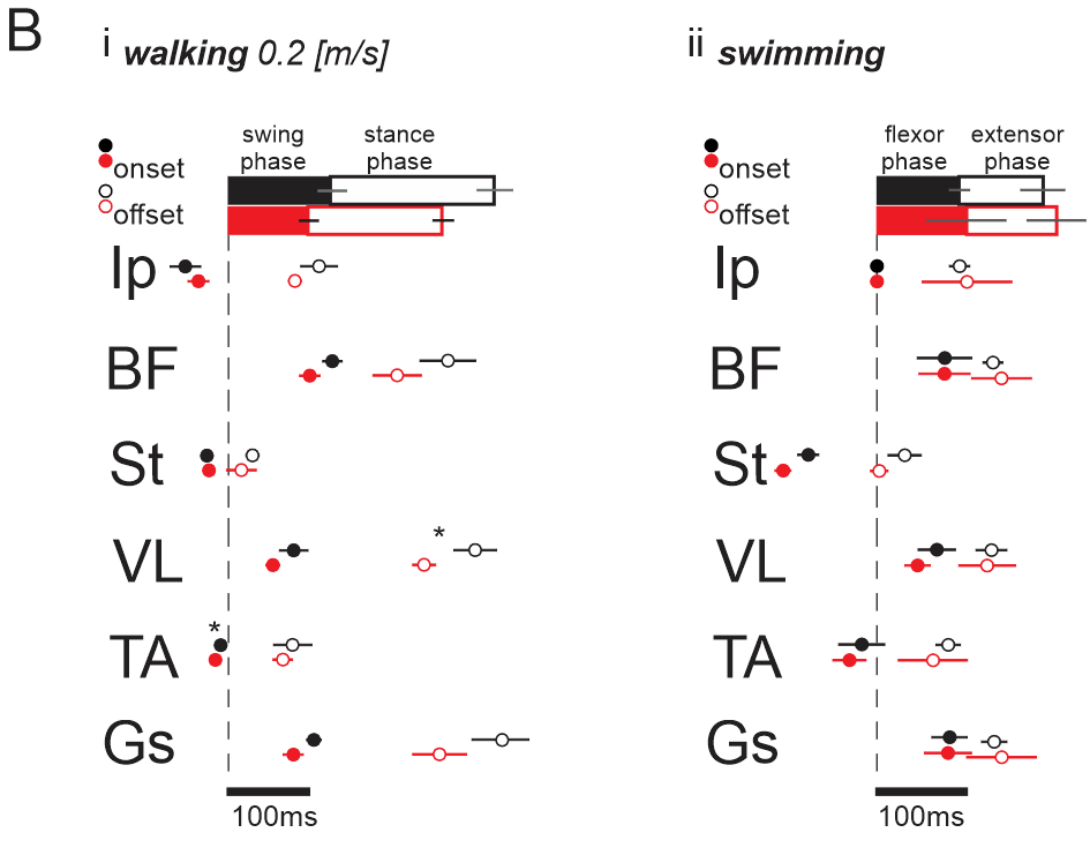
B
i walking 0.2 [m/s]
ii swimming
swing phase
stance phase
onset
offset
Ip
BF
St
VL
TA
Gs
*
*
100ms
flexor phase
extensor phase
onset
offset
Ip
BF
St
VL
TA
Gs
100ms

The overall results presented in this chapter demonstrated that functional walking or swimming requires proprioceptive feedback (section 2.3.1 and 2.3.2). Furthermore, combining gene delivery with AAV9 and *Pv::cre* mice allowed us to investigate the role of muscle spindle feedback selectively from single joints of the hindlimb (section 2.3.4). Our findings suggest that, in contrast to muscle spindle feedback from the hip (section 2.3.4.1) and knee (section 2.3.4.2) joints, muscle spindle feedback from the ankle joint (section 2.3.4.3) affects the timing parameters of limb movement during walking but not during swimming.

2.4 Discussion

The primary goal of this chapter was to provide a framework to understand the role of proprioceptive feedback from muscle spindles and Golgi tendon organs over different aspects of locomotion in freely behaving mice. Our results suggest that the temporal and spatial parameters of coordinated movements such as in walking or swimming require proprioceptive sensory input.

2.4.1 Dysfunctional Locomotor Pattern without Proprioceptive Feedback

We have shown that proprioceptive sensory feedback is necessary for the generation of functional locomotor patterns. When proprioceptive feedback from group Ia/II and group Ib afferents from muscle spindles and GTOs, respectively, were killed in *Pv:Cre*;*Isl2:DTA* (*Pkill*) mice, we observed severe flaws in walking and swimming behavior. During these

tasks, EMG recordings from flexor and extensor muscles controlling hip, knee, and ankle joints revealed a synchronous rather than an alternated pattern of activation. The reason for this observation and dysfunction in *Pkill* mice is that the group Ia/II sensory feedback from muscle spindles have a dominance patterning the motor output of flexor muscles (Akay et al., 2014; Hiebert et al., 1996), whereas is likely the group Ib afferents from GTOs determine the pattern of activation on the extensor muscles (Akay et al., 2014; Hiebert & Pearson, 1999; Pearson, 2004). Moreover, the lack of proprioceptive feedback during the embryonic development may cause disorganization of premotor interneurons that control the activity of flexor and extensor muscles in *Pkill* animals (Tripodi et al., 2011), and the consequence of this structural disarrangement may result in general activation of flexor end extensor motoneurons mingled within the same pool. Therefore, it was important to do experiments with a mouse line with milder changes of the nervous system, such as in the *Egr3*$^{-/-}$ mice. Nevertheless, our data support the findings that proprioceptive feedback is required for well-coordinated functional locomotion.

2.4.2 Influence of Group Ia/II on Different Locomotor Programs

The *Egr3*$^{-/-}$ mice provided us with an opportunity to assess the impact of selective loss of group Ia/II afferents (Chen et al., 2002; Tourtellotte & Milbrandt, 1998). The group Ib feedback from the GTOs that inform the CNS with changes related to muscular tension are intact. However, the engagement of *Egr3*$^{-/-}$ mice in swimming diminishes the phasic component of group Ib feedback due to the lack of gravitational influence on water. The outcome of this condition was an EMG activity pattern qualitatively comparable to that observed in *Pkill* mice during walking. Interestingly, the *Egr3*$^{-/-}$ swimming behavior was

pronounced by onset and offset of flexor muscles occurring almost simultaneously, while the extensor muscle activation occurred more in a sequential fashion, tending to start with the hip extensor and propagating towards the ankle extensor. The explanation for this might be that the patterning of flexor activity is partially controlled by group Ib feedback generated by the unloading of the GTOs at the end of stance phase (Whelan et al., 1995), therefore attenuating group Ib influence due to water buoyancy, and without having feedback from muscle spindles, has changed the typical flexor muscle activation pattern to a staggered pattern of activation during swimming.

During walking, the flexor muscles are mostly activated during the swing phase, while extensor muscles are typically active during stance phase. However, our recordings have shown that onset and offset activity is way more complex than that simple interpretation. The precise timing relationship of flexor muscle activities around the swing phase, but not of the extensor muscles, was altered in the absence of feedback from muscle spindles. The temporal parameters of the step cycle such as swing duration changed when proprioceptive feedback from muscle spindles was absent, while stance duration remained the same. This is in accordance with previous findings that the stance phase is stronger controlled by the group Ib feedback from the GTO (Donelan & Pearson, 2004a; Donelan & Pearson, 2004b; Duysens & Pearson, 1980; Pearson, 2008) during walking. Our data corresponds with previous findings suggesting that the stance phase is likely controlled by feedback from muscle spindles and the GTOs, whereas the swing phase is mostly controlled by the muscle spindle feedback.

2.4.3 Single Joint Group Ia/II Feedback and Fluency of Locomotion

We demonstrated that fluent and functional locomotor pattern requires proprioceptive feedback from muscle spindles and GTOs. However, it is unknown whether proprioceptive feedback from specific joints play more important roles than the other joints in pattern generation. We acutely eliminated group Ia/II feedback only from a subset of muscles within the hip, knee or ankle joints using a new methodology developed in collaboration with Dr. Andrew Murray (Mayer et al., 2018) to understand how feedback from a specific joint or group of muscles modulate motor output. Although the results do not represent complete ablation of muscle spindle proprioceptive feedback, since there are slight variations in viral infectivity ranging from 55% to 73%, we at least, successfully attenuated the feedback input towards the CNS.

Our data indicated that manipulating the proprioceptive feedback from muscle spindle of a single joint in the hindlimb is not enough to induce major changes in the locomotor pattern. This could be due to several reasons: first, the CPG circuitry might compensate for the sudden loss of muscle spindle feedback in a single joint. Second, the loss of sensory information from one joint might be compensated by sensory feedback from other joints of the same limb or joints of other appendages. It is documented in spinalized cats that Ia afferents feedback from the hindlimb provide excitatory inputs to motoneurons of muscles responsible to move the same joint (Eccles, Eccles, & Lundberg, 1957), but Ia impulses also provide excitation to motoneurons of muscles moving different joints (Eccles & Lundberg, 1958). Third, possibly the partial attenuation of feedback from muscle spindles may not have been enough to generate a detectable effect. Our current data do not allow

the differentiation between these three possibilities and therefore requires further investigation.

An interesting result of our study was that the localized ablation of group Ia/II feedback tends to cause changes in the angular movement of the same joints. Specifically, removal of group Ia/II feedback from the hip or knee joints evoked minor kinematic variations in the same joint that led to changes in the foot positioning at the swing onset and offset. The exception was the ankle joint, which appeared to have a more wide-spread effect, although the results were statistically inconsistent. Removal of muscle spindle feedback from the ankle joint, caused changes in the swing and stance durations, and the cycle period during walking at different speeds, partially similar to the results observed in *Egr3*$^{-/-}$ mice. That is, the swing durations significantly decreased following muscle spindle removal from the ankle joint with a significant decrease in the stance duration leading to a significant decrease in the cycle period. Interestingly, removing the muscle spindle afferents from the hip or knee joint resulted in much milder effects on swing duration and the cycle period and no effect on the stance duration. These results suggest that muscle spindles from the ankle muscles have a more prominent effect on the step duration parameters than the muscle spindles from the hip or knee muscles.

Despite these very interesting observations with clear tendencies, the small number of successful experiments in each group does not allow for definitive conclusion. Increasing the number of animals in each group would be necessary to reach statistically significant results that would lead to a solid conclusion.

CHAPTER 3 MUSCLE SPINDLE FEEDBACK ENSURING PRECISE FOOT PLACEMENT

Mayer, W. P., & Akay, T. (2018). Stumbling corrective reaction elicited by mechanical and electrical stimulation of the saphenous nerve in walking mice. *The Journal of Experimental Biology*, jeb.178095.

https://doi.org/10.1242/jeb.178095

3.1 INTRODUCTION

The typical locomotor behavior of terrestrial mammals is achieved by rhythmic and coordinated movement of two (bipeds) or four (quadrupeds) limbs with multiple joints (Grillner, 1981). The rhythmic stepping movement of the limbs is divided into stance and swing phases. Throughout the stance phase, the foot is on the ground, carries the body weight and provides propulsion. As the body moves forward, the foot moves backward relative to the body, beginning from an anterior extreme position (AEP) towards the posterior extreme position (PEP) (Cruse, Kindermann, Schumm, Dean, & Schmitz, 1998). Once the foot reaches the PEP at the end of the stance phase, it lifts off the ground and moves forward (swing phase) to reach the AEP to begin the next stance phase.

The transition from stance to swing phase requires extension of the hip joint followed by reduction of weight-bearing in the hindlimb (Grillner and Rossignol 1978, Hiebert et al 1996, and Duysens and Pearson 1980). It has been suggested that muscle spindles in the hip joint and GTOs in calf muscle are the key structures signaling the timing of the

transition from stance to swing phase to the CNS (Grillner and Rossignol 1978; Hiebert et al., 1996; Pearson, 2004). Contrary to the stance to swing transition, proprioceptive control of AEP at the swing to stance transition is not well understood, McVea et al. (2005) found no indication that activating proprioceptors in ankle extensor muscles during the swing phase would influence the regulation of swing to stance transition. However, there is solid evidence that modifying proprioceptive input from hip flexor muscles affects the duration and amplitude of flexor activity (Lam & Pearson, 2001) and that may affect the end of the swing phase. Previous research on stick insect suggests that the swing movement of a posterior leg is guided by the ipsilateral anterior leg (Dean & Wendler, 1983) and this aimed movement is guided by proprioceptive sensory feedback (Cruse, Dean, & Suilmann, 1984). Furthermore, research on human walking suggests that visual information can guide the foot trajectory (Reynolds & Day, 2005). However, visual feedback is not viable in quadrupedal mammals, because their body structure blocks visualization of the hindlimb during walking.

Although the lack of visual feedback, forelimb to hindlimb coordination is easily achieved in quadrupedal locomotion. This organized movement among appendages is also observed when mammals are requested to walk on a horizontal ladder. Rats for example, spontaneously walk from a starting point towards an ending point along the rungs in front of them. Such behavior requires skilled walking that depends on the placement of the foot in a precise location at the rungs in the end of the swing phase (Metz & Whishaw, 2002). Animals showing deficits in limb positioning or coordination, for example, due to nervous system injuries, show difficulties in performing this task (Farr et al., 2006). In addition to injuries, previous research with rats (Vincent et al., 2016) and mice (Akay et al 2014) have

shown that without proprioceptive feedback from the muscle spindles, severe deficits in placing the foot from rung to rung is observed, suggesting that proprioceptive feedback from muscle spindles is important in targeted movements of the limb during walking.

Another relevant aspect to consider regarding locomotion is that the central nervous system has the ability to change the stepping pattern according to the challenges imposed by the environment. For example, an unexpected obstacle intercepting the normal path of the foot during swing movement requires the central nervous system (CNS) to respond with a "stumbling corrective reaction/response" (SCR) (Forssberg, 1979; Forssberg et al., 1975, 1977; Prochazka et al., 1978). Whenever an object collides with the limb during swing phase, cutaneous mechanoreceptors are activated, eliciting a flexor response that moves the foot higher to clear the obstacle (Wand et al., 1980). However, if this same perturbation occurs during a stance phase, no flexor response is triggered but an enhanced extensor activation is observed (Forssberg, 1979; Forssberg et al., 1977). This phenomenon shows an example of reflex reversal: that is when identical stimuli cause opposite effects depending on the context of the stimulation (Duysens, Trippel, Horstmann, & Dietz, 1990; Pearson & Collins, 1993).

Traditionally, insights into the neural control of SCR have been provided by kinematic and electromyographic (EMG) analysis of the step cycle, with a particular focus on the cat hindlimb (Doperalski et al., 2011). By using the cat as an animal model, it has been shown that stimulation of cutaneous afferents is sufficient to elicit SCR (Buford & Smith, 1993; Quevedo, Stecina, Gosgnach, et al., 2005; Wand et al., 1980). There is further evidence that the network controlling the SCR is located within the spinal cord, as SCR can be elicited

in spinalized cats (Forssberg et al., 1977). Electrical stimulation of the superficial peroneal nerve, activating cutaneous afferent fibers that otherwise would signal obstacle touch on the dorsum of the paw, have been shown to elicit a motor response closely resembling the SCR. These experiments have been done during fictive locomotion in the absence of any physical movement, and consequently movement-related (phasic) sensory feedback (Quevedo, Stecina, Gosgnach, et al., 2005). Because of the lack of any physical movement in these experiments, Quevedo et al named these reactions "fictive" SCR. Furthermore, the same authors performed intracellular recordings from different motoneurons during fictive SCR to infer that di-, oligo-, and polysynaptic pathways mediate SCR (Quevedo, Stecina, & McCrea, 2005). In addition, SCR with similar characteristic has been characterized in humans (Schillings et al., 1996). As in the cat, electrical stimulation of the superficial peroneal nerve elicits SCR in a phase-dependent manner in humans (Van Wezel et al., 1997; Zehr et al., 1997). Hence, this whole body of work from experiments on human and cats have provided considerable insights into the neuronal mechanisms that control SCR, but a clear understanding of the spinal interneuronal network that controls SCR still up to debate.

Recently, mice have become a preferred animal-model for studying locomotion due to the possibilities of genetic manipulation of the neural circuits, and capability for measuring its effect on locomotor behavior in either *in vivo* or *in vitro* experiments (Goulding, 2009; Grillner & Jessell, 2009; Kiehn, 2016). By combining genetics and behavioral observations, a recent study identified a group of interneurons, distinguished by selective retinoid-related orphan receptor (ROR) alpha expression that was important for corrective reflex movements during walking on a narrow beam (Bourane et al., 2015). Furthermore, many

more interneurons have been identified based on gene expression patterns that are interconnected between sensory afferents and motoneurons (Alvarez et al., 2005; Bourane et al., 2015; Bui et al., 2013; Hilde et al., 2016; Koch et al., 2017; Zagoraiou et al., 2009; Zhang et al., 2008). Nevertheless, it is not known whether any of the previously identified interneurons are part of the neuronal network underlying the SCR, and how much they contribute in targeting limbs to its final destination after a swing phase. This is mainly because methods to elicit SCR in freely behaving mice have not been available.

In this chapter, we sought to develop a reliable method to trigger SCR in mice that allows experiments in combination with mouse genetics to identify the neuronal circuits underlying the SCR, as well as to understand the mechanisms that the hindlimb employs to achieve foot precision at the end of swing phase in its Anterior Extreme Position - AEP. Thus, this swing to stance transition was investigated under conditions where the proprioceptive feedback from muscle spindles were attenuated or abolished, concomitantly to perturbations or manipulation of the swing phase to gain insights regarding the role of proprioceptive feedback controlling the swing phase and achievement of AEP targeting.

3.2 METHODS

3.2.1 Animals

Experiments were carried out on nine wild type mice of either sex, ages ranging from 74 to 141 days. Four *Egr3* knock-out mice (*Egr3*$^{-/-}$) mice of either sex, ages ranging from 74 to 178 days, and 18 parvalbumin-cre (*Pv::cre*) mice of either sex, ages ranging from 68 to

107 days. None of the mice were trained prior to the experiments. All procedures were in accordance with the Canadian Council on Animal Care and were approved by the University Committee on Laboratory Animals at Dalhousie University.

3.2.2 Removal of Muscle Spindle

We used two methods to remove proprioceptive feedback from the muscle spindles. The first model used the *Egr3*$^{-/}$ where all muscle spindles are ablated (Chen, Tourtellotte & Frank, 2002; Tourtellotte & Milbrandt, 1998). Muscle spindles fail to form properly during development while the proprioceptive feedback from the GTOs is left intact as described in chapter 2 (section 2.2.3).

The second method acutely eliminates muscle spindle feedback from a subset of muscles We used a *Pv::cre* mouse line infected with AAV9 in target muscles and later administration of diphtheria toxin to eliminate muscle spindles as described in chapter 2 (section 2.2.4, and Figure 2.8).

3.2.3 Electrode Implantation Surgeries

Each mouse received an electrode implantation surgery as previously described **(**Akay et al., 2014). Briefly, mice were anesthetized with isoflurane, ophthalmic eye ointment was applied to the eyes, and the skin of the mice was sterilized with three-part skin scrub using hibitane, alcohol, and povidone-iodine. A set of six bipolar EMG electrodes was implanted

in all animals (Akay et al., 2006; Pearson et al., 2005). Five wild type animals and four *Egr3*$^{-/-}$ received an additional nerve stimulation cuff electrode implant (Akay, 2014).

Small skin incisions were made in the neck region and to the right hindlimb to expose the target muscles and the saphenous nerve (SPN). Electrodes were drawn subcutaneously from the neck incision to the limb incisions, and the headpiece connector was stitched to the skin around the neck incision. The EMG recording electrodes were implanted into hip flexor (iliopsoas, Ip) and extensor (anterior biceps femoris, BF), knee flexor (semitendinosus, St) and extensor (vastus lateralis, VL), and ankle flexor (tibialis anterior, TA) and extensor (gastrocnemius, Gs).

The cuff stimulator electrode was implanted around the saphenous nerve, a nerve carrying cutaneous afferent fibers from the anterior part of the distal hindlimb to the spinal cord. The hindlimb incisions were then closed and anesthetic was discontinued. Analgesics, buprenorphine (0.03 mg/kg) and ketoprofen (5 mg/kg), were injected subcutaneously one hour prior to the surgery to avoid pain. Additional injections were performed in 12-hour intervals for 48 hours. Mice were housed separately, placed in a warmed cage with a fresh mass of hydrogel for the first three days and then returned to their regular mouse rack. Any handling of the mouse was avoided until mice were fully recovered, and the first recording session started at least ten days after electrode implantation surgeries.

3.2.4 Behavioral Recording Sessions

Following the full recovery from electrode implantation surgeries, the behavioral recordings were performed as previously described (Akay et al., 2006; Pearson et al., 2005). Under brief anesthesia with isoflurane, custom-made cone-shaped reflective markers (1-2 mm diameter) were attached to the skin at the level of the anterior tip of the iliac crest, hip, knee, ankle, the metatarsal phalangeal joint (MTP), and the tip of the fourth digit (toe). The anesthesia was discontinued, and the mouse was placed on a mouse treadmill (model: MA 102; custom built in the workshop of the Zoological Institute, University of Cologne, Germany).

The electrodes were connected to an amplifier (model 102, custom-built in the workshop of the Zoological Institute, University of Cologne, Germany) and to a stimulus insulation unit (Iso-flex). We waited at least five minutes to begin the recording session to allow the mice to fully recover from anesthesia. The mice started stepping on the treadmill when it was turned on. The speed of the treadmill was set to 0.3 m/s. In the four wild type mice that did not receive the nerve cuff electrode, a custom-made metallic hook was placed in the path of the moving foot during the swing phase to elicit a stumbling corrective reaction. For the other five wild type and the four *Egr3*$^{-/-}$ mice, with the nerve cuff electrode implanted, the saphenous nerve was electrically stimulated with five brief impulses (duration: 0.2 ms, frequency: 500 Hz).

Only one recording session was performed with each mouse to avoid a learning effect. Therefore, mice in which SCRs were elicited by mechanical stimulation were different than

the mice in which SCRs were elicited by electrical nerve stimulation. The strength of the stimulation was set to be 1.2 times the current that was necessary to elicit the slightest response in the tibialis anterior muscle during resting, which varied between 96 to 1200 μA from animal to animal.

The stepping mouse was filmed from the sagittal plane with a high-speed video camera (IL3, Fastec Imaging) at 250 frames per second, and video files were stored in a computer for later motion analysis. The EMG data were stored separately on the computer by using the Digitizer (Power 1401, Cambridge Electronics Design, UK) combined with spike2 software (Version 8, Cambridge Electronic Design, UK).

The precise foot placement ability during locomotion was assessed by recording the animals walking on the treadmill and on the horizontal ladder. During the treadmill walk, we measured electromyogram (EMG) activities of multiple muscles (Figure 3.1A) together with kinematic parameters of the limb movements (Figure 3.1B). The Hindlimb Anterior Extreme Position (HL_{AEP}) was defined as the initial point of contact of the toe with the treadmill while starting a stance phase, and the Forelimb Posterior Extreme Position (FL_{PEP}) as the last contact of the forelimb with the treadmill before initiating its swing phase. The measurements of relative HL_{AEP} and FL_{PEP} position were given by having the hip joint as a reference in the x-axis. The forelimb was digitized in its last frame of contact with the treadmill, just before starting a swing phase, and distance was taken between forelimb and the toe marker in the hindlimb (FL_{PEP} - HL_{AEP}) (Figure 3.1C). All measurements were performed between ipsilateral limbs.

Figure 3. 1 Illustration of EMG and kinematics recording techniques of stepping during mouse walking. **A**: representation of implanted animal with six EMG electrodes coupled with a headpiece sending signals to an amplifier and cuff electrode attached to a stimulation box. EMG activities are recorded during treadmill walk to produce a locomotor pattern. **B**: kinematic data are obtained by reconstruction of the hindlimb by means of detecting the coordinates of markers attached to the skin above hindlimb segments. Stick diagrams are reconstructed by connecting marker's coordinates. **C**: hindlimb targeting is obtained by measurements of distances between toe to the hip joint (HL_{AEP}) and forelimb paw to hip joint (FL_{PEP}) along the horizontal x-axis (A and B are adapted with permission Akay et al., 2014).

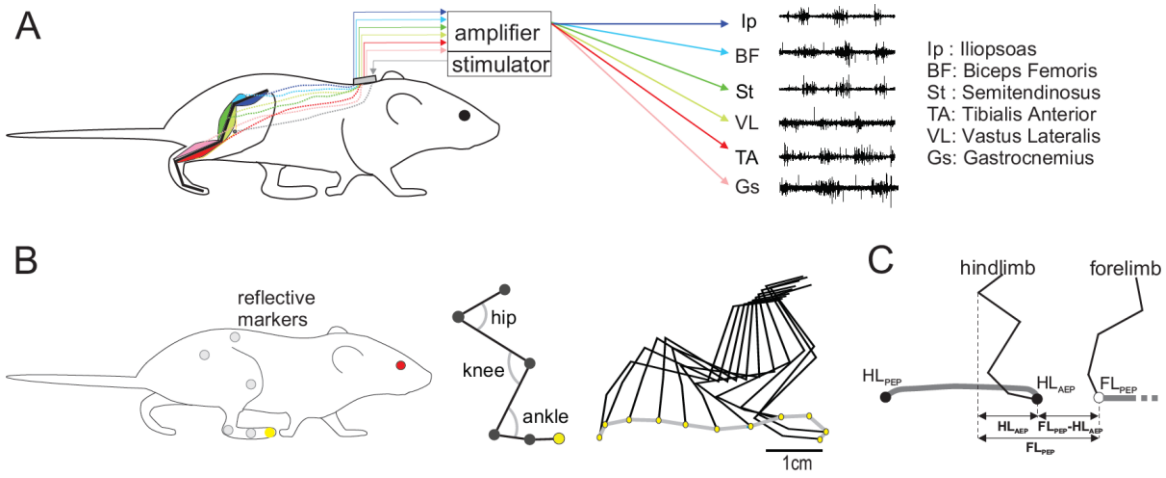

Errors in foot placement accuracy were also tested in the horizontal ladder task. The horizontal ladder was custom built in the workshop of the Zoological Institute, University of Cologne, Germany, made of Plexiglas and metal rungs with a distance of 2 cm between rungs.

A quantitate analysis of skilled walking was achieved by allocating the mice in an initial point where required to across the ladder, stepping rung to rung towards the end of the ladder. During this task, mice were filmed performing 10 consecutive steps in the sagittal

plane. Later the steps were counted accurate if the foot securely landed and held on a rung, or missed step if the foot dropped down missing or slipping dropping down in between the rungs (Akay et al., 2014).

3.2.5 Data Analysis

The kinematic parameters of stepping were obtained from the video files using Motus Vicon or a custom-made software written by Dr. Nicolas Stifani with ImageJ (KinemaJ) and R (KinemaR) (Bui et al., 2016; Fiander et al., 2017). The coordinates and the angular joint movements were then imported into the spike2 files containing the EMG data in a way that the kinematic and EMG data were synchronized with a custom-written spike2 script. The data analysis was performed using this final spike2 file containing the merged EMG and kinematic data. All plots were done using Excel 2016 software, and statistical analysis with the data analysis package for Excel: the statistiXL (version 1.8). Comparisons of swing durations, swing amplitudes, relative HL_{AEP} and FL_{PEP} position during control steps and SCR were performed after Mann and Whitney test using statistiXL.

3.3 RESULTS

3.3.1 Mechanical Perturbation of Swing Movement with Obstacle Elicits "Stumbling Corrective Reaction"

When the hindlimb encountered an obstacle (the rod in our experiments) during the swing phase, the foot was lifted higher to clear the obstacle and placed on the AEP without disrupting the ongoing stepping, a response previously described as SCR (Forssberg, 1979)

(Figure 3.2). In these experiments, mice stepped on the treadmill at a constant speed of 0.3 m/s and in a random sequence, a rod was manually placed briefly along the path of the hindlimb movement during the swing phase. When the limb touched the rod during swing phase, the foot was lifted higher to clear the obstacle, and the swing continued until the foot touched the ground at the AEP (Figure 3.2A and B).

The lifting of the foot over the obstacle was achieved by an extra burst of activity in the knee and ankle flexor muscles (Figure 3.2A, green arrows). The SCR could be elicited regardless of whether the swing was perturbed during early-, mid-, or late-swing (Figure 3.2Bii-iv). Of the perturbed swing phases, neither the swing amplitude (distance between PEP and AEP) ($P \geq 0.674$) nor the duration of the swing phase ($P \geq 0.170$) changed compared to the unperturbed swing phases (statistical comparison with Mann and Whitney test) (Figure 3.2C). These data indicate that the SCR can be elicited in mice, as previously described in cats (Forssberg et al., 1977; Forssberg, 1979), and humans (Schillings et al., 1996; Van Wezel et al., 1997; Zehr et al., 1997).

The high stepping frequency (4.14 Hz, ± 0.91) and short swing duration (0.113 sec, ± 0.017) made mechanical perturbation of the swing phase without additionally disturbing the following stance phase very challenging. Therefore, a large number of trials (188 trials) were performed and only trials in which the rod only touched the foot a single time during the swing phase (64 trials) were analyzed. This present a major limitation to the feasibility of this method as a tool for further projects.

Figure 3. 2 Stumbling corrective reaction elicited by mechanically perturbing hindlimb movement during swing phase. Kinematics and EMG pattern during a stepping sequence that includes two swing phases (shaded background) before and two swing phases after mechanically evoked stumbling corrective reaction (SCR). **A**: hip, knee, and ankle joint angles, rel. toe_x, and y coordinates (toe height) synchronized with raw EMG activity of Flexor (Ip, St, TA) and Extensor (BF, VL, Gs) muscles. Mechanical perturbation of the swing phase is represented by the darker gray inside the third swing phase. Green arrows point to the activity of knee and ankle flexor muscle initiated by the perturbation. Stick diagram reconstruction of a swing phase before SCR, an SCR, and after SCR are illustrated below. **B**: average toe trajectories during control swing phase (i), SCR elicited during early (ii), mid (iii), and late swing (iv). Thin lines indicate toe trajectories from individual trials from one animal and bold line the average trajectory. **C**: box and whisker diagrams illustrating average swing duration (left) and average swing amplitude (right) from control unperturbed swing phases (open bars, $24<n<90$ swing phases) and SCRs elicited by mechanical perturbation (blue bars, $8<n<30$ SCRs) from four mice. None of these comparisons were statistically significant after Mann and Whitney test. M1-M4 represents the four individual mice used in this study.

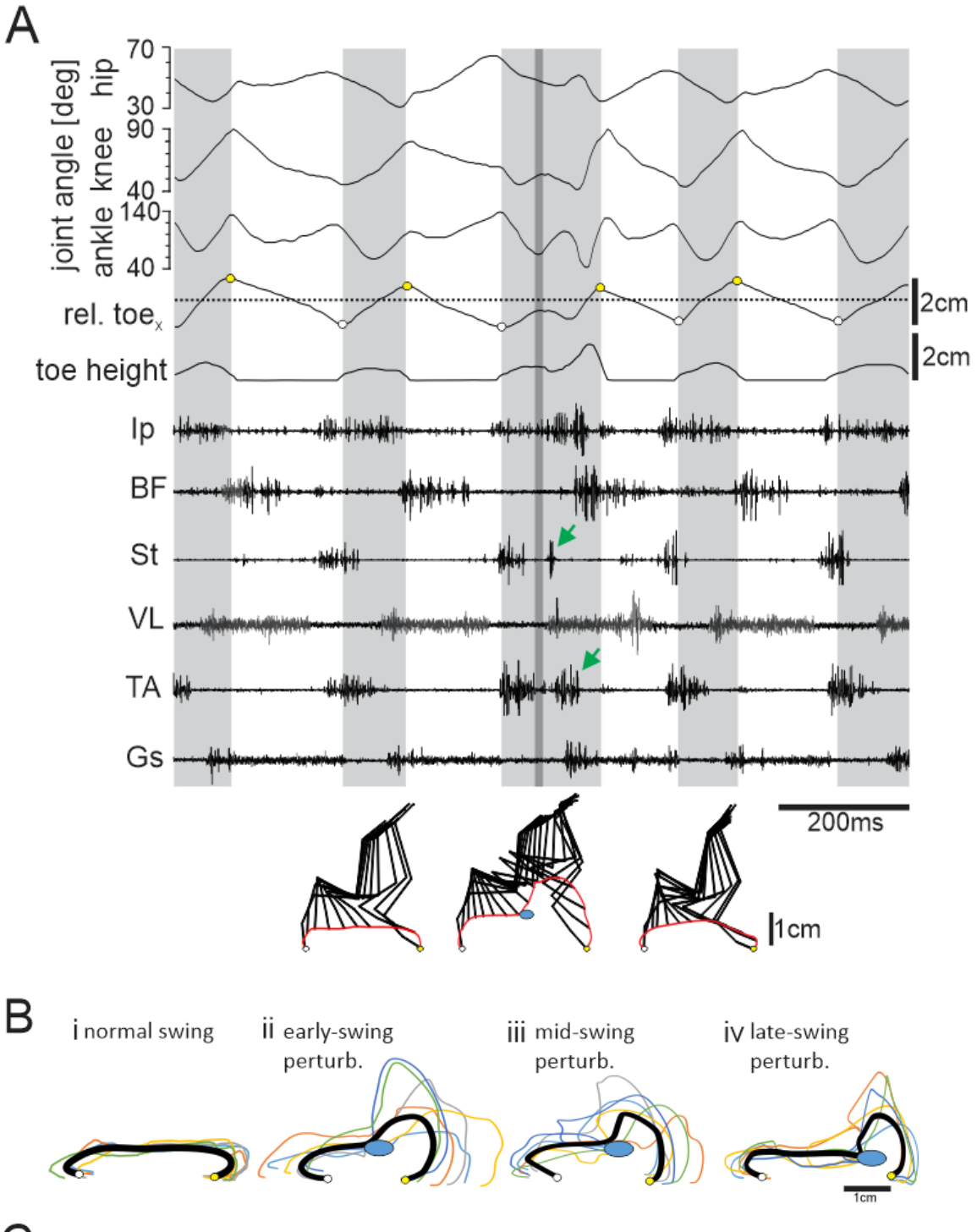
A
joint angle [deg]
hip
knee
ankle
70
30
90
40
140
40
rel. toe$_x$
toe height
2cm
2cm
Ip
BF
St
VL
TA
Gs
200ms
1cm
B
i normal swing
ii early-swing perturb.
iii mid-swing perturb.
iv late-swing perturb.
1cm
C
swing duration [sec]
0.6
0.4
0.2
0.0
CONTROL
SCR
M1
M2
M3
M4
swing amplitute [cm]
5.0
4.0
3.0
2.0
1.0
M1
M2
M3
M4

One could imagine that an automated system could be developed to carry out the mechanical perturbation of the swing movement in a much more precise way, nevertheless, the SCR could be elicited by electrical stimulation of peripheral nerves, activating sensory afferents selectively that would signal obstacle touch. This has been done in the past in cats and humans by stimulating the superficial peroneal nerve (Quevedo, Stecina, Gosgnach, et al., 2005; Van Wezel et al., 1997; Zehr et al., 1997). However, implanting cuff electrodes around the superficial peroneal nerve was not feasible, due to the small size of mice. Therefore, we hypothesized that the saphenous nerve, which also innervates the skin of the dorsum of the foot (Dezhdar et al., 2016; Zimmermann et al., 2009) might be similarly effective in mice.

3.3.2 Saphenous Nerve Stimulation Elicits Stumbling Corrective Reaction in Mice During Walking

Previously in the cat, it was shown that the SCR can be evoked either by electrically stimulating the superficial peroneal nerve in intact animals (Buford & Smith, 1993) or during fictive locomotion (Quevedo, Stecina, Gosgnach, et al., 2005; Quevedo, Stecina, & McCrea, 2005).

We thought that a similar approach with the saphenous nerve (SPN) would overcome the limitations of mechanical stimulation. When SPN was electrically stimulated at 1.2 times the threshold current to elicit any motor response during rest, we could provoke a strikingly similar SCR as elicited by mechanical stimulation (see above). When the stimulation of the SPN occurred during the swing phase, angular joint movements, toe trajectory, and EMG

pattern of muscles reacted in a similar fashion as in SCR evoked by mechanical stimulation (Figure 3.3).

Furthermore, during SCR elicited with electrical SPN stimulation, the lifting of the foot to clear the "virtual obstacle" was achieved by activation of flexor muscles moving knee (St) and ankle (TA) joints (Figure 3.3A, green arrows). Only when the stimulation occurred later in swing phase the hindlimb tends to terminate the swing and proceed to the next stance phase instead of clearing the "virtual obstacle" (Figure 3.3Biv).

When the SPN was stimulated, as in the mechanical stimulation, we could not detect any changes either in the swing amplitude ($P \geq 0.629$ after Mann and Whitney test) or the swing duration ($P \geq 0.580$ after Mann and Whitney test) (Figures 3.3C) compared to unperturbed swing phases. Our data provide evidence that electrical stimulation of the SPN during the ongoing swing phase consistently elicits a response that strongly resembles the SCR elicited by mechanical stimulation.

Our data suggest that the SCR can be evoked when electrical stimulation of the SPN occurs within the first- and second-third of the swing phase. The movement of joints during SCR evoked by mechanical stimulation and electrical stimulation was very similar. The only difference we could detect was, when the electrical stimulation occurred at the end of the swing phase, SCR was not elicited but the swing was terminated. In contrast, mechanical stimulation at the end of swing phase consistently initiated SCR. Nevertheless, the SCR elicited by electrical stimulation provides advantages over mechanical stimulation since it can be applied with more accuracy as well as elicited cleaner responses.

Figure 3. 3 Stumbling corrective reaction elicited by electrical stimulation of the saphenous nerve during swing phase. Kinematics and EMG pattern during a stepping sequence including two swing phases (shaded background) before and two swing phases after electrically evoked SCR. **A**: hip, knee, and ankle joint angles, rel. toe_x, and y coordinates (toe height) synchronized with raw EMG activity of Flexor (Ip, St, TA) and Extensor (BF, VL, Gs) muscles. Electrical stimulation of the saphenous nerve during the swing phase is indicated by the darker gray inside the third swing phase. Arrows point to the activity of knee and ankle flexor muscle initiated by the stimulation. Stick diagram reconstruction of a swing phase before SCR, an SCR, and a swing phase after SCR are illustrated below. **B**: individual and average toe trajectories during control swing phase (i), SCR elicited during early (ii), mid (iii), and late swing (iv). Thin lines indicate toe trajectories from individual trials from one animal and bold line the average trajectory. **C**: box and whisker diagrams illustrating average swing duration (left) and average swing amplitude (right) from control unperturbed swing phases (open bars, $21<n<87$ swing phases) and SCRs elicited by electrical stimulation (red bars, $7<n<29$ SCRs) from five mice. None of these comparisons were statistically significant after Mann and Whitney test. M1-M5 represents the five individual mice used in this study.

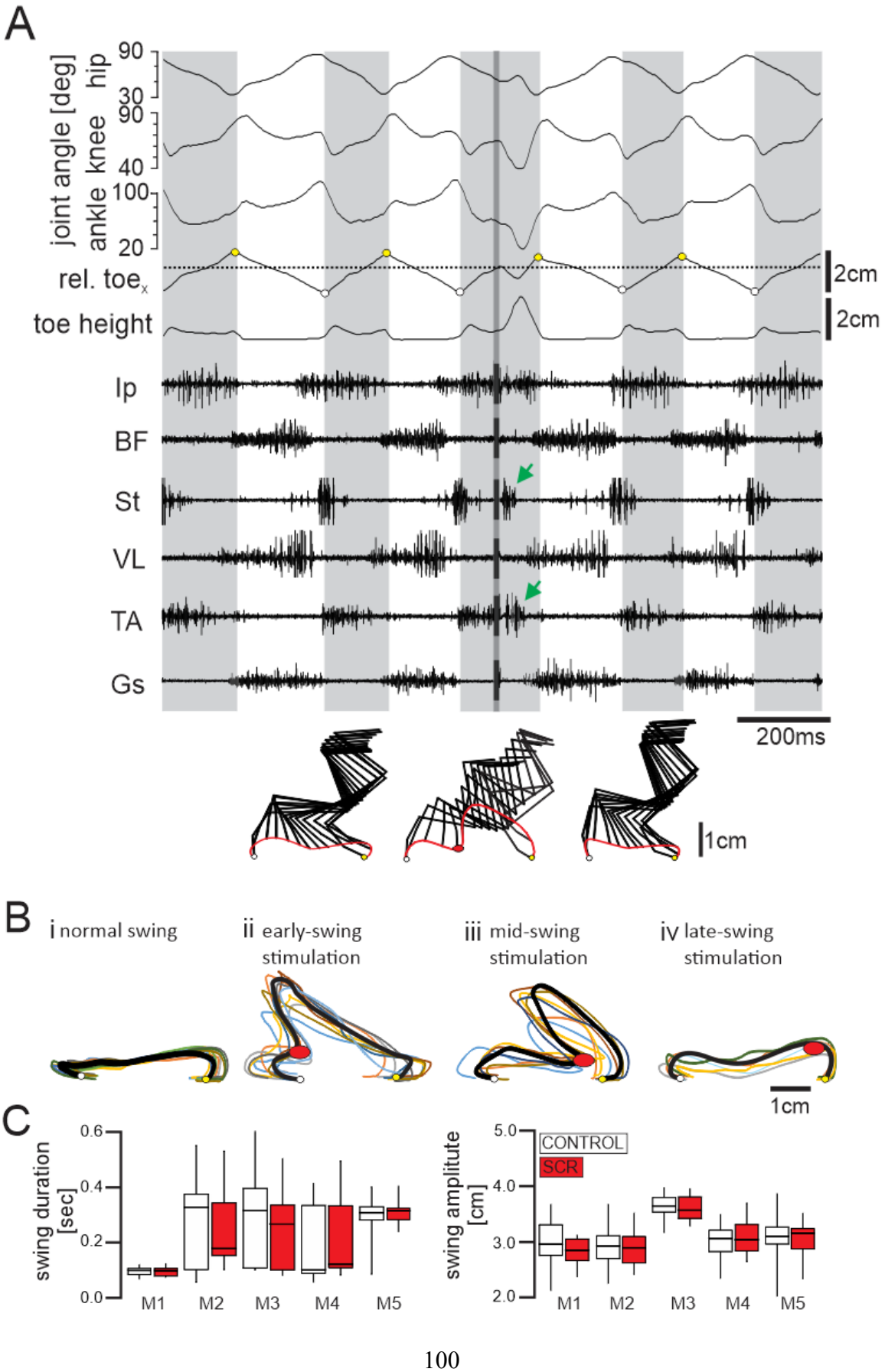
A
joint angle [deg]
hip
90
30
knee
90
40
ankle
100
20
rel. toe$_x$
toe height
2cm
2cm
Ip
BF
St
VL
TA
Gs
200ms
1cm
B
i normal swing
ii early-swing stimulation
iii mid-swing stimulation
iv late-swing stimulation
1cm
C
swing duration [sec]
0.6
0.4
0.2
0.0
M1
M2
M3
M4
M5
swing amplitute [cm]
5.0
4.0
3.0
2.0
CONTROL
SCR
M1
M2
M3
M4
M5

3.3.3 Stumbling Correction Reaction in Absence of Muscle Spindle Feedback Lack Uniform Response and Temporal Control

Previous studies have shown that only cutaneous stimulation is enough to trigger stumbling corrective reactions (Buford & Smith, 1993; Quevedo, Stecina, & McCrea, 2005; Zehr et al., 1997). Here we sought to establish the role of muscle spindle feedback during such reaction. Is the SCR a spinal program that once initiated by cutaneous signals does not require further sensory feedback? Or does the execution of SCR further require muscle spindle feedback? To address these questions, we performed SCR experiments via saphenous nerve stimulation in six *Egr3*$^{-/-}$ mice (Figure 3.4).

Stimulating the SPN during the swing phase in *Egr3*$^{-/-}$ mice evoked angular reactions in hip, knee and ankle joints qualitatively different than in wild type (joint angle traces Figure 3.4A). The rel. toe$_x$ recordings have shown that the SPN stimulation elicited a paw withdraw (rel. toe$_x$ Figure 3.4A) similar to those recorded in the wild types (rel. toe$_x$ Figure 3.3A). The toe, although lifted after the stimulation, revealed no qualitative regular pattern of progression compared with wild type animals.

Similar as in wild types, during SCR in *Egr3*$^{-/-}$ mice, the foot lifting to clear the "virtual obstacle" was achieved by activation of flexor muscles mostly moving the hip (Ip) and ankle (TA) joints (Figure 3.4A, green arrows) when the stimulation occurred in early- or mid-swing (Figure 3.4Bii-iii). However, when stimulating the SPN in late-swing, the hindlimb tended to terminate the swing and proceed to the next stance phase (Figure 3.4Biv) same as performed by the wild type mice (Figure 3.3Biv). These data suggest that

the overall muscle activation pattern during SCR is not dependent on muscle spindle feedback.

Qualitative differences were also observed regarding the toe trajectory in *Egr3*$^{-/-}$ SCR. The individual responses after the stimulation proved to be more variable in comparison to wild type animals, as well as the average toe trajectory presented particular dissimilarities (Figure 3.4Bi-iv). The swing duration after the SCR has changed in two out of 6 animals as well the swing amplitude (Figure 3.4C) compared to unperturbed swing phases. Those results suggest that muscle spindle feedback is not necessary to elicit the SCR, however, it provides evidence that it plays a role in fine-tuning the movement during the SCR.

Figure 3. 4 Stumbling corrective reaction elicited by electrical stimulation of the saphenous nerve during swing phase in *Egr3*$^{-/-}$. Kinematics and EMG pattern during a stepping sequence including two swing phases (shaded background) before and two swing phases after electrically evoked SCR. **A**: hip, knee, and ankle joint angles, rel. toe_x, and y coordinates (toe height) synchronized with raw EMG activity of Flexor (Ip, St, TA) and Extensor (VL and Gs) muscles. Electrical stimulation of the saphenous nerve during swing phase is indicated by the darker gray inside the third swing phase. Green arrows point to the activity of the hip and ankle flexor muscle initiated by the stimulation. Stick diagram reconstruction of a swing phase before SCR, during SCR, and a swing phase after SCR are illustrated below. **B**: individual and average toe trajectories during control swing phase (i), SCR elicited during early (ii), mid (iii), and late swing (iv). Thin lines indicate toe trajectories from individual trials from one animal and bold line the average trajectory. **C**: box and whisker diagrams illustrating average swing duration (left) and average swing amplitude (right) from control unperturbed swing phases (open bars) and SCRs elicited by electrical stimulation (red bars) from six mice. Two animals recorded longer swing duration (M1= control 0.08sec and SCR 0.10sec; and M3= control 0.08sec and SCR 0.12sec. Two animals modified swing amplitude (M1= control 2.80cm and SCR 3.42cm; and M4= control 2.62cm and SCR 2.46cm). Statistically significant after Mann and Whitney test $*P < 0.05$ and $***P < 0.001$, M1-M6 represents the six individual mice used in this study.

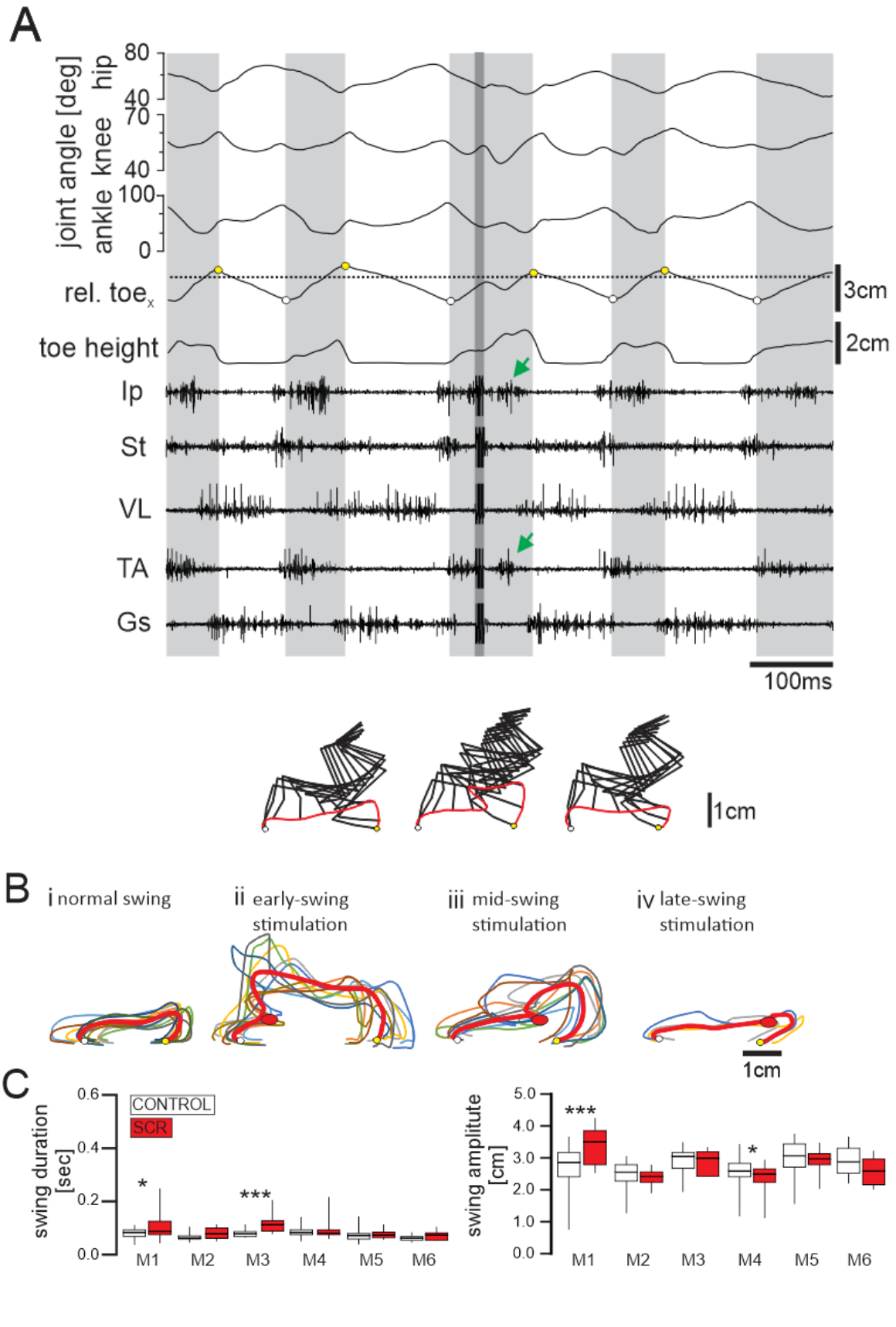
A
joint angle [deg]
hip
knee
ankle
80
40
70
40
100
0
rel. toe$_x$
toe height
3cm
2cm
Ip
St
VL
TA
Gs
100ms
1cm
B
i normal swing
ii early-swing stimulation
iii mid-swing stimulation
iv late-swing stimulation
1cm
C
swing duration [sec]
0.6
0.4
0.2
0.0
CONTROL
SCR
*
***
M1
M2
M3
M4
M5
M6
swing amplitute [cm]
5.0
4.0
3.0
2.0
1.0
0.0
***
*
M1
M2
M3
M4
M5
M6

3.3.4 Targeting of the Hindlimb During Walking is Compromised in Absence of Muscle Spindles

To assess the precision of the foot placement during walking, we measured the distance between the hip marker to the toe landing at AEP (HL_{AEP}), and the hip marker to the paw position of the ipsilateral forelimb at the end of stance (FL_{PEP}). Both measurements were taken on the horizontal axis (x-axis, see methods 3.2.4). These measurements were taken from control steps (three steps before perturbation) and the SCR steps (steps that had directly suffered stimulation to evoke a stumbling corrective reaction) in wild type and *Egr3*$^{-/-}$ mice.

The HL_{AEP} measured during normal walking, without perturbation in four wild types, had an average of 1.45 cm ± 0.23 while that distance was shorter in *Egr3*$^{-/-}$ mice, 0.90 cm ± 0.42 ($P < 0.001$ after Mann and Whitney test). Moreover, not only was the average lower, the variability of the HL_{AEP} in *Egr3*$^{-/-}$ mice was significantly larger compared to wild types ($P < 0.001$ after f-test) (Figure 3.5A – control steps). After the SCR, wild type mice managed to land their foot at an average distance of 1.29 cm ± 0.24, which is closer to the hip joint compared to control walking ($P < 0.001$ after Mann and Whitney test). On the other hand, after the SCR the HL_{AEP} *in Egr3*$^{-/-}$ mice was 1.03 cm ± 0.81, with wider distribution ($P < 0.001$ after f-test) but no changes in average distance ($P = 0.696$ after Mann and Whitney test) (Figure 3.5A – SCR steps). These data suggest that the proprioceptive feedback from muscle spindles is necessary for precise foot placement at the end of the swing phase during normal walking and after SCR.

What determines the HL_{AEP} during normal walking? In humans, it is known that if precision is required, visual information is essential to determine the location at which the foot is placed during walking (Reynolds & Day, 2005). In quadrupedal animals however, visual guidance is not an option because of the limitation due to body posture. Therefore, we alternatively hypothesized that the forelimb position during stance guides the hindlimb foot placement at the end of swing. In fact, this has been shown to be the case using insect models (Cruse, 1979; Dean & Wendler, 1983).

To test this hypothesis, we measured the FL_{PEP} and investigated its relation with the HL_{AEP}. The position of the FL_{PEP} relative to the hip joint was similar in either group under both circumstances (control steps and SCR). Wild type scored an average of $FL_{PEP=}$ 2.18cm ± 0.45 during control steps while the *Egr3*$^{-/-}$ recorded FL_{PEP} = 1.91cm ± 0.42 (Figure 3.5B – control steps). During the SCR wild type FL_{PEP} = 1.99cm ± 0.47 and *Egr3*$^{-/-}$ FL_{PEP} = 1.99cm ± 0.54 (Figure 3.5B – SCR steps). These data illustrate that the FL_{PEP} shifts to a more posterior position when SCR is elicited compared to normal walking.

To quantify the hindlimb targeting related to the forelimb, we measured the distance between the two ipsilateral limbs during the stance phase, the Hindlimb Anterior Extreme Position subtracted from the Forelimb Posterior Extreme Position (HL_{AEP} **-** FL_{PEP}). During control walking, wild type mice showed a more concentrated distribution of this distance compared to their *Egr3*$^{-/-}$ littermates ($P < 0.01$, f-test). The average distance in wild type HL_{AEP} **-** FL_{PEP} was 0.73cm ± 0.51, whereas the *Egr3*$^{-/-}$ showed a less concentrated distribution ($P < 0.005$ after f-test) with longer HL_{AEP} - FL_{PEP} = 1.01cm ± 0.62 ($P < 0.001$, Mann and Whitney test) (Figure 3.5C control steps). In the SCR experiments, wild type

animals had a distribution HL_{AEP} - FL_{PEP} similar to those recorded in control steps as the *Egr3*$^{-/-}$ noted even more scattered distribution ($P < 0.001$, f-test) (Figure 3.5C - SCR steps histogram), the average values for wild type SCR HL_{AEP} - FL_{PEP} were 0.69cm ± 0.49 and *Egr3*$^{-/-}$ SCR HL_{AEP} - FL_{PEP} were 0.96cm ± 0.76 ($P < 0.005$, Mann and Whitney test). This set of results showed that the distribution of HL_{AEP} and HL_{AEP} - FL_{PEP} are more variable in the absence of proprioceptive feedback from the muscle spindles during normal walking. After SCR, the HL_{AEP} was brought closer to the hip joint in wild types but not in the *Egr3*$^{-/-}$ mice.

When the swing phase was perturbed with SCR, both, HL_{AEP} and FL_{PEP} shifts posteriorly in wild type mice, however, *Egr3*$^{-/-}$ mice showed no changes in the HL_{AEP} and FL_{PEP} but a more variable positioning was noticed. Figure 3.6A illustrates detailed information on such performance. In addition, Figure 3.6B shows that no significant changes were observed in the HL_{AEP} - FL_{PEP} distances for both experimental groups after the SCR. This supports our hypothesis that the hindlimb is guided by the forelimb and this mechanism requires proprioceptive feedback from the muscle spindles.

Figure 3. 5 Foot placement during walking and after Stumbling Corrective Reaction in wild type and *Egr3*$^{-/-}$. **A**: histogram demonstrates the hindlimb anterior extreme position HL_{AEP} (black bars: wild types and red bars: *Egr3*$^{-/-}$). Notice on the left histogram that the distribution of the muscle spindle deficient animals is scattered and less precise compared to the wild types during control steps. During SCR wild types tend to concentrate their response in the same range as during the control steps (black bars on left and right histograms). In contrast, *Egr3*$^{-/-}$ responses get spread along the histogram spectrum after the SCR (red bars on right histograms). **B**: distribution of Forelimb Posterior Extreme Position related to the hip joint (FL_{PEP}) show similar behavior during control and SCR steps for wild types and *Egr3*$^{-/-}$ mice. **C**: distribution of distances between ipsilateral hindlimb anterior extreme position and forelimb posterior extreme position (HL_{AEP} - FL_{PEP}) in wild type animals remain similar during normal stepping and after perturbations. In *Egr3*$^{-/-}$ mice, slightly wider spread was observed in both conditions. Trials from four wild type animals, n= 252 control steps and 84 stumbling corrective reaction steps, and six *Egr3*$^{-/-}$, n= 288 control steps and 96 stumbling corrective reaction steps.

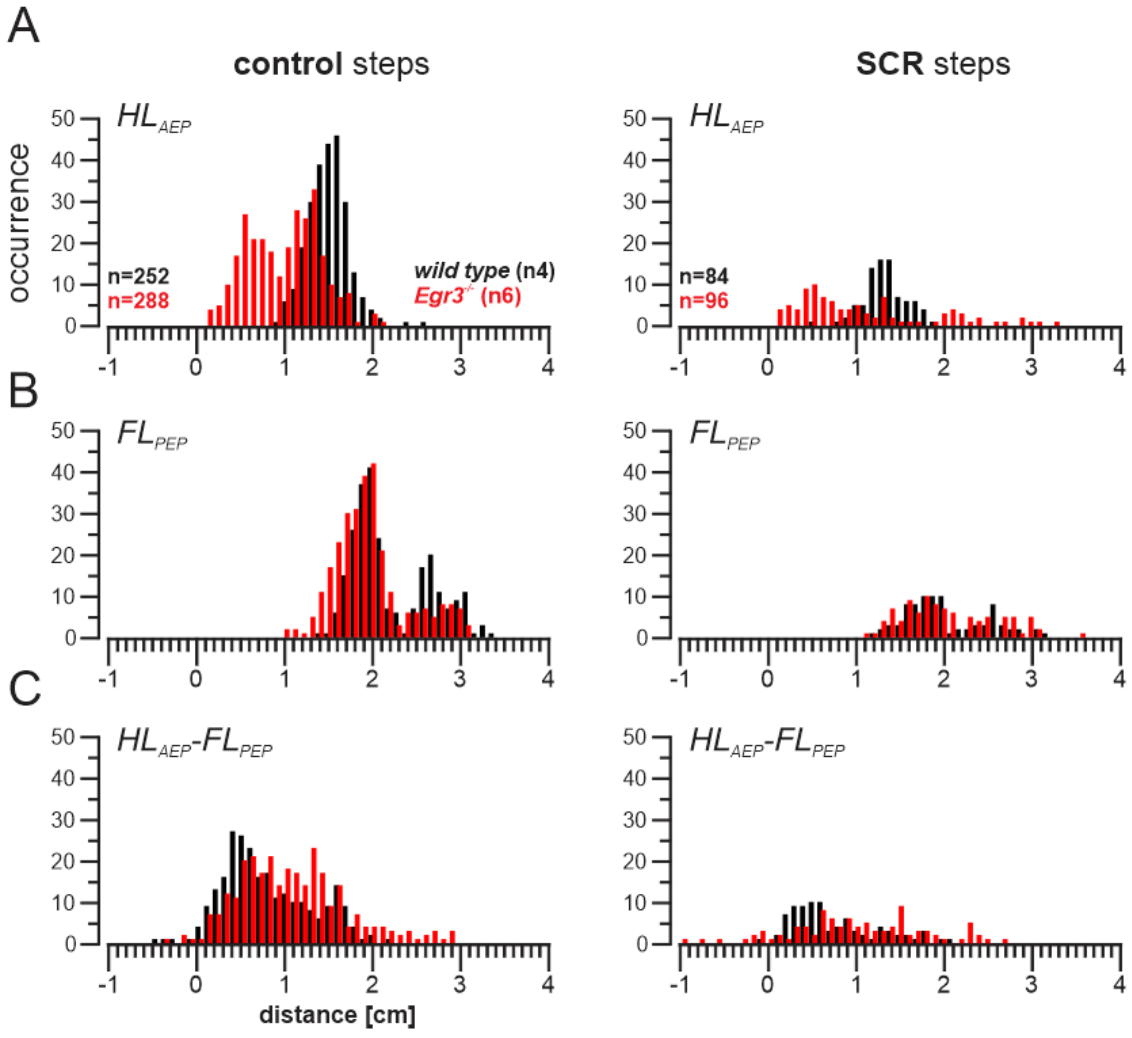

Figure 3. 6 Hindlimb targeting after stumbling corrective reaction. Schematics of hindlimb segments and forelimb position in wild types (black circles) and *Egr3*$^{-/-}$ mice (red circles). **A**: hindlimb position in control steps and after SCR. Notice that hindlimb and forelimb moved posteriorly after perturbation in wild types. In *Egr3*$^{-/-}$, the variability of these parameters but not the averages increased during SCR (closed circles: HL_{AEP}, and open circles: FL_{PEP}). **B**: distance between ipsilateral hindlimb anterior position and forelimb posterior extreme position (HL_{AEP} - FL_{PEP}). Notice that HL_{AEP} - FL_{PEP} has not changed during SCR in wild types, while in *Egr3*$^{-/-}$ mice the variability increase but the average remained unchanged. N= four wild types, 252 control steps, and 84 SCR steps; N= six *Egr3* $^{-/-}$, 288 control steps and 96 SCR steps, statistically significant after Mann and Whitney test ***$P < 0.001$.

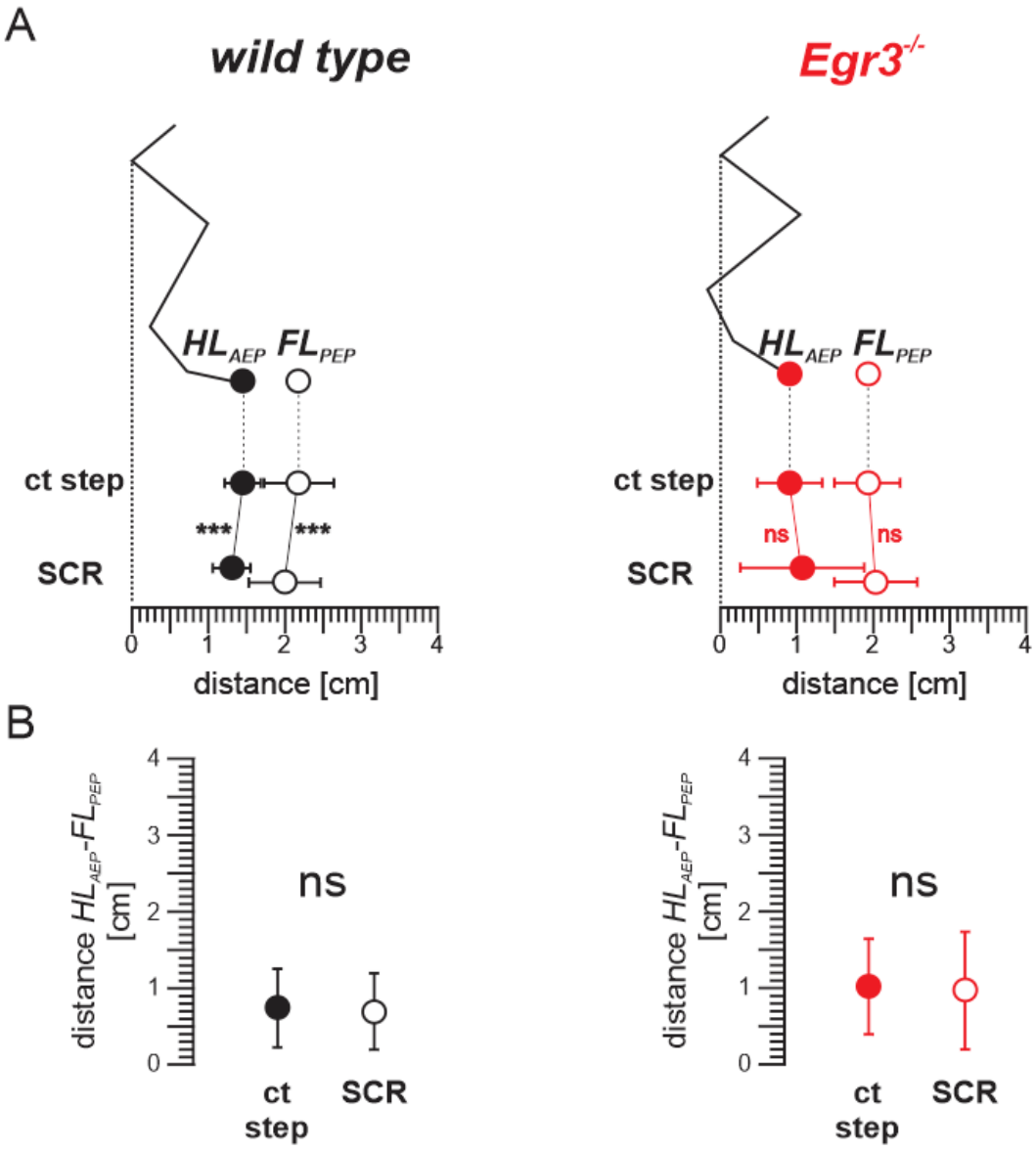

3.3.5 Muscle Spindle Feedback Ensuring Accuracy in Skilled Motor Behavior

We were further interested to know whether the targeting is achieved by proprioceptive feedback from a particular joint, or whether proprioceptive feedback from all joints contributed collectively. To differentiate between these possibilities, we counted correct foot placement or misplacements of the paw in the rungs during horizontal ladder walking in wild type, *Egr3*$^{-/-}$ (total absence of muscle spindle feedback) or from a particular joint in *Pv::cre* (partial lack of proprioceptive feedback) mice as previously described in methods session.

In the absence of proprioceptive feedback from all muscle spindles, the *Egr3*$^{-/-}$ mice had severe difficulty in placing their limbs accurately on the rungs while walking in the horizontal ladder. The *Egr3*$^{-/-}$ showed reduced precision in foot placement during this skilled task. Wild types performed a well-defined hindlimb placement when walking on the rungs of a horizontal ladder, with a placement error of only 2% ± 5. In contrast, we detected a higher inaccuracy in *Egr3*$^{-/-}$ mice (39% ± 18), with the difference being statistically significant ($P < 0.001$, two-tailed *t*-test) (Figure 3.7).

Figure 3. 7 Performance of wild type and *Egr3*$^{-/-}$ mice on the horizontal ladder. Higher incidence of errors occurred while *Egr3*$^{-/-}$ mice walking on the horizontal ladder compared to wild types. Black bars indicate the number of steps that precisely landed on the rung and the red bars specify the number of steps in which the foot was dropped between the rungs. Data from three wild type and three *Egr3*$^{-/-}$ mice (adapted with permission Akay et al., 2014).

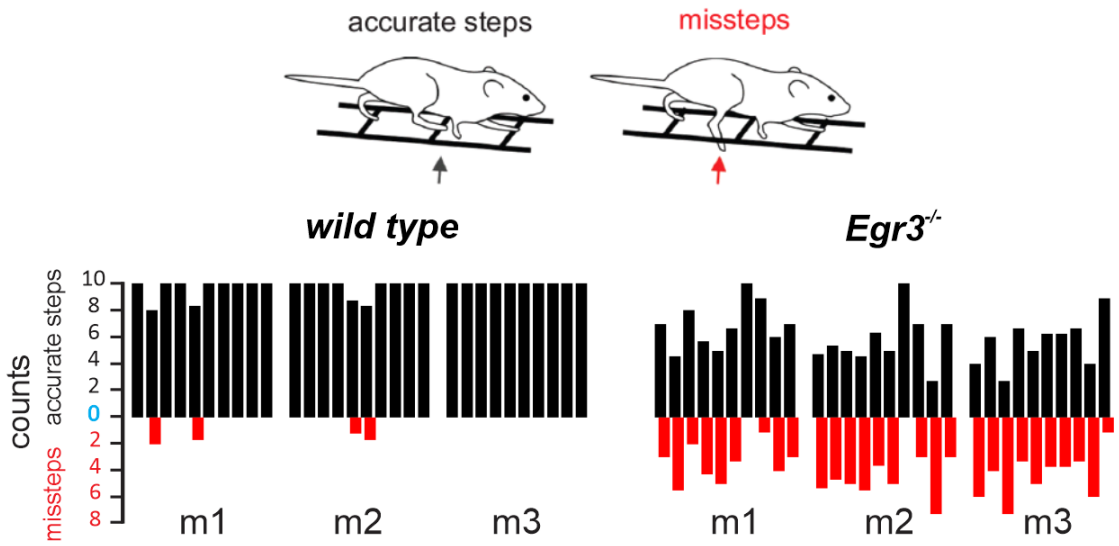

After demonstrating that *Egr3*$^{-/-}$ mice had severe difficulties performing a task that requires precise foot placement as walking on the horizontal ladder, we sought to investigate if there was any specific group of muscle that would contribute more to the hindlimb final target during horizontal ladder walking. To do this, we eliminated proprioceptive afferent from muscle spindles in specific muscles of the hindlimb by using the AAV9/DTX method and evaluated the horizontal ladder walking as previously described. The attenuation of muscle spindles from the hip joint has altered the scoring target rates when compared to normal conditions. In pre-DTX experiments, the animals had a placement error of 7% ± 6 while post-DTX the scores were 13% ± 5 of inaccuracy. Although four out of six mice had increased inaccuracy, the number was not strong enough to be statistically significant in paired *t*-test (P = 0.178) (Figure 3.8A). In the second group of DTX experiments, where

the knee muscles were targeted for muscle spindle elimination, six out of six animals had increased the inaccuracy rate while reaching the rungs of the horizontal ladder, average values pre-DTX = 4% ± 2, and post-DTX = 10% ± 3, $P < 0.05$ two-tailed *t*-test with paired dataset (Figure 3.8B). For the last set of experiments, with the muscle spindle feedback being removed from ankle joints, only two out of six mice had increased their inaccuracy rate, the average pre-DTX = 6% ± 4, and post-DTX = 5% ± 4, P = 0.688 under two-tailed *t*-test with paired dataset (Figure 3.8C). These data suggest that muscle spindles from the knee joint is necessary for precise foot placement. In addition, muscle spindles from hip joint might contribute to the targeting as we could see a tendency, however, the difference was not statistically significant.

Figure 3. 8 Performance of mice before and after attenuation of muscle spindle feedback from the hip (A), knee (B), or ankle (C) joint on horizontal ladder. Control data are represented by pre-DTX graphs and feedback attenuation is given by the post-DTX graphs. Note that there is a tendency to increase mistakes while removing feedback from hip muscles (**A**) but this change was not statistically significant. The only statistical significance could be detected after removing spindle afferents from the knee muscles (**B**). Spindle removal from ankle has not changed performance on the horizontal ladder. Each burst of bars represents 5 runs of a single animal, black bars are accurate steps and red bars missteps. N= 18 animals, six for each experiment performing 30 steps pre- and post-DTX.

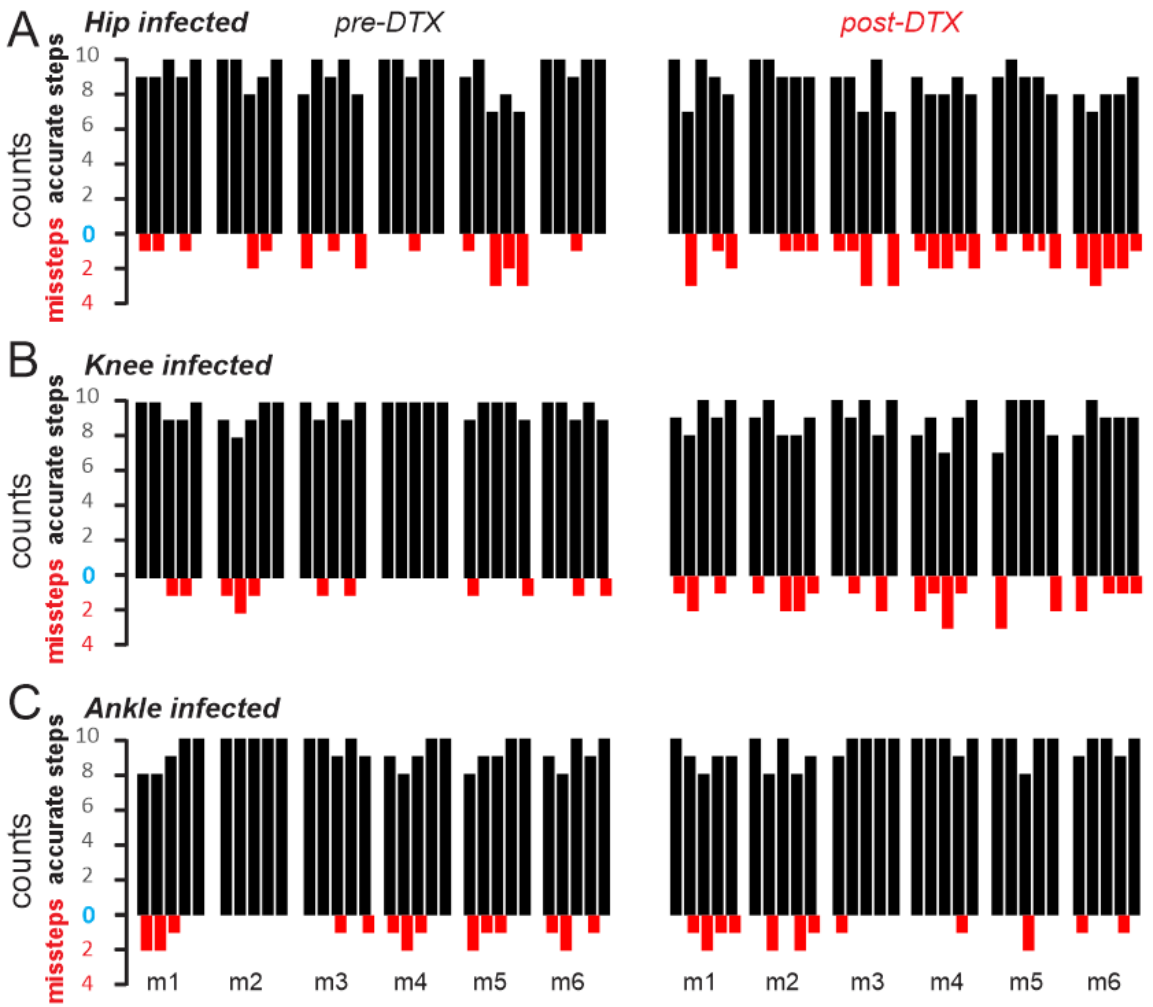

The results presented in this chapter indicate that stumbling corrective reaction can be elicited in mice, either by mechanical stimulation or through electrical stimulation of the saphenous nerve, and those findings are qualitatively similar to those described in cats. Furthermore, we show that at the end of the swing phase, the foot lands on a specific location that the HL_{AEP} is predetermined by the forelimb. However, in the absence of proprioceptive feedback from the muscle spindles, this guidance of the hindlimb by the forelimb is compromised.

3.4 Discussion

Proprioceptive feedback has been known to be important for the generation of the locomotor pattern (McCrea, 2001; Pearson, 2004). However, the role of muscle spindle feedback in targeting limbs on the ground after a swing phase is still obscure. Especially how proprioceptive information is processed to enable targeting is not known. Here we have shown that proprioceptive feedback from muscle spindles is important in targeting the hindlimb during normal locomotion and in skilled locomotion where precise foot placement is required. Furthermore, although cutaneous stimulation is sufficient to trigger stumbling corrective reaction, normal kinematic responses with normal duration of the swing phase, and limb positioning required muscle spindle feedback to achieve appropriate performance. Finally, we have shown that muscle spindle feedback from proximal muscles in the hindlimb, especially knee muscles, appears to have more influence on precise foot placement such as required to walk on a horizontal ladder.

3.4.1 Stumbling Corrective Reaction in Mice

We have shown that, in mice, if the swing phase is perturbed by inserting an obstacle in the pathway of the foot moving from the posterior extreme position to the anterior extreme position elicits an SCR without affecting the fluency of the locomotion. The kinematics of the hindlimb during SCR and activation pattern of multiple flexors and extensor muscles closely resemble the pattern previously described in cats (Buford & Smith, 1993; Forssberg, 1979; Quevedo, Stecina, Gosgnach, et al., 2005). The knee joint flexed as a response to the obstacle, whereas the ankle joint initially extend and then flexed, hence the combination of these movements lifted the foot higher to clear the obstacle. Accordingly, we detected the activation of flexor muscle as a response to the obstacle contact during the swing phase (Figure 3.2). In previous cat experiments, it has been shown that the elevation of the foot is mainly achieved through the activation of the flexor muscles of distal hindlimb joints leading to increased flexion (Wand et al., 1980). Our data suggest that SCR characterized in cats also occurs in mice with striking similarities (Figure 3.2). That is, when the foot encounters an obstacle during swing movement, regardless of early-, mid- or late-swing, the knee joint simply flexes, while the ankle joint initially extends and later flexes.

We also recorded that flexor muscles of knee were activated prior ankle flexors and that the ankle joint described a brief extension after stimulation, while no consistent changes in activity in the hip flexor muscles was observed. What is the reason for the short-latency initial ankle extension prior to ankle flexion? Two explanations for this kinematic behavior during SCR could be explored. First, it is likely we simply have not recorded the extensor

muscle that would underlie the early ankle extension. Multiple muscles extend the ankle joint, and we only recorded from one head of the gastrocnemius muscle (lateral gastrocnemius). It is conceivable that other ankle extensors, with no EMG electrodes implanted, such as the medial gastrocnemius, soleus or the plantaris muscles might have had increased activity assisting the movement. Second, the initial extension of the ankle joint occurs passively due to ongoing flexion of the hip joint that would push the foot towards the obstacle causing the ankle joint to extend. Once the foot is cleared, the ankle would then start flexion due to flexor muscle activity. We do not think the latter is true, as we observed a similar early extension of the ankle joint during nerve stimulation where there is no actual obstacle to cause a passive ankle extension. Therefore, we believe that the early ankle extension is an active part of the SCR that is presumably caused by another ankle extensor muscle not recorded in our experiments.

Furthermore, electrical stimulation of the saphenous nerve, activating cutaneous afferent neurons that would normally signal the contact of an object with the leg, elicits SCR. Both SCRs, regardless of whether they were elicited by mechanical or electrical stimulation, were similar in kinematic parameters and muscle activation patterns. Moreover, we have observed that when electrical stimulation of the saphenous nerve occurred during ongoing stance phase, it did not generate any kinematic changes or flexor muscle activation as described in previous studies (Forssberg, 1979; Forssberg et al., 1975, 1977; Mayer & Akay, 2018). Our data provide a detailed description of the SCR in mice and will be crucial for future attempts to address neuronal control mechanisms of SCR by combining this method with mouse genetics.

3.4.2 Cutaneous Afferent Signaling is Sufficient to Elicit SCR

Mechanical stimulation leaves open the question of whether a functional SCR can be elicited by only cutaneous afferent signals, as suggested from experiments in cats (Forssberg, 1979). Alternatively, proprioceptive feedback that signals changes in the natural angular joint movement due to obstacle contact (McVea & Pearson, 2007) could also contribute to the initiation of the SCR.

To differentiate between these two possibilities, we recorded the SCR initiated by cutaneous afferent activation by electrical stimulation of the saphenous nerve that would mimic obstacle contact. Here, as there is no actual physical object preventing leg movement, the proprioceptive component of obstacle detection was eliminated. Therefore, we could conclude that a response can be initiated by cutaneous afferent signaling only. Indeed, electrical stimulation of the SPN, activating only cutaneous afferents, is sufficient to generate an SCR very similar to the SCR initiated by contact of the foot with an obstacle during swing phase (Figure 3.3). These data provide evidence that cutaneous afferent signals are sufficient to initiate SCR.

The only major difference between mechanically and electrically evoked SCRs was found at the end of the swing phase. When mechanical stimulation occurred at the end of swing phase, kinematic changes were triggered to overcome the obstacle. In contrast, the electrical stimulation of the SPN at the end of swing did not elicit SCR. Our current data cannot elucidate this discrepancy. However, one possible explanation is that proprioceptive

feedback, although not necessary to elicit SCR in early- or mid-swing phase might have a more important role at the end of swing phase.

3.4.3 Muscle Spindle Feedback Standardize SCR

Our results suggest that cutaneous feedback is sufficient to elicit SCR, however muscle spindle feedback is required for the accurate execution of the SCR. In the absence of muscle spindles in *Eg3*$^{-/-}$ mice, we could clearly see SCR being elicited when cutaneous afferents were stimulated, but the regularity of the movement was compromised (Figure 3.4). In wild type mice, the swing duration and swing amplitude during SCR are maintained within the same parameters of normal unperturbed steps. In contrast, in *Egr3*$^{-/-}$ mice, the duration of the swing phase, swing amplitude and regularity of the movement were not as consistent as in the wild type mice. It has been shown that sensory feedback is important to regulate the motor output (Akay et al., 2014; Pearson, 2004; Rossignol et al., 2006). The data presented here suggest that after an SCR event, the group Ia/II feedback acts to regulate the temporal and spatial properties of response after perturbation of the swing phase. However, the data are inconclusive regarding the role of GTO feedback in the SCR. Future studies may clarify how feedback through group Ib afferents are integrated with the rhythm-generating circuits that control SCR.

3.4.4 Targeted Responses and Skilled Locomotor Behavior Rely on Muscle Spindle Feedback

Previous work by Akay et al. 2014 showed that reaching the rungs of a horizontal ladder with precision worsens without muscle spindle feedback, however, such compromised precision has not been investigated during normal walking. We sought to address whether foot placement at the end of the swing phase during normal walking is a targeted movement and whether proprioceptive feedback from muscle spindles is necessary to such mechanism.

We have shown that the swing movement of the hindlimb is a targeted movement in which the foot is placed in a specific location related to the forelimb, and the determination of the target as well as the precision of this movement requires proprioceptive feedback. The targeting mechanism that is guided by the more anterior leg has been previously shown in walking insects (Cruse, 1979; Dean & Wendler, 1983). In our study, when the swing phase was disrupted causing an SCR, wild type animals with intact proprioceptive feedback were able to place their foot precisely to the AEP as during normal locomotion. However, without proprioceptive feedback, the AEP became more variable during normal walking and degraded even more after an SCR event (Figures 3.5 and 3.6).

Next, we wanted to know whether muscle spindle feedback from a specific joint was more important than the other joints in precise foot placement. Our results implied that removing muscle spindle feedback from only the knee joint caused sufficient deterioration of accurate foot placement on the horizontal ladder, although a tendency for deterioration was observed by removing muscle spindle feedback from hip muscles as well. Finally removing muscle

spindles from the ankle joint did not cause changes on precise foot placement. Therefore, our data suggest that muscle spindle feedback from knee joint has a more prominent role in precise foot placement.

We have mainly focused on sensory feedback from the measured limb. However, further consideration has to be given to the spinal interneurons that are involved in left and right coordination (Lanuza et al 2006; Talpalar et al 2013; Kiehn 2016; Zhang et al., 2008). Because our experiments with the AAV9/DTX only removed muscle spindle feedback from one hindlimb, it is conceivable that sensory information from the contralateral hindlimb could also function to guide the limb movement. Our data do not provide any information regarding the influence of sensory feedback from the contralateral limbs and future studies focusing in cross reflexes with mice (Laflamme & Akay, 2018) may shed light on this issue.

CHAPTER 4 ROLE OF MUSCLE SPINDLE FEEDBACK IN REGULATING MUSCLE ACTIVITY STRENGTH

Mayer, W. P., Murray, A. J., Brenner-Morton, S., Jessell, T. M., Tourtellotte, W. G., & Akay, T. (2018). Role of muscle spindle feedback in regulating muscle activity strength during walking at different speed in mice. *Journal of Neurophysiology*, *120*(5), 2484–2497. https://doi.org/10.1152/jn.00250.2018

4.1 INTRODUCTION

In terrestrial legged animals, the stereotyped and rhythmic limb movements (step cycle) during locomotion can be divided into two phases, the swing and the stance. The swing phase starts with lifting the foot off the ground and moving it toward the direction of the locomotion in the air and ends with placing the foot back on the ground. Once the foot is placed on the ground, the stance phase starts, in which the foot stays stationary while the body moves in the direction of locomotion. Thus the limb carries the body weight and provides propulsion. In mammals, this limb movement is mainly achieved by the precisely patterned contraction pattern of multiple extensor and flexor muscles that move the hip, knee, and ankle joints (Akay, Tourtellotte, Arber, & Jessell, 2014; Engberg & Lundberg, 1969; Grillner, 2011; Rossignol, 2011). In a simplified version, extensor muscles are mostly activated during stance and flexor muscles during the swing phase. This coordinated action of muscles is in turn controlled by the patterned activity of pools of motoneurons (locomotor pattern) in the spinal cord. This locomotor pattern is known to be the result of the integrated function of a network of interconnected interneurons in the spinal cord (central pattern generator, CPG) and the sensory feedback from cutaneous and

proprioceptive systems in the periphery (McCrea, 2001; Pearson, 2004; Rossignol, Dubuc & Gossard, 2006).

Animals can move around their environment at different speeds to fulfill diverse purposes such as hunting, escape, migration, or foraging. When the locomotor speed is increased, the step cycle duration decreases. This is caused by a decrease in the stance phase duration, whereas the swing phase duration stays relatively constant (Grillner, 2011). Furthermore, electromyogram (EMG) activity recordings from flexor and extensor muscles during different speeds revealed that with increasing speed, the EMG activity of mainly the extensor muscles increases accordingly (Pierotti, Roy, Gregor, & Edgerton, 1989; Prilutsky, Herzog, & Allinger, 1994; Roy, Hutchison, Pierotti, Hodgson, & Edgerton, 1991; Walmsley, Hodgson, & Burke, 1978). However, the circuits that give rise to this speed-dependent regulation of extensor activity are not understood. One possibility is that the speed-dependent amplitude regulation is controlled by proprioceptive sensory feedback.

Experiments with walking cats and humans suggest that proprioceptive sensory feedback regulates the activity strength of extensor muscles during stance phase (Donelan, McVea, & Pearson, 2009; Donelan & Pearson, 2004a; Donelan & Pearson, 2004b; Grey, Nielsen, Mazzaro, & Sinkjaer, 2007; Sinkjaer, Andersen, Ladouceur, Christensen, & Nielsen, 2000). Experiments with humans suggest that extensor activity strength during walking is regulated by proprioceptive sensory feedback from the Golgi tendon organs (GTO) and from the muscle spindles (af Klint, Mazzaro, Nielsen, Sinkjaer, & Grey, 2010; Grey, Mazzaro, Nielsen, & Sinkjær, 2004; Grey et al., 2007; Mazzaro, Grey, & Sinkjær, 2005; Sinkjaer et al., 2000; Yang, Stein, & James, 1991). In contrast, experiments with cats

suggest that the extensor activity during stance is regulated by the GTO feedback, but no evidence has been found regarding the feedback from muscle spindles (Donelan et al., 2009; Donelan & Pearson, 2004a; Donelan & Pearson, 2004b). In this chapter, we present evidence that proprioceptive sensory feedback from the muscle spindles regulates the EMG activity of extensor muscles during stance and that this regulation is necessary for locomotion at higher speeds.

To address the role of proprioceptive sensory feedback from muscle spindles in the regulation of activity strength of extensor muscle during walking at different speeds, we recorded EMG activities of multiple muscles while mice walked on a treadmill at various speeds, as previously described (Akay et al., 2014). We hypothesize that "proprioceptive sensory feedback from muscle spindles is necessary for extensor muscle EMG activity upregulation during walking at different speeds." To address the global role of muscle spindles in speed-dependent amplitude modulation, we performed the same experiments with the *Egr3*$^{-/-}$ mice, in which muscle spindles fail to properly develop postnatally (Oliveira Fernandes & Tourtellotte, 2015; Tourtellotte & Milbrandt, 1998).

Furthermore, we developed a viral and mouse genetics-based strategy to acutely eliminated muscle spindles only from quadriceps femoris (QF; knee extensor muscles) or triceps surae muscles (TS; ankle extensor muscles). In these experiments, data from the same animal obtained before and after the removal of the muscle spindles were compared to gain insight into the role of the muscle spindle feedback from specific muscles in the speed-dependent amplitude modulation. Our data suggest that speed-dependent amplitude modulation

requires proprioceptive sensory feedback from the muscle spindles specifically from the TS, but not from the QF, muscle groups.

4.2 METHODS

4.2.1 Animals

The experiments were done on adult mice, ages ranging from 60 days to 90 days of either sex. None of the mice were trained prior to the experiments. All procedures were in accordance with the Canadian Council on Animal Care and were approved by the University Committee on Laboratory Animals at Dalhousie University.

4.2.2 Removal of Muscle Spindles

We used two methods to remove proprioceptive feedback from the muscle spindles. The first utilized the *Egr3* knock-out mice (*Egr3*$^{-/-}$) in which all muscle spindles are ablated (Chen, Tourtellotte, & Frank, 2002; Tourtellotte & Milbrandt, 1998). In these mice, the muscle spindles fail to form properly during development, whereas the proprioceptive feedback from the GTOs are left intact. The second method allowed us to acutely eliminate muscle spindle feedback from a subset of muscles (Figure 4.1). For this method, we used a mouse line that expresses the *cre*-recombinase under the control of the calcium-binding protein parvalbumin (Pv) expression (*Pv::cre*) (Hippenmeyer et al., 2005). To conditionally and selectively ablate proprioceptors, we generated adeno-associated virus (AAV) serotype 9 encoding diphtheria toxin receptor-green fluorescent protein (DTR-GFP) fusion in a Flex-

switch (AAV9-DTR-GFP) (Azim, Jiang, Alstermark, & Jessell, 2014). When injected into the muscle of *Pv::cre* animals, the AAV9 infects sensory neurons and expresses DTR-GFP in Pv^{+} proprioceptors.

We injected each one of the QF muscles or the TS muscles when the *Pv::cre* mice were 7 to 10 days old (P7–P10). As a control, AAV9 encoding only GFP was injected into the same muscle groups of the contralateral limb. After these AAV9 injections, *Pv::cre* mice were kept until adulthood when they underwent EMG implantation. EMG and kinematic data recordings were performed before and 5–15 days after intraperitoneal injection of diphtheria toxin (DTX; 400 ng dissolved in sterile phosphate buffer).

Figure 4. 1 Acute elimination of proprioceptive afferents from selected muscles. Adeno-associated virus (AAV) was used to deliver a *cre* conditional (flexed) gene encoding the receptor for diphtheria toxin (DTX) into specific muscle of a *Pv::cre* mouse, where parvalbumin (Pv) is selectively expressed in proprioceptive afferents and some interneurons. **A**: *Pv::cre* mice were injected at less than 2 weeks of age, infecting proprioceptive afferents and motoneurons innervating that muscle. Because motoneurons do not express Pv, the diphtheria toxin receptor (DTR) gene was only expressed in proprioceptive afferents. Once the mice were older than 50 days, electromyogram electrodes were implanted into their muscles and control recordings were performed. Their locomotor pattern was recorded again 5–15 days after intraperitoneal (IP) DTX injection. The locomotor patterns recorded during pre- and post-DTX sessions were compared. IN, interneurons; MN, motoneurons. **B**: confocal images of proprioceptive afferents innervating muscle spindle (*top*) and a Golgi tendon organ (GTO; *bottom*) from a vastus lateralis (VL) muscle. Afferent fibers were labeled with antibody staining against VGluT1. Control muscle is from the left hindlimb, which did not receive an AAV9 injection. Experimental muscle shown is from the right hindlimb after AAV9 and DTR injection. Notice that the typical anulospiral structure is degraded to some punctuated structures in the experimental limb after DTX injection, but the GTOs appear normal. Scale bars, 50 μm.

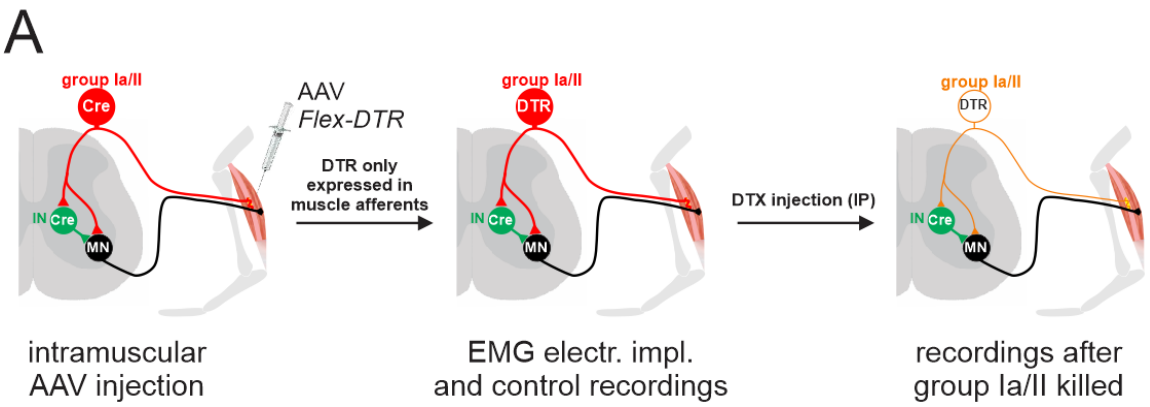
A
group Ia/II
Cre
IN
Cre
MN
AAV
Flex-DTR
DTR only
expressed in
muscle afferents
group Ia/II
DTR
IN
Cre
MN
DTX injection (IP)
group Ia/II
DTR
IN
Cre
MN
intramuscular
AAV injection
EMG electr. impl.
and control recordings
recordings after
group Ia/II killed

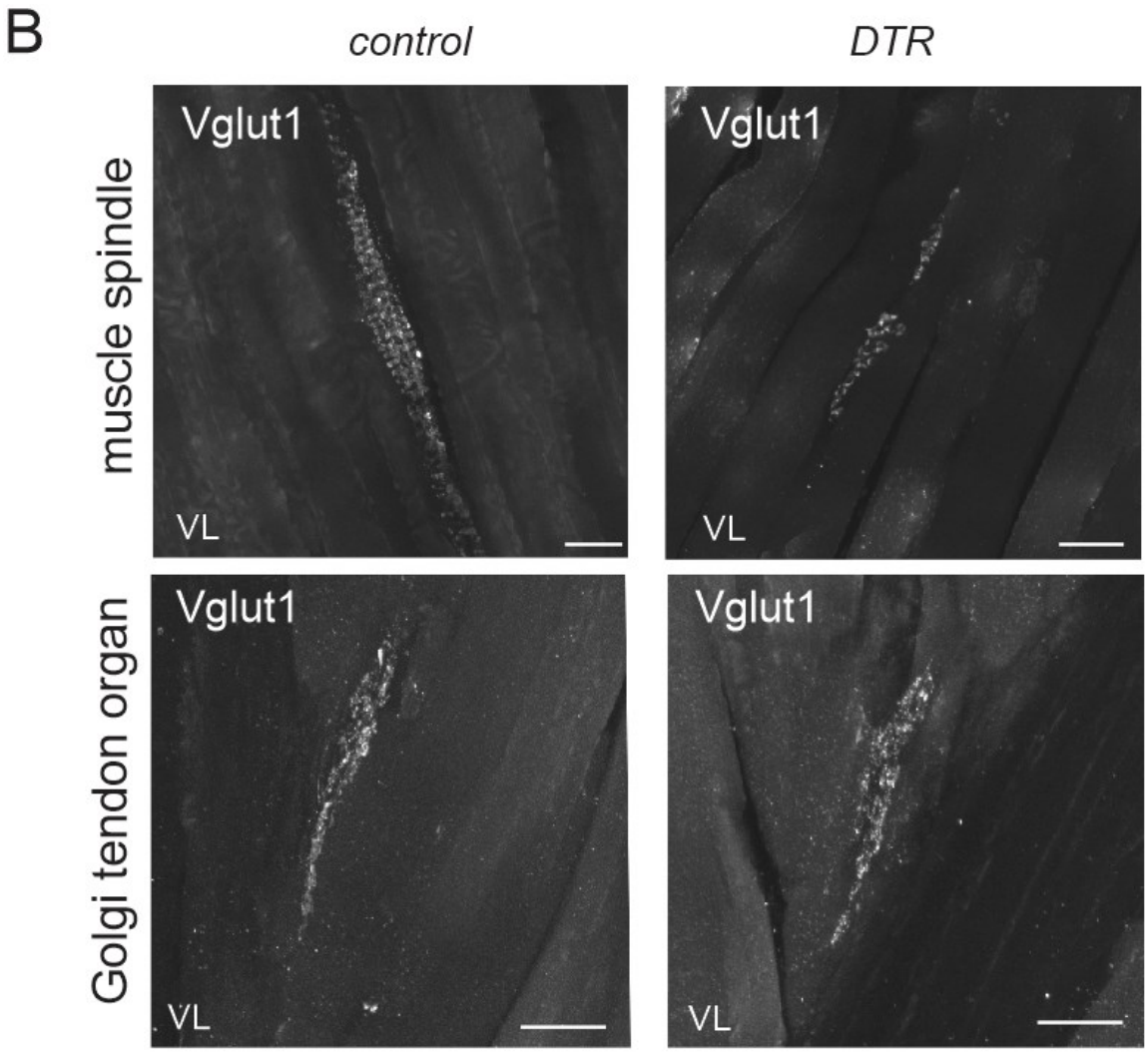
B
control
DTR
muscle spindle
Golgi tendon organ
Vglut1
VL
Vglut1
VL
Vglut1
VL
Vglut1
VL

4.2.3 Electrode Implantation Surgeries

Each wild type, *Egr3*$^{-/-}$, or *Pv::cre* mouse injected with AAV9-DTR-GFP received an electrode implantation surgery as previously described **(**Akay et al., 2014; Mayer & Akay, 2018). Briefly, the animals were anesthetized with isoflurane, ophthalmic eye ointment was applied to the eyes, and the skin of the mice was sterilized with three-part skin scrub using Hibitane, alcohol, and povidone-iodine. A set of six bipolar EMG electrodes were implanted in all experimental mice (Akay et al., 2006; Pearson, Acharya & Fouad, 2005) as follows: The neck region and the right hindlimb were shaved. Small incisions were made to the neck region and in the hindlimb above muscles. The electrodes were drawn subcutaneously from the neck incision to the limb incisions, and the headpiece connector was stitched to the skin around the neck incision.

The EMG recording electrodes were implanted into hip flexor (iliopsoas, Ip) and extensor (anterior biceps femoris, BF), knee flexor (semitendinosus, St) and extensor (vastus lateralis, VL), and ankle flexor (tibialis anterior, TA) and extensor (gastrocnemius, Gs). The incisions were closed, and buprenorphine (0.03 mg/kg) and ketoprofen (5 mg/kg) were injected subcutaneously as analgesics. Additional buprenorphine injections were performed at 12-h intervals for 48 h. The anesthetic was discontinued, and mice were placed in a heated cage for 3 days and then finally returned to their regular mouse rack. Food mash and hydrogel were provided for the first 3 days after the surgery. Handling of the mice was avoided until they were fully recovered. The first recording session was started no earlier than 10 days after electrode implantation surgeries.

4.2.4 Behavioral Recording Sessions

Following the full recovery from electrode implantation surgeries, the behavioral recordings were performed as previously described (Akay et al., 2006; Pearson et al., 2005). Under brief anesthesia with isoflurane, custom-made cone-shaped reflective markers (1–2 mm in diameter) were attached to the skin at the level of anterior tip of the iliac crest, hip, knee, ankle, and metatarsal phalangeal joint (MTP) and the tip of the fourth digit (toe). The anesthesia was discontinued and the mouse placed on the mouse treadmill (model 802; custom built in the workshop of the Zoological Institute, University of Cologne, Germany). The electrodes were connected to the amplifier (model 102; custom built in the workshop of the Zoological Institute, University of Cologne, Germany). We waited at least 5 minutes before the session started to allow the mouse to fully recover from anesthesia. The mouse started walking when the treadmill was turned on. The speed of the treadmill was changed, starting from 0.2 m/s and increasing to 0.6 m/s, a speed at which all wild type mice could walk. The walking mouse was filmed from the sagittal plane with a high-speed video camera (IL3; Fastec Imaging) at 250 frames/s, and video files were stored on the computer for later motion analysis. The EMG data were stored separately on the computer by using the Digitizer (Power 1401, Cambridge Electronic Design, Cambridge, UK) combined with Spike2 software (version 8; Cambridge Electronic Design). Only walking sequences where the mouse would walk stationary without drifting forward or backward, indicating equal walking speed and treadmill speed were considered for data analysis. These recordings were performed once with each wild type and *Egr3*$^{-/-}$ mouse.

In most of the experiments with the *Pv::cre* mice that received AAV9 injection, three sets of recordings on different days were performed before the DTX injection, and three sets of recordings were performed after DTX injection. The three recordings before and after DTX injections were used to ensure stable EMG recordings over multiple days. Because Pv is also expressed in some extrafusal muscle fibers (Celio & Heizmann, 1982) and AAV9 is known to also infect extrafusal muscle fibers (Katwal et al., 2013), we did histological assessments to show that in our experiments, DTX injection did not affect extrafusal muscle fibers (Figure 4.2; see discussion).

Figure 4. 2 No sign of muscle fiber degeneration in *Pv::cre* mice previously injected with adeno-associated virus serotype 9 (AAV9) to deliver gene encoding diphtheria toxin receptor (DTR) after diphtheria toxin (DTX) injection. **A**: fluorescence microscope images of a cross-section through a gastrocnemius (Gs) muscle previously injected with AAV9 to deliver *DTR-GFP* gene and after DTX injection. Parvalbumin (Pv)-expressing fibers (red; *left*) have a very healthy appearance in toluidine blue (TB) staining (*right*). Occasional fibers with centralized nuclei were observed in either Pv^+ (white arrow) and Pv^- (blue arrows) muscle fibers, indicating that this feature was independent of DTX effect. **B**: fluorescence images of muscle previously injected with AAV9 to deliver *DTR-GFP* gene and after DTX injection. The fibers that are expressing GFP are Pv^+ fibers that were infected with AAV9 (asterisks; *left*). The same fiber successfully infected with AAV9 and expressing the delivered *DTR-GFP* gene shows no sign of any degeneration (asterisks; *right*). Scale bars, 50 µm.

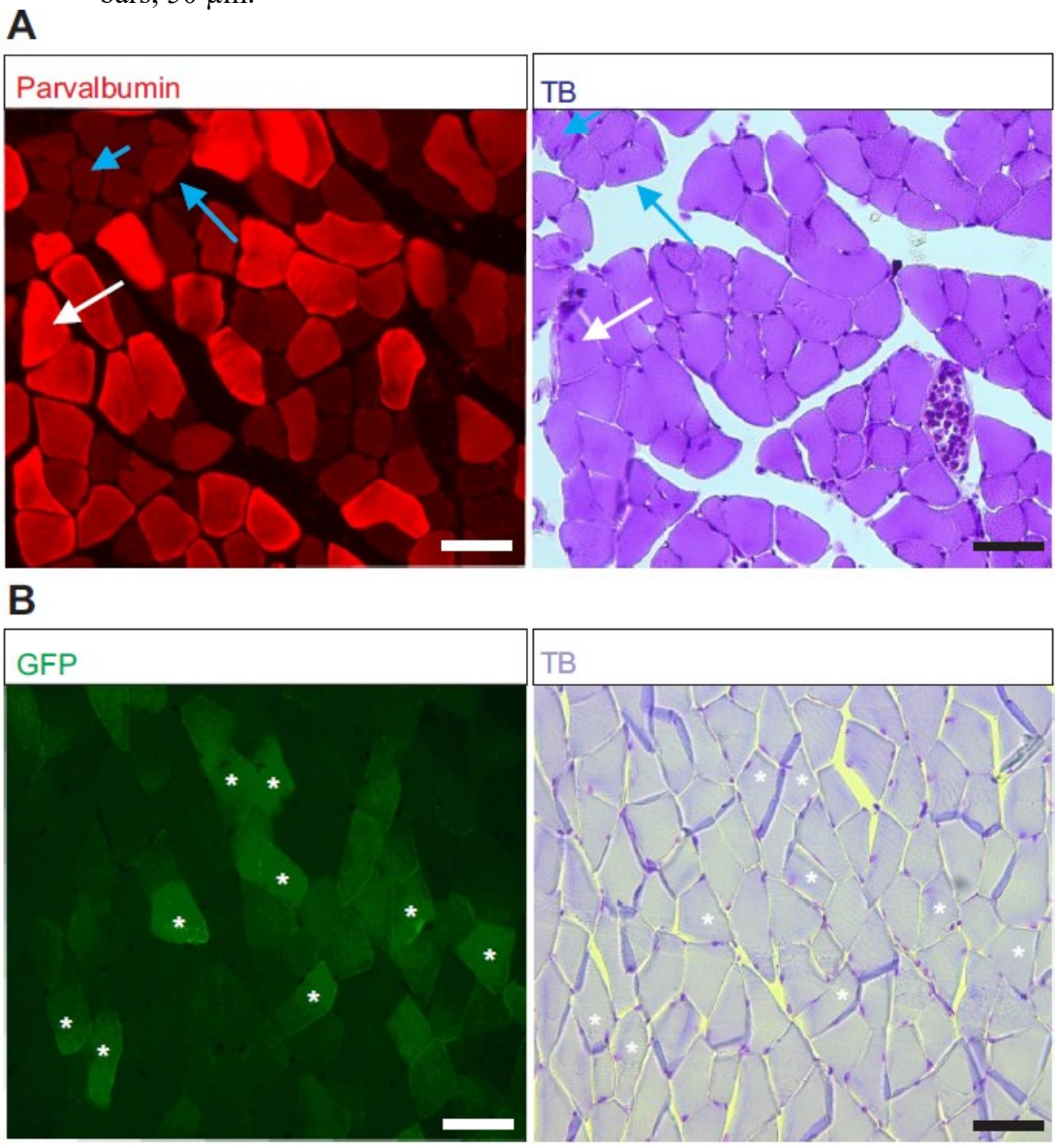

4.2.5 Immunohistochemistry

After each experiment where muscle spindle afferents were removed acutely by AAV9 and DTX injections in *Pv::cre* mice, the efficiency of muscle spindle removal was assessed with Immunohistology. After the last recording sessions following DTX injection, mice were euthanized with an intraperitoneal injection of pentobarbital sodium (40 mg/kg). After thoracotomy, the animals were perfused with 20 ml of saline solution followed by 10 ml of 4% paraformaldehyde (PFA) through the left cardiac ventricle. The Gs or the VL were dissected and then cryoprotected by immersion in 30% sucrose-PBS solution overnight at 4°C. The following day, the muscles were embedded in optimal cutting temperature compound (OCT) mounting medium, flash-frozen on dry ice, and stored at -80°C.

Muscle tissue was sectioned longitudinally at 80µm by using a cryostat (Leica CM3050 S), and the sections were placed on microscope slides. For immunofluorescence staining, the sections were washed in PBS to remove the OCT, incubated in blocking solution (PBS-1% BSA-0.3% Triton) for 1 h, and later incubated overnight with primary rabbit antibody against vesicular glutamate transporter 1 (anti-VGluT1, 1:8,000) (de Nooij et al., 2015). The next day, tissues received multiple washes in blocking solution and were incubated overnight at room temperature with secondary antibody (goat anti-rabbit conjugated to Alexa Fluor 488, 1:500; Life Technologies) in the blocking solution. The sections were washed with blocking solution, followed by a wash with PBS to remove the BSA. Finally, the microscope slides with the sections were coverslip using mounting medium (Permafluor).

4.2.6 Data Analysis

The kinematic parameters of walking were obtained from the video files using custom-made software written by Dr. Nicolas Stifani with ImageJ (KinemaJ) and R (KinemaR) (Bui, Stifani, Akay, & Brownstone, 2016; Fiander, Stifani, Nichols, Akay, & Robertson, 2017). The coordinates and the angular joint movements were then imported into the Spike2 files containing the EMG data by using a custom-written Spike2 script to analyze the kinematic and EMG data. All plots were created with Excel 2016 software and statistical analysis with the data analysis package for Excel (statistiXL; version 1.8). Student's *t*-test was used to compare data between wild type and *Egr3*$^{-/-}$ mice and for the walking at 0.2 and 0.4 m/s in wild type mice. Moreover, a *t*-test for paired data was used to compare data before and after DTX injection in *Pv::cre* mice injected with AAV9. The changes were considered statistically significant if $P < 0.05$.

4.3 RESULTS

4.3.1 Speed Dependent Amplitude Modulation in Wild Type Mice

To provide insights into the mechanisms of amplitude modulation, we first examined the muscle EMG activities of different muscles in wild type mice. None of the seven recorded wild type mice had any difficulty walking on the treadmill at speeds up to 0.6 m/s (Figure 4.3). In Figure 4.3A, kinematic and EMG recording data during three episodes of walking at 0.2, 0.4, and 0.6 m/s speed are illustrated including three, five, and seven swing phases (shaded backgrounds), respectively. As the walking speed increased, the step duration

decreased (Figure 4.3B). The decrease in the step duration was largely the result of a decrease in the stance phase and, to a lesser extent, a change in the swing duration (Figure 4.3B). Note also that the EMG activity recorded from the BF (hip extensor), VL (knee extensor), and the Gs (ankle extensor) increased with increased walking speed.

Figure 4. 3 Locomotor pattern during walking at different speeds in wild type mice. All wild type mice (n = 7) were able to walk on the treadmill up to the 0.6 m/s speed. **A**: angular movement of hip, knee, and ankle joints, toe coordinates represented as toe height and horizontal toe position relative to hip position (rel. toe_x; dashed horizontal line), and electromyogram activities of the 6 recorded flexor and extensor muscles at 3 different speeds are shown. Shaded background indicates swing phase. Ip, iliopsoas; BF, anterior biceps femoris; St, semitendinosus; VL, vastus lateralis; TA, tibialis anterior; Gs, gastrocnemius. **B**: bar graphs illustrating means and SD of step cycle period, swing duration, and stance duration at 3 different walking speeds. Notice that all parameters decrease with the increasing walking speed, with a stronger effect in cycle period and stance duration than in swing phase.

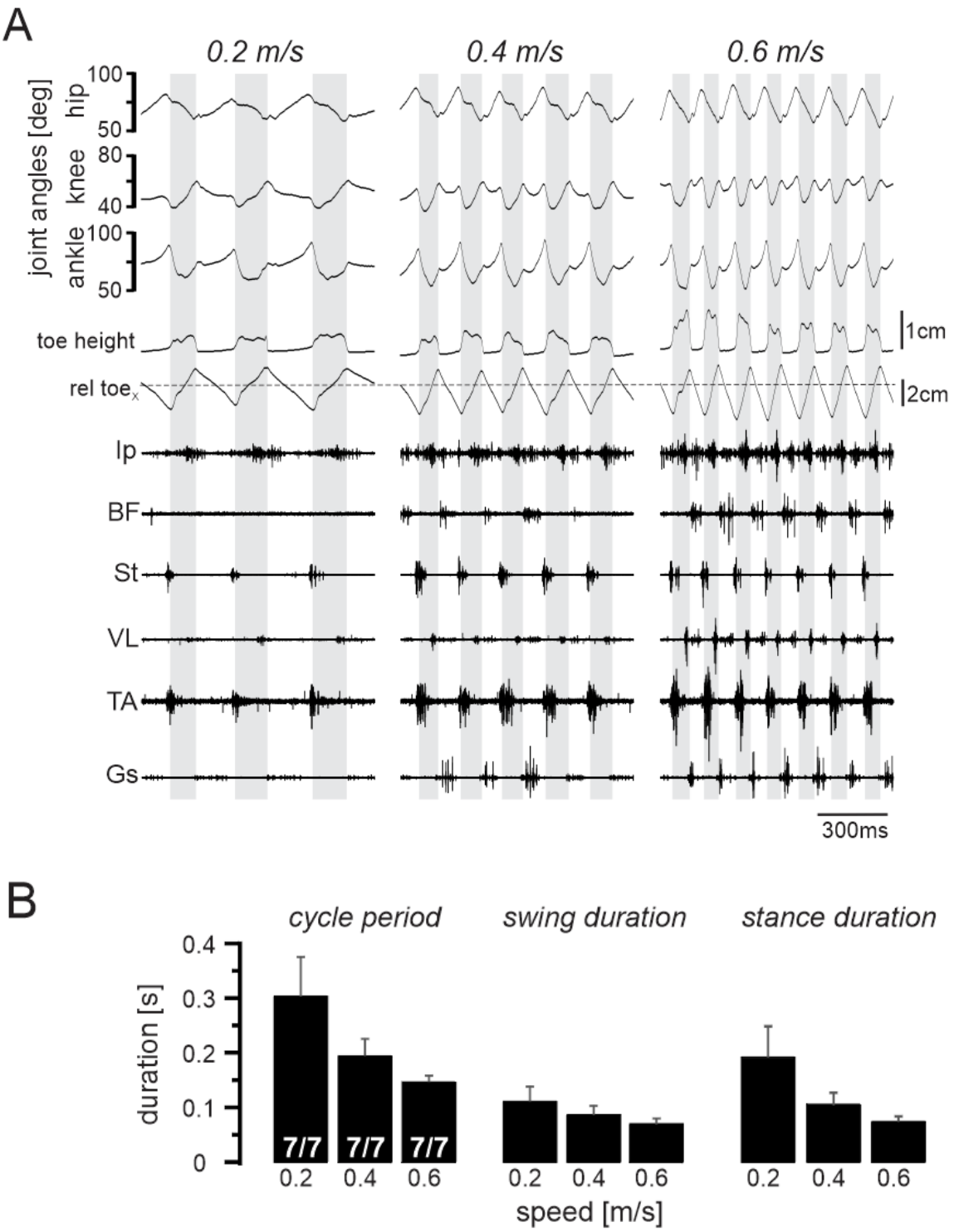
A
0.2 m/s
0.4 m/s
0.6 m/s
joint angles [deg]
hip
knee
ankle
100
50
80
40
100
50
toe height
rel toe$_x$
1cm
2cm
Ip
BF
St
VL
TA
Gs
300ms
B
cycle period
swing duration
stance duration
duration [s]
0.4
0.3
0.2
0.1
0
7/7
7/7
7/7
0.2
0.4
0.6
0.2
0.4
0.6
0.2
0.4
0.6
speed [m/s]

The increase in the extensor muscle activity was also shown in pooled average traces of the rectified EMG traces from all muscle in Figure 4.4, showing minor increase in the flexor muscles (*left* traces) but major upregulation in the extensor muscles (*right* traces). These data suggest that during walking, the EMG activity of the extensor muscles are upregulated in a speed-dependent manner.

Figure 4. 4 Electromyogram (EMG) activity in hindlimb muscles increases at higher walking speeds. Average EMG activities (rectified and smoothed) from all flexor (*left*) and extensor (*right*) muscles at different speeds (black, 0.2 m/s; yellow, 0.4 m/s; blue, 0.6 m/s) recorded in this study indicate that the EMG activity of extensor muscles increases at higher speeds. Durations of stance and swing are shown by horizontal bars (*top*) indicating averages ± SD. Ip, iliopsoas; BF, anterior biceps femoris; St, semitendinosus; VL, vastus lateralis; TA, tibialis anterior; Gs, gastrocnemius.

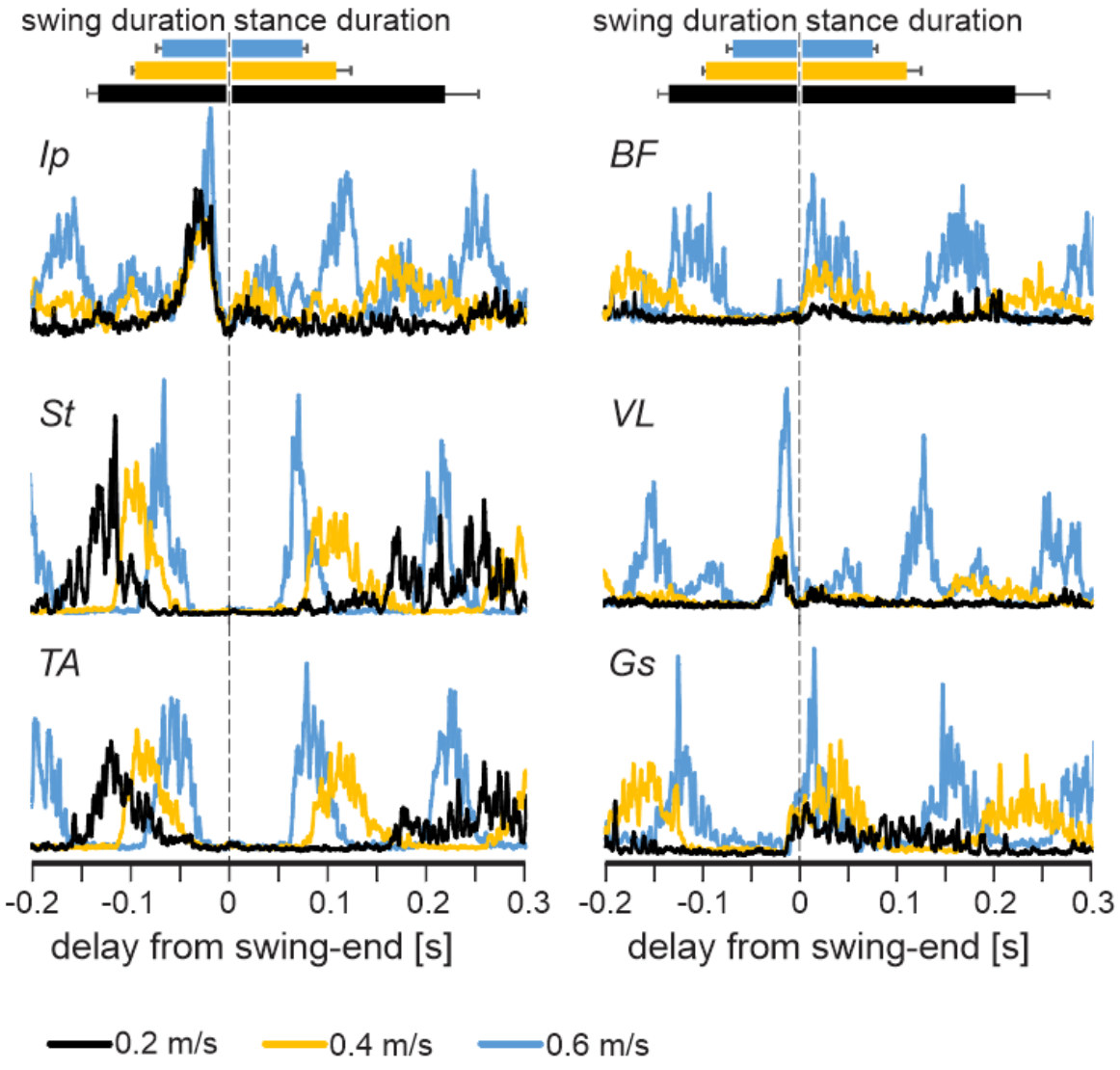

The maximal EMG activities normalized to the EMG amplitude at 0.2 m/s walking speed in individual animals are plotted against walking speed to more easily visualize the speed-dependent amplitude modulation (Figure 4.5). The EMG amplitude of all extensor muscles was upregulated depending on the speed of locomotion (Gs and VL, $P < 0.05$; BF, $P < 0.01$; after ANOVA). In contrast, the activity amplitude of the other flexor muscles was not dependent on the walking speed, except for that of the TA muscle ($P < 0.05$; after ANOVA).

Figure 4. 5 Speed-dependent amplitude modulation of extensor electromyogram (EMG) activities in wild type mice. Maximal EMG activities (peak-to-peak amplitude, PTP ampl.) in all recorded flexor (*left*) and extensor (*right*) muscles, normalized (norm.) to the maximal activity at 0.2 m/s as a function of walking speed. Note that activity in extensor muscles increases with increasing speed, but flexor muscle activities remain relatively unchanged. Colors indicate individual animals (n = 7). Ip, iliopsoas; BF, anterior biceps femoris; St, semitendinosus; VL, vastus lateralis; TA, tibialis anterior; Gs, gastrocnemius.

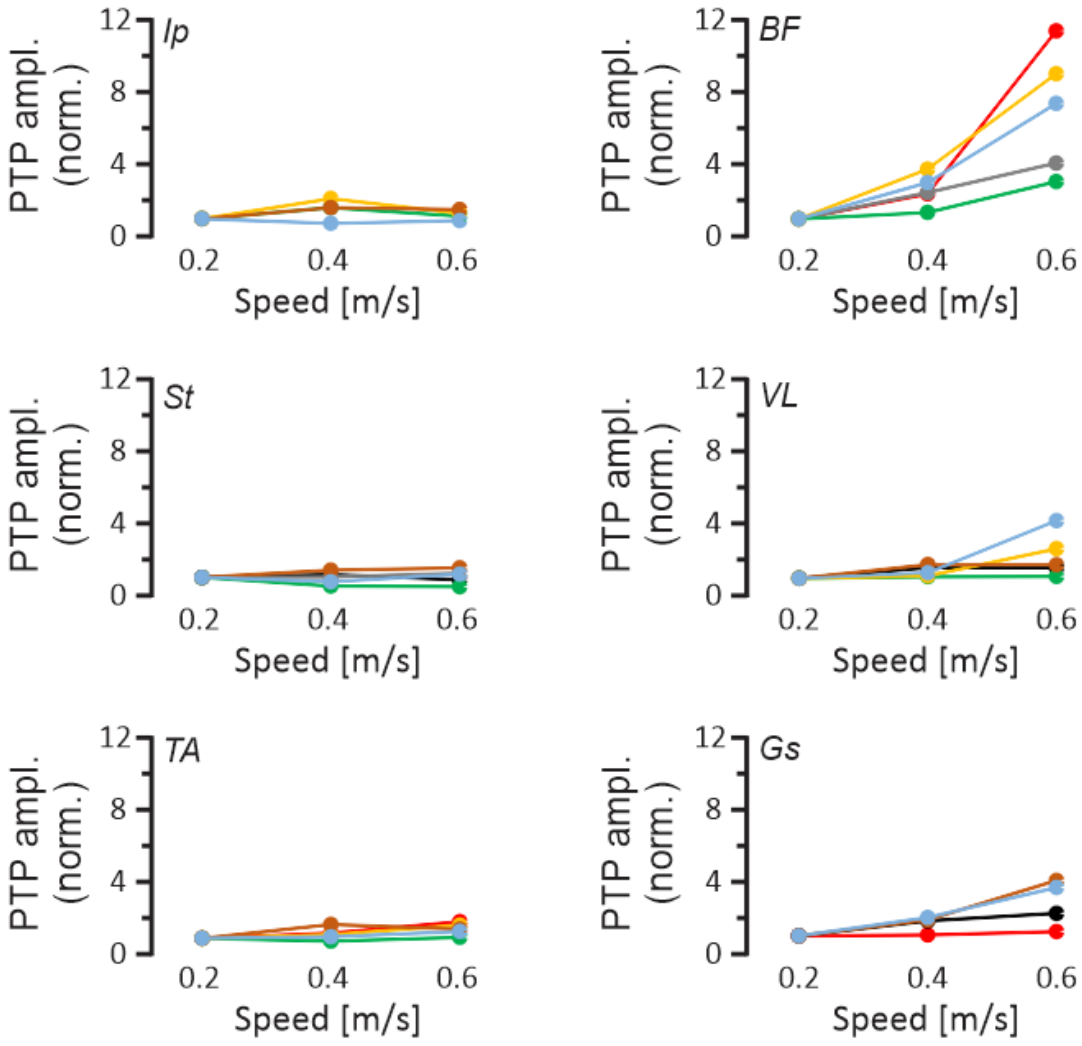

4.3.2 Speed Dependent Amplitude Modulation is Compromised in *Egr3* $^{-/-}$ Mice

To address the role of proprioceptive sensory feedback from muscle spindles in the speed-dependent modulation of muscle activity, we measured EMG signals from hindlimb muscles during walking at different treadmill speeds in *Egr3*$^{-/-}$ mice. In contrast to wild type mice, none of the seven *Egr3*$^{-/-}$ mice could walk at speeds higher than 0.4 m/s, and only five of seven mice could reach the 0.4 m/s speed. The kinematic and EMG recording data during two episodes of walking at 0.2 and 0.4 m/s speeds, shown in Figure 4.6A, that include four and five swing phases (shaded backgrounds), respectively. As in wild type mice, the step duration decreased as the walking speed increased from 0.2 to 0.4 m/s (Figure 4.6B). Furthermore, in the *Egr3*$^{-/-}$ mice, the decrease in the step duration was the result of the decreasing stance duration with lesser contribution of a change in the swing duration, similar to that in wild type animals (Figure 4.6B). Comparing the duration from *Egr3*$^{-/-}$mice and wild type mice revealed that the cycle periods and the swing durations were significantly shorter in *Egr3*$^{-/-}$ mice than in wild type mice. Stance duration, however, was not significantly different at 0.2 m/s but was significantly shorter at 0.4 m/s in *Egr3*$^{-/-}$ mice compared with wild type mice ($P < 0.05$). One possible explanation for the altered swing phase with minor change in stance phase is that the lack of muscle spindle feedback may be compensated by GTO signaling during stance (Akay et al., 2014). These data suggest that proprioceptive sensory feedback from the muscle spindles is important or regulating the temporal characteristics of hindlimb movement during walking at different speeds. Further examination of extensor muscle activity revealed that the strength of the EMG signal of each extensor muscle did not change considerably when *Egr3*$^{-/-}$ mice increased walking speed from 0.2 to 0.4 m/s (Figure 4.6A). This missing upregulation of the extensor

muscles is illustrated in Figure 4.7, where the pooled averages of the rectified EMG activities from flexor (*left*) and extensor muscles (*right*) during walking at 0.2 and 0.4 m/s are shown. Our data, therefore, suggest that in the absence of muscle spindles, mice are unable to reach walking speeds >0.4 m/s. Furthermore, when they do increase their walking speed, there is no speed-dependent amplitude modulation of extensor muscles.

Figure 4. 6 Locomotor pattern during walking at different speeds in *Egr3*$^{-/-}$ mice. None of the *Egr3*$^{-/-}$ mice would walk at 0.6 m/s, and only 5 of 7 could walk at 0.4 m/s. **A**: hip, knee, and ankle joint movements, along with toe height and horizontal toe position relative to hip position (rel. toe_x; dashed horizontal line) and electromyogram activities of the 6 recorded flexor and extensor muscles at 3 different speeds are shown. Shaded background indicates swing phase. Ip, iliopsoas; BF, anterior biceps femoris; St, semitendinosus; VL, vastus lateralis; TA, tibialis anterior; Gs, gastrocnemius. **B**: all means and SD of step cycle period, swing duration, and stance duration at 3 different walking speeds in the *Egr3*$^{-/-}$ mice were smaller than the same parameters in wild type mice. *$P < 0.05$; **$P < 0.01$; ***$P < 0.001$; ns, not significant (after Student's *t*-test to detect statistical significance in differences between these parameters with the wild type parameters shown in Figure 4.2).

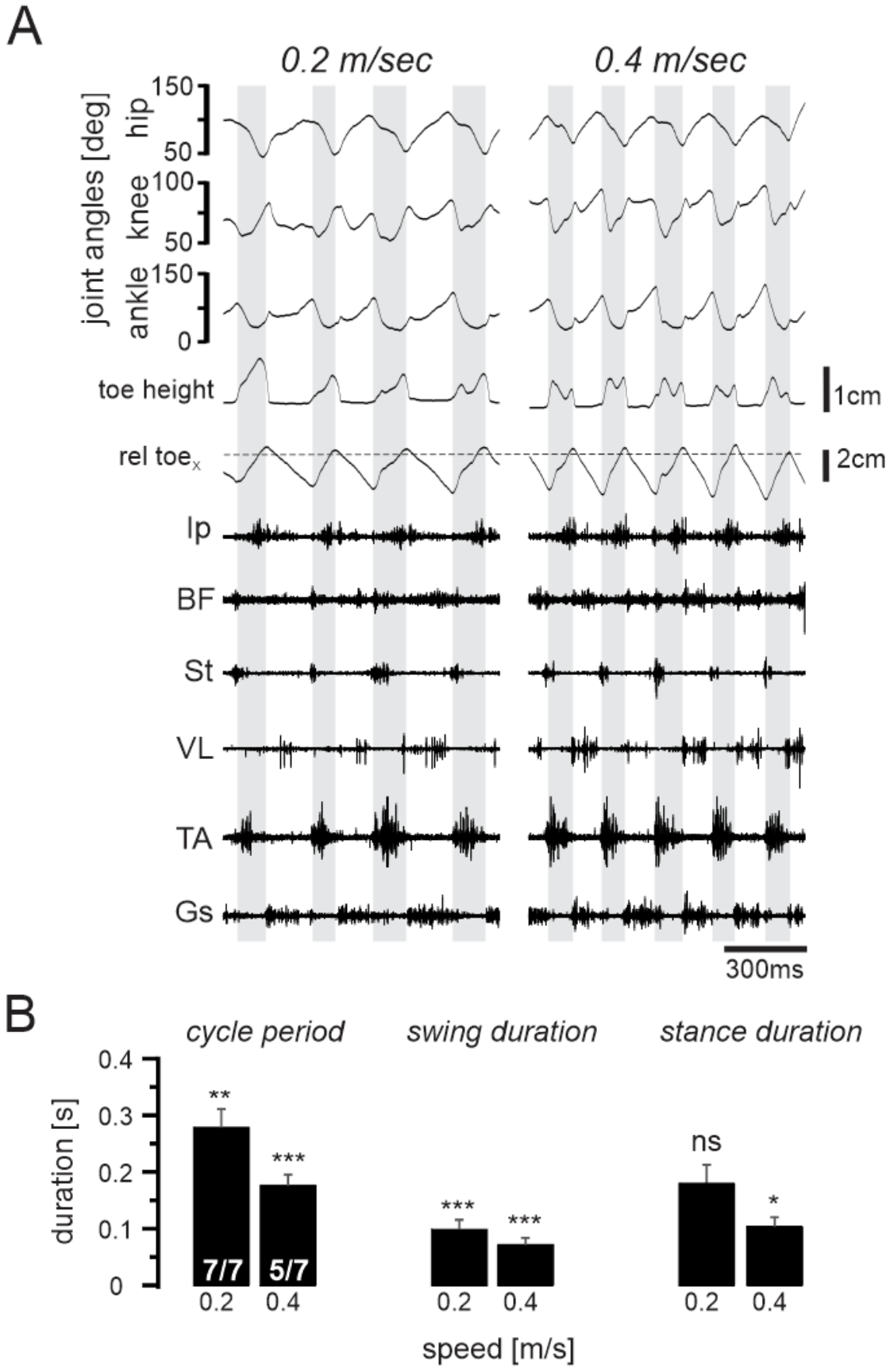
A
0.2 m/sec
0.4 m/sec
joint angles [deg]
hip
knee
ankle
150
50
100
50
150
0
toe height
1cm
rel toe$_x$
2cm
Ip
BF
St
VL
TA
Gs
300ms
B
cycle period
swing duration
stance duration
duration [s]
0.4
0.3
0.2
0.1
0
**
***
***
***
ns
*
7/7
5/7
0.2
0.4
0.2
0.4
0.2
0.4
speed [m/s]

Figure 4. 7 Electromyogram (EMG) activity in extensor muscles does not increase as the walking speed increases from 0.2 to 0.4 m/s in *Egr3*$^{-/-}$ mice. Average EMG activities (rectified and smoothed) from all flexor (*left*) and extensor (*right*) muscles recorded at different speeds (black, 0.2 m/s; yellow, 0.4 m/s) indicate that the EMG activity of extensor muscles increases at higher speeds. Durations of stance and swing are shown by horizontal bars (*top*) indicating averages ± SD. Ip, iliopsoas; BF, anterior biceps femoris; St, semitendinosus; VL, vastus lateralis; TA, tibialis anterior; Gs, gastrocnemius.

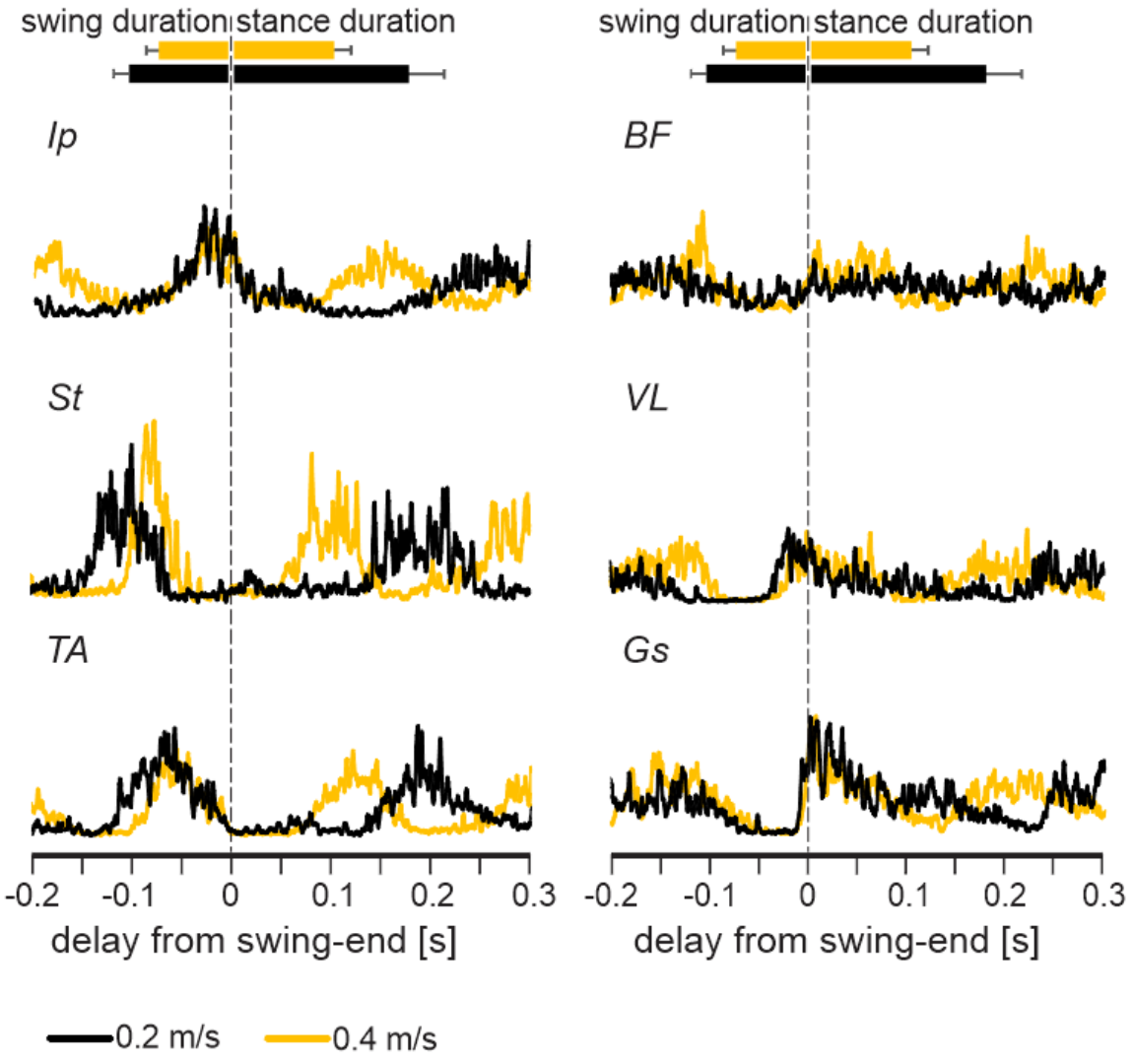

Comparison of maximal EMG activities in wild type mice and *Egr3*$^{-/-}$ mice during walking at 0.2 and 0.4 m/s revealed that the amplitude modulation in hip extensor muscle was reduced (Figure 4.8). When the overall increases in the amplitudes at 0.4 m/s were compared between *Egr3*$^{-/-}$ and wild type mice, only the amplitude modulation in BF activity was significantly different. When wild type mice walked at 0.4 m/s, the BF EMG amplitude increased, on average, 260 ± 88% (SD). In *Egr3*$^{-/-}$ mice, the EMG amplitude increase was 142 ± 42%, which was statistically smaller (P = 0.045, Student's t-test; Figure 4.8). There were no significant differences in VL (wild type: 138 ± 29%; *Egr3*$^{-/-}$:168 ± 73%; P = 0.43) or Gs (wild type: 170 ± 44%; *Egr3*$^{-/-}$: 131 ± 68%; P = 0.34). We could not detect any significant change in EMG amplitudes at 0.4 m/s in wild type vs. *Egr3*$^{-/-}$ mice in any of the recorded flexor muscles (Ip: P = 0.24; St: P = 0.13; TA: P = 0.44). These data suggest that in the five of seven *Egr3*$^{-/-}$ mice that could walk at 0.4 m/s, the increase in extensor EMG activity was compromised but strong and consistent enough to be statistically significant only in the hip extensor muscle. Our data suggest that the speed-dependent increase of the hip extensor EMG activity requires proprioceptive sensory feedback from the muscle spindles. In the absence of feedback from muscle spindles, the hip extensor amplitude modulation is compromised, preventing the animal from reaching higher walking speeds.

Figure 4. 8 Speed-dependent amplitude modulation of extensor electromyography (EMG) activities is compromised in *Egr3*$^{-/-}$ mice. Maximal EMG activities (peak-to-peak amplitude, PTP ampl.) in all recorded flexor (*left*) and extensor (*right*) muscles, normalized (norm.) to the maximal activity at 0.2 m/s at 0.2 and 0.4 m/s walking speeds in individual (color-coded) *Egr3*$^{-/-}$ mice (n = 7). Each color represents data from one animal. Based on the Student's t-test, only in biceps femoris (BF) muscle was the amplitude modulation at 0.4 m/s sufficiently weaker in *Egr3*$^{-/-}$ mice compared with wild type mice to reach statistical significance (*P < 0.05). Ip, iliopsoas; St, semitendinosus; VL, vastus lateralis; TA, tibialis anterior; Gs, gastrocnemius.

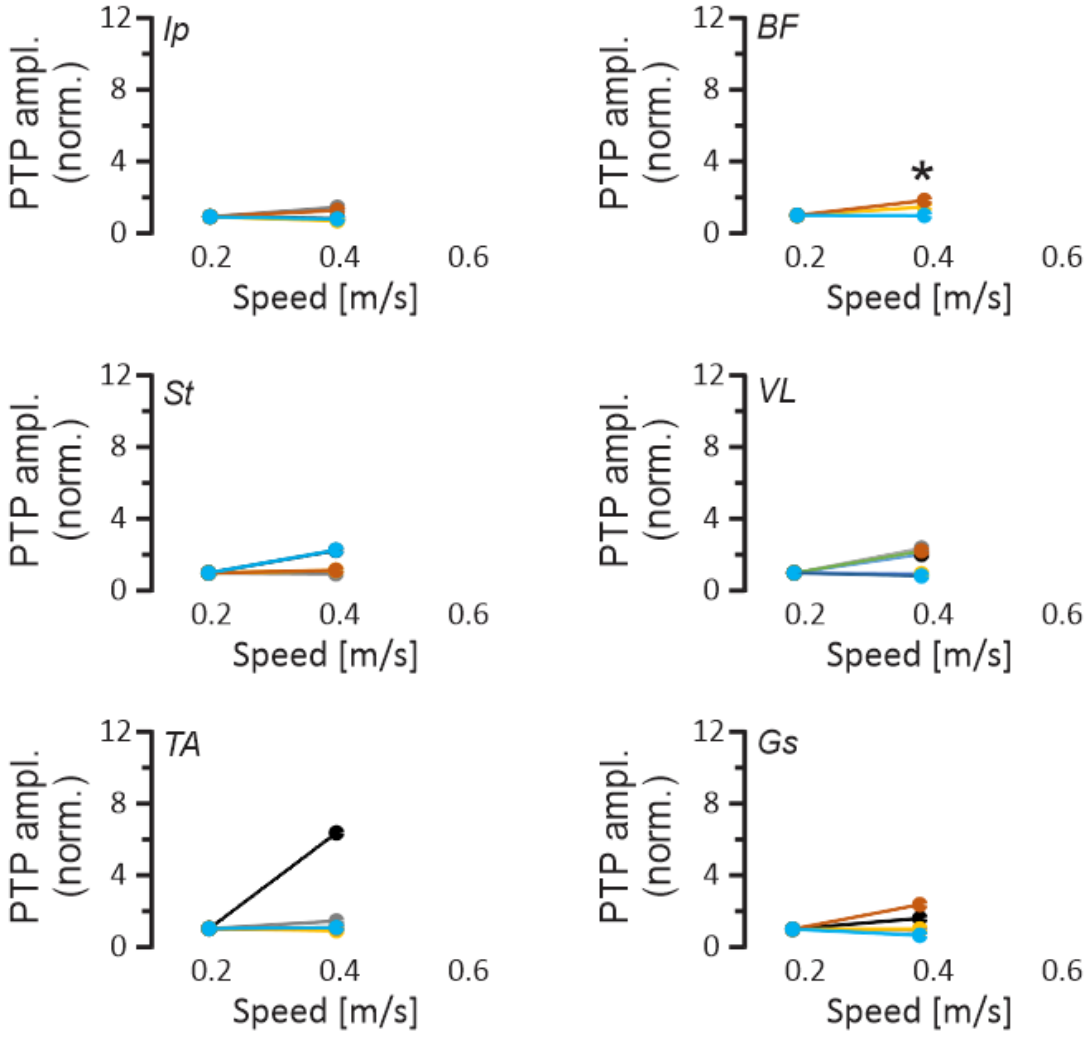

4.3.3 Muscle Spindle Feedback Specifically from The TS Muscle Group Is Particularly Important in Speed Dependent Amplitude Modulation

How is the information from the muscle spindle processed by the central nervous system to achieve the speed-dependent amplitude modulation of the extensor muscle activities? We reasoned that one possibility might be that information signaling individual joint proprioception could affect the amplitude modulation of the extensor muscles of the same joints (local processing). Alternatively, the information from muscle spindles of multiple joints could be collectively processed in the central nervous system to regulate all or a larger group of the extensor muscles (global processing). To differentiate between these two possibilities, we selectively removed feedback from either the ankle extensor TS muscles (including Gs muscles) or the knee extensor QF muscles (including VL muscle) and measured the amplitude modulation as described above.

If the information from the muscle spindles is processed locally, elimination of the muscle spindles only from the TS muscles should selectively affect speed-dependent amplitude modulation only in Gs muscle, which is one of the three TS muscles. To ensure that with this method we were effectively removing muscle spindle innervation, we counted all the afferent endings at the muscle spindles in the Gs muscle of the right limb and the left limb (Figure 4.9A). The left limb received AAV9 injections that only express GFP and did not envelop the gene that encodes the DTR (control limb), and therefore no ablation of nerve endings after the DTX infection. The right limb was injected with AAV9 enveloping the gene that encodes the DTR (experimental limb), which would affect the nerve endings after the DTX infection. After the final post-DTX recording session was performed, we counted the VGluT1-positive afferent endings at muscle spindles and the GTOs in the left (control)

and right (experimental) limbs. The results suggested that, on average, 55 ± 23% of the muscle spindle afferents in the Gs muscle were eliminated after DTX injection, whereas GTOs were not affected (Figure 4.9A).

The averaged EMG traces from all recorded muscles before and after DTX injection to acute elimination of proprioceptive feedback from muscle spindles from only the TS muscles are illustrated in Figure 4.9B. Note that in all muscles and at all speeds, pre-DTX and post-DTX EMG traces overlapped, except for the Gs and, to a lesser extent, the VL and TA muscles. These three muscles showed reduced activity already at 0.2 m/s speed, and the difference increased with increasing locomotor speed in Gs and VL, whereas the difference diminished in TA at 0.6 m/s. These observations were consistent when EMG traces from individual animals were investigated. That is, in seven of nine Gs recordings and in five of nine TA recordings, the speed-dependent amplitude modulation was absent. Moreover, in VL muscle the amplitude modulation was present but less prominent in three of four recordings and absent in the one remaining recording. Our data suggest that acute elimination of muscle spindles from only TS muscles reduced amplitude modulation in two distal extensor muscles, the VL and Gs, and partly in one of the distal flexor muscles, the TA.

Figure 4. 9 Acute elimination of the muscle spindle afferents only from triceps surae (TS) muscle group affects speed-dependent amplitude modulation in distal extensor muscles. **A**: graphs show that, on average, 55 ± 23% (mean ± SD) of afferent endings at muscle spindles (GrIa/II; *left*) were degenerated in the gastrocnemius (Gs) muscle (**$P < 0.01$ after paired *t*-test), whereas no difference (ns) was found in the number of afferents to Golgi tendon organs (GrIb; *right*). Comparisons were made between the right limbs (control) and the left limbs (experimental). **B**: average electromyogram (EMG) activities (rectified and smoothed) from all recorded muscles at different speeds recorded before (black) and after (red) the elimination of muscle spindles in TS muscle group through diphtheria toxin (DTX) injection. Note that the Gs EMG traces after removal of muscle spindles (red trace) in TS are much lower than before removal (black trace) at 0.4 and 0.6 m/s. In vastus lateralis (VL), there is a milder change that is more obvious only at 0.6 m/s. Durations of swing and stance are shown by horizontal bars (*top*) indicating averages ± SD. **$P < 0.01$; ***$P < 0.001$; ns, not significant (after paired *t*-test). Ip, iliopsoas; BF, anterior biceps femoris; St, semitendinosus; TA, tibialis anterior.

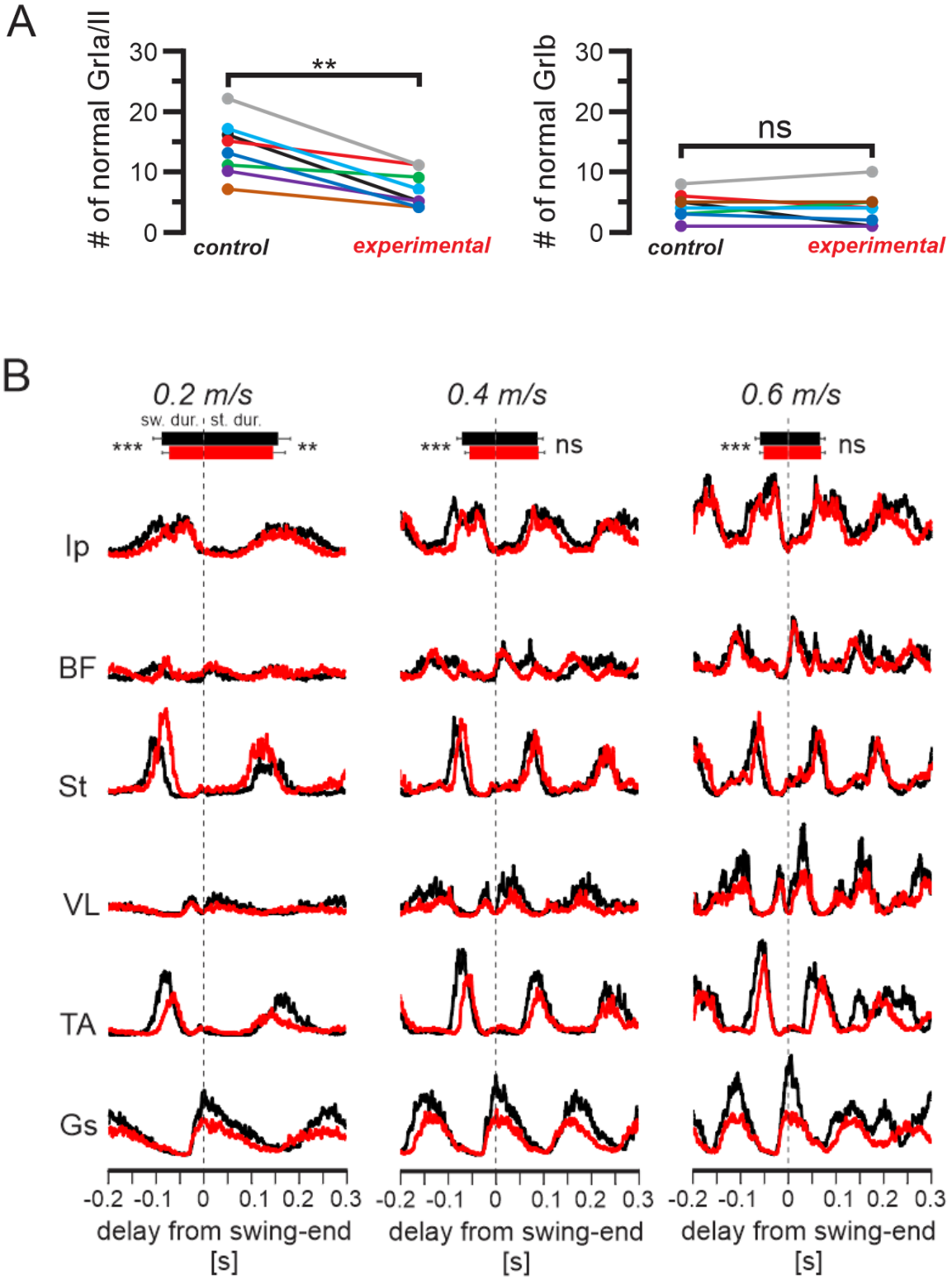
A
# of normal GrIa/II
30
20
10
0
**
control
experimental
# of normal GrIb
ns
B
0.2 m/s
0.4 m/s
0.6 m/s
sw. dur.
st. dur.
***
**
ns
Ip
BF
St
VL
TA
Gs
-0.2 -0.1 0 0.1 0.2 0.3
delay from swing-end
[s]

As in Figure 4.5 and 4.8, the maximum of rectified EMG activity in each step was averaged and normalized to the average amplitude of that value at 0.2 m/s and is plotted as a function of treadmill speed before and after the DTX injection (Figure 4.10A). The values at each speed were then compared before and after the DTX injection using a paired *t*-test. Only the amplitude increase at Gs muscle at 0.6 m/s was significantly compromised after the removal of muscle spindle feedback from the TS muscles by DTX injection (pre-DTX: 229 ± 156%, post-DTX: 175 ± 125%, $P = 0.018$). There was no difference in the amplitude modulation of all other recorded muscles. Analysis of the cycle period, swing duration, and stance duration revealed that cycle period and swing duration consistently decreased after removal of muscle spindle feedback from TS muscles, but changes in stance duration were limited to 0.2 m/s only (Figure 4.10B). This result suggests that muscle spindle feedback from the TS muscles mainly regulates the amplitude modulation selectively in the one TS muscle that was recorded in this experiment: the Gs muscle.

Figure 4. 10 Decline of speed-dependent amplitude modulation is only statistically significant in gastrocnemius (Gs) muscle after acute removal of muscle spindle afferents from the triceps surae (TS) muscles. **A**: maximal electromyogram activities (peak-to-peak amplitude, PTP ampl.) in all recorded flexor (*left*) and extensor (*right*) muscles, normalized norm.) to the maximal activity at all 3 walking speeds in individual (color-coded) *Pv::cre* mice in which TS muscle groups were infected with adeno-associated virus before and after diphtheria toxin (DTX) injection. Each color represents data from one animal. Based on the paired *t*-test, the decrease in amplitude modulation at 0.6 m/s was only statistically significant (*$P < 0.05$) for Gs muscle. **B**: means and SD of step cycle period, swing duration, and stance duration at 3 different walking speeds before (black) and after (red) DTX injection indicate that after DTX injection, cycle period and swing duration decreased at all speeds, whereas stance duration only decreased at 0.2 m/s. **$P < 0.01$; ***$P < 0.001$; ns, not significant (after paired *t*-test). Ip, iliopsoas; BF, anterior biceps femoris; St, semitendinosus; VL, vastus lateralis; TA, tibialis anterior.

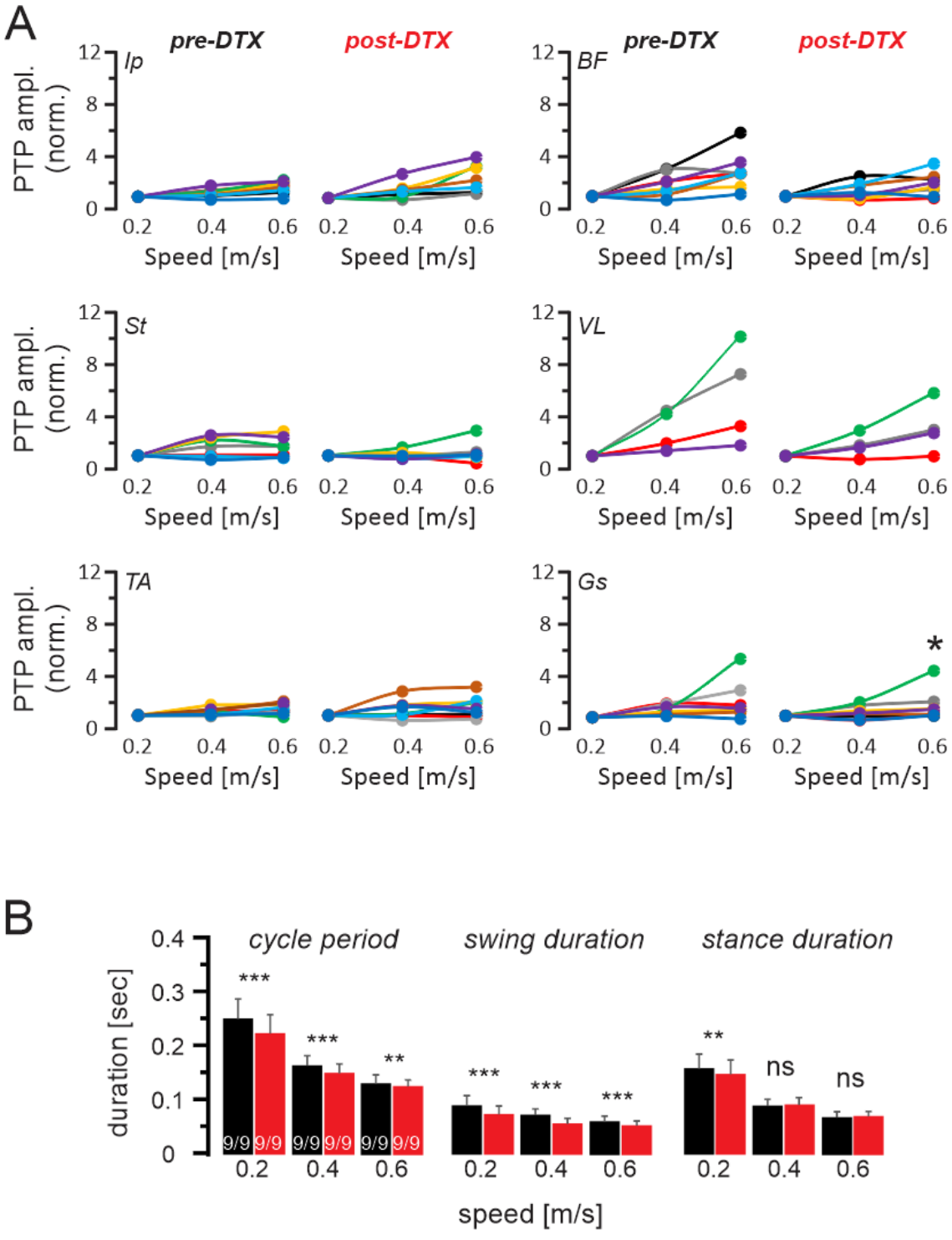
A
pre-DTX
post-DTX
pre-DTX
post-DTX
Ip
BF
St
VL
TA
Gs
PTP ampl. (norm.)
Speed [m/s]
*
B
cycle period
swing duration
stance duration
duration [sec]
***
**
ns
9/9
speed [m/s]

To address the question of whether the amplitude modulation was achieved by muscle spindles only from the TS group, we performed another set of experiments where muscle spindle afferents only to the QF muscles were removed. As for the Gs muscle presented in Figure 4.9A, we counted the afferent endings at muscle spindles and the GTOs. Similar to the Gs muscles, we found a 73 ± 10% reduction of muscle spindle afferents in the VL muscles after DTX injection, whereas the GTOs were not affected (Figure 4.11A).

The average EMG traces from the recorded muscles before and after DTX injection to remove muscle spindles only from QF muscles are illustrated in Figure 4.11B. After the elimination of the proprioceptive sensory feedback from muscle spindles of the QF muscles, no visual effect could be detected on the speed-dependent amplitude in any of the recorded muscles. As for the Gs recordings, these observations were consistent when EMG traces from individual animals were investigated. That is, the speed-dependent amplitude modulation was present in all recorded extensor muscles. This finding suggests that proprioceptive sensory feedback from the QF muscle spindles are not used to regulate the activity strength in any of the recorded muscles.

Figure 4. 11 Acute elimination of the muscle spindle afferents only from the quadriceps femoris (QF) muscle group does not cause a systematic change in speed-dependent amplitude modulation. **A**: graphs show that, on average, 73 ± 10% (mean ± SD) of afferent endings at muscle spindles (GrIa/II; *left*) were degenerated in the vastus lateralis (VL) muscle (**$P < 0.01$ after paired *t*-test), whereas no differences were found in the afferents to the Golgi tendon organs (GrIb; *right*). Comparisons were made between the right limbs (control) and the left limbs (experimental). **B**: average electromyogram (EMG) activities (rectified and smoothed) from all recorded muscles at different speeds recorded before (black) and after (red) the elimination of muscle spindles in the QF muscle group through diphtheria toxin injection. Notice that all black and red EMG traces overlap at all speeds. Durations of stance and swing are indicated by horizontal bars (*top*) indicating averages ± SD. **$P < 0.01$; ns, not significant (after paired *t*-test). Ip, iliopsoas; BF, anterior biceps femoris; St, semitendinosus; TA, tibialis anterior.

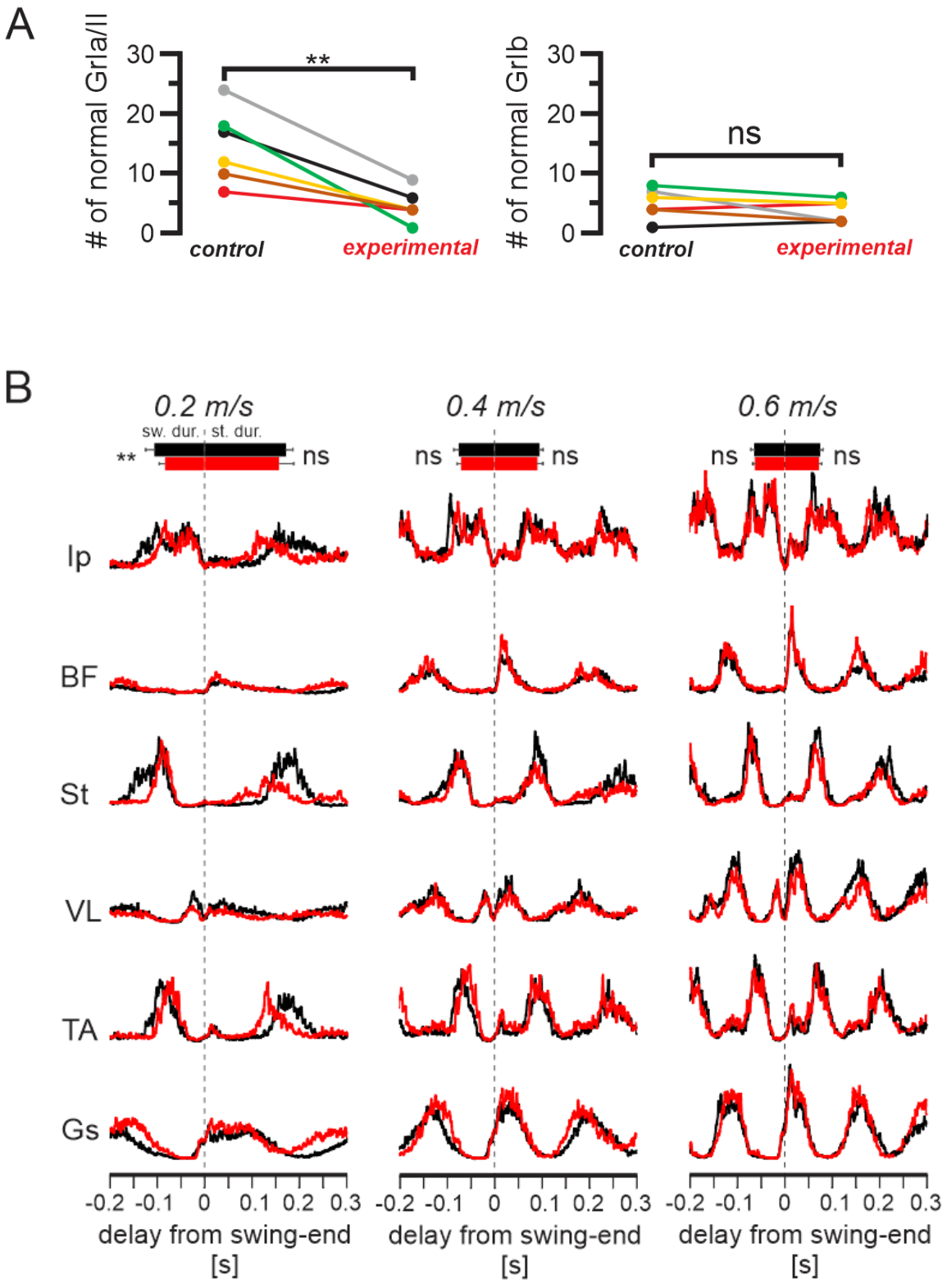
A
# of normal GrIa/II
30
20
10
0
**
control
experimental
# of normal GrIb
ns
B
0.2 m/s
0.4 m/s
0.6 m/s
sw. dur.
st. dur.
**
ns
Ip
BF
St
VL
TA
Gs
-0.2 -0.1 0 0.1 0.2 0.3
delay from swing-end [s]

To quantify this observation, we analyzed the maximum EMG activity in all muscles at different speeds before and after DTX injection (Figure 4.12). Note that the changes in amplitude modulation were not statistically significant in any of the recorded muscles (Figure 4.12A). Following the removal of muscle spindle feedback from the QF muscles, a consistent decrease was only detected in cycle period, whereas only a minor change in swing duration limited to 0.2 m/s was observed (Figure 4.12B). No change could be detected in stance duration following DTX injection (Figure 4.12B). These data confirm that muscle spindle feedback from QF muscles is not used in speed-dependent amplitude regulation.

Figure 4. 12 Decline of speed-dependent amplitude modulation is not statistically significant in any muscle after acute removal of muscle spindle afferents from the quadriceps femoris (QF) muscles. **A**: maximal electromyogram activities (peak-to-peak amplitude, PTP ampl.) in all recorded flexor (*left*) and extensor (*right*) muscles, normalized to the maximal activity at all 3 walking speeds in individual (color-coded) *Pv::cre* mice in which QF muscles were infected with adeno-associated virus before and after diphtheria toxin (DTX) injection. Based on the paired *t*-test, amplitude modulation did not change significantly change after DTX injection. **B**: means and SD of step cycle period, swing duration, and stance duration at 3 different walking speeds before (black) and after (red) DTX injection indicates that after DTX injection, cycle period decreased at all speeds whereas swing duration only decreased at 0.2 m/s. No change could be detected in stance duration at any speed. **P* < 0.05; ***P* < 0.01; ns, not significant (after paired *t*-test). Ip, iliopsoas; BF, anterior biceps femoris; St, semitendinosus; VL, vastus lateralis; TA, tibialis anterior; Gs, gastrocnemius.

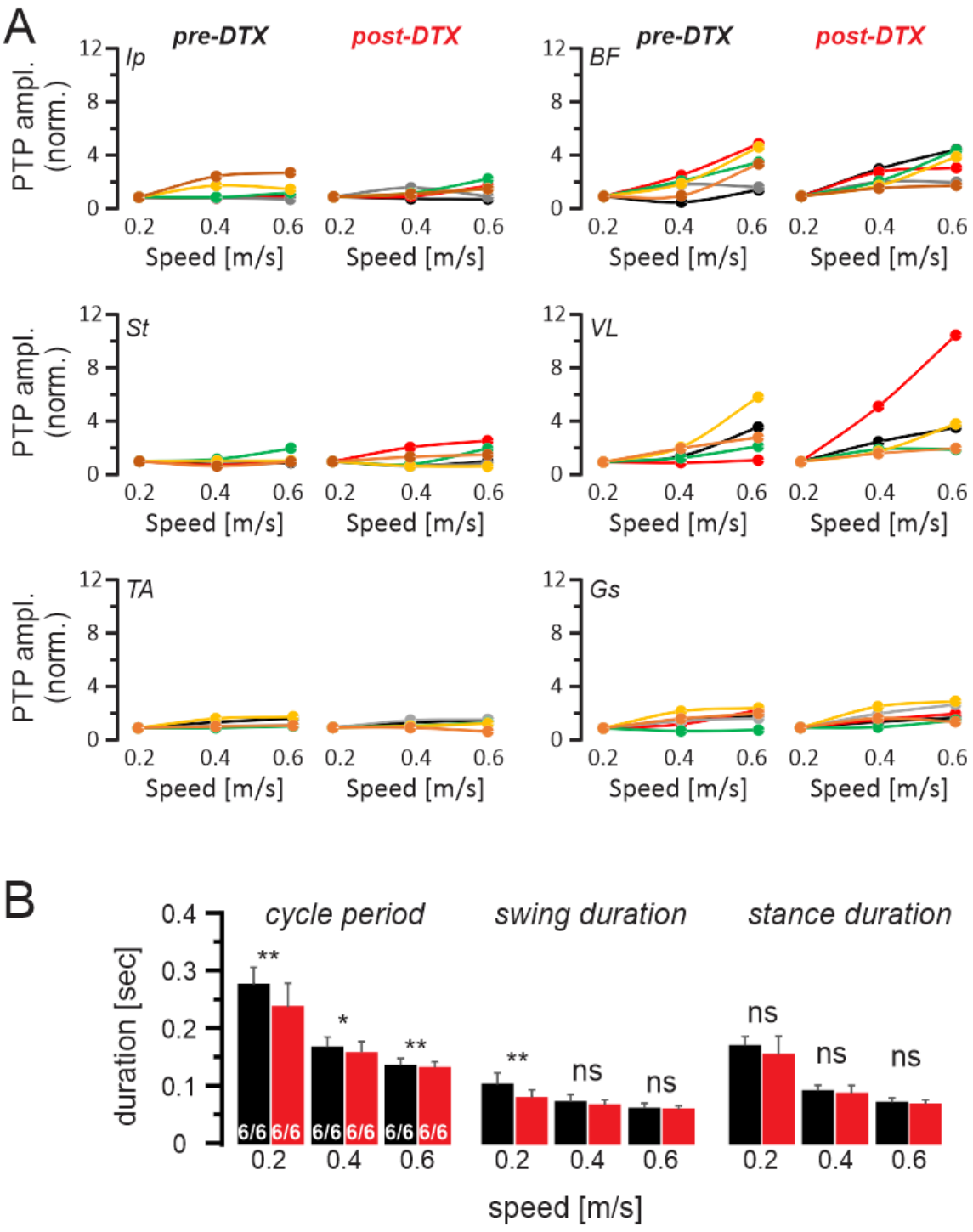
A
pre-DTX
post-DTX
Ip
BF
St
VL
TA
Gs
PTP ampl. (norm.)
Speed [m/s]
B
cycle period
swing duration
stance duration
duration [sec]
speed [m/s]
6/6
ns

4.4 Discussion

Proprioceptive feedback has been known to play a major role in the regulation of muscle activity strength during walking in humans and cats. However, the type of proprioceptive sensory feedback used for this amplitude control is somewhat controversial, and how this proprioceptive information is processed is not known. We have shown that proprioceptive feedback from muscle spindles is important in regulating muscle activity strength during locomotion in mice. Furthermore, the amplitude modulation required muscle spindle feedback to regulate the extensor activity increase at higher speeds. Finally, we have shown that muscle spindle feedback from knee extensor muscles did not have an effect on amplitude modulation, whereas muscle spindle feedback from the ankle was important for the regulation of activity mainly in ankle extensor muscles.

4.4.1 Speed Dependent Amplitude Modulation of Extensor Muscle Activity Requires Feedback from Muscle Spindles

Proprioceptive feedback is known to be important for regulating muscle activity strength during walking (Donelan & Pearson, 2004b; Hiebert & Pearson, 1999; Pearson, 2004). In humans, proprioceptive sensory feedback from the group Ib afferents that innervate GTOs as well as the afferent fibers that innervate muscle spindles are both important for regulating muscle activity strength during walking (af Klint et al., 2010; Grey et al., 2004; Mazzaro et al., 2005; Sinkjaer et al., 2000; Yang et al., 1991). In contrast, in a quadrupedal animal, the cat, group Ib afferent feedback from the GTOs has been shown to be important for

amplitude modulation (Donelan et al., 2009; Donelan & Pearson, 2004a; Donelan & Pearson, 2004b), but the contribution from muscle spindles has not been appreciated.

Our data provide evidence that muscle spindle feedback is important for regulating muscle contraction strength during walking in a quadrupedal animal. When wild type mice walk at different speeds, increasing activity is observed in extensor muscles (Figure. 4.3–5) as has been described previously in cat (Kaya, 2003; Prilutsky et al., 1994; Smith et al., 1993; Walmsley et al., 1978). However, in a mutant mouse model in which muscle spindles do not properly form, the *Egr3* knock-out mice (*Egr3*$^{-/-}$), the mice no longer walk at speeds higher than 0.4 m/s (Figure 4.6) and the extensor amplitude modulation is compromised (Figure 4.7–9). Furthermore, the swing duration is significantly shorter at the measured speeds in *Egr3*$^{-/-}$ mice with minor changes in the stance duration leading to decreased cycle period (Figure 4.6B). These data suggest that muscle spindle feedback is necessary for both the increased speed of walking and the speed-dependent amplitude modulation.

Because the *Egr3*$^{-/-}$ mice could not walk at 0.6 m/s, we measured muscle activity at different walking speeds in another model, where muscle spindles were removed only from a subset of muscles in an acute way, which resulted in a milder phenotype. Using this method that combines *Pv::cre* mice and gene delivery with AAV9 and later DTX injection, we could successfully acutely eliminate muscle spindle afferents only in a subset of muscles while leaving the GTO afferents intact (Figure 4.10). This is an interesting observation given that the group Ib proprioceptive afferent fibers from the GTOs have also been shown to express Pv (de Nooij et al., 2015). Why then did we not observe significantly lower number of GTOs after DTX injection, even though the number of MS afferents was consistently

decreased? One possible explanation is that the AAV9 was injected approximately in the center of the belly of the muscles. This could possibly avoid the infection of the group Ib afferents because the GTOs are typically located at the myotendinous junctions, farther away from the injection site. Nevertheless, regardless of the explanation as to why GTOs were not eliminated by the AAV9/DTX method, our data clearly suggest the number of GTOs after DTX injection remained unaffected.

Using the AAV9/DTX method to acutely eliminate MS feedback, we have shown that acute elimination of muscle spindle feedback from only a subset of muscles does not affect the animals' ability to walk at higher speed but compromises the amplitude modulation in the extensor muscles (Figure 4.9 and 4.10). Our data provide evidence that proprioceptive feedback from the muscle spindles is important for the regulation of muscle activity strength during walking. Previous studies with humans (Sinkjaer et al., 2000) concluded that afferent feedback from the group II afferents from the muscle spindles and group Ib afferents from the GTOs are important for the regulation of muscle activity strength during walking. Our results provide evidence that muscle spindle feedback-dependent amplitude modulation is necessary for the animals to walk at higher speeds.

One concern with the elimination of muscle spindle afferents with AAV9 injection into *Pv::cre* mice is the possibility of DTX also killing extrafusal muscle fiber that also expresses Pv (Celio & Heizmann, 1982). It is known that AAV9 can infect extrafusal muscle fibers (Katwal et al., 2013). Therefore, it is conceivable to expect that in our experiments, DTX injections would have killed Pv-expressing muscle fibers that could also compromise amplitude modulation measured in this study. To exclude this possibility, we

performed histological assessment to provide proof that extrafusal muscle fibers were not affected (Figure 4.2). We have shown that Pv-expressing extrafusal muscle fibers do not present any sign of damage. Therefore, we are confident that the effect measured in the AAV9/DTX experiments is due to elimination of proprioceptive feedback from the muscle spindles.

Could the reduced activity modulation at higher speeds be an indirect effect produced by inability to achieve the faster speeds because of the ataxia previously observed in *Egr3*$^{-/-}$ mice (Akay et al., 2014; Takeoka, Vollenweider, Courtine, & Arber, 2014) rather than a direct influence of spindle feedback on muscle activity? Our data suggest that compromised amplitude modulation in the absence of muscle spindle feedback is due to the elimination of direct influence of spindle feedback on muscle activity. Our observation is that amplitude modulation is compromised when muscle spindles are degenerated in only a small group of muscles with the AAV9/DTX approach. None of these animals showed any sign of ataxia or had any difficulty walking on the treadmill at higher speeds. The only change we could detect after DTX injection was that the speed-dependent amplitude modulation, mostly in the Gs muscle after muscle spindle feedback from the TS, was significantly attenuated.

4.4.2 Sensory Feedback from Muscle Spindles of Only TS Muscles Regulate the Strength of Distal Extensor Muscle Activity

The results from the experiments in which muscle spindles were removed acutely and selectively from the TS or the QF muscle groups strongly suggest that proprioceptive feedback from only TS muscles is necessary for speed-dependent amplitude modulation.

Speed-dependent amplitude modulation of extensor muscle activity was described in the past in rat (Hutchison et al., 1989; Roy et al., 1991) and cat (Kaya, 2003; Prilutsky et al., 1994; Smith et al., 1993; Walmsley et al., 1978) model systems, but the mechanism for this modulation was not understood. We have presented evidence that proprioceptive sensory feedback from muscle spindles in the ankle extensors, the TS muscle group, is necessary for the speed-dependent amplitude modulation of distal extensor muscles. Interestingly, our data also suggest that the muscle spindles of the QF group, the knee extensor muscles, are not necessary for the speed-dependent amplitude modulation. These data, however, do not suggest that this is the exclusive picture of amplitude control. Muscle spindles from other muscles that were not infected with AAV9 in this project could have additional function, and also, QF muscle spindles might have influence on other muscles not recorded in this study. Nevertheless, the data presented suggest distinctive roles of muscle spindles in specific muscles such that TS, but not QF, controls the amplitude modulation in muscles recorded. This finding is in accordance with the previous finding that activation of muscle afferents from the ankle extensor muscles, but not from the knee extensor muscles, strongly enhances ipsilateral extensor activity during fictive locomotion elicited by electrical stimulation of the mesencephalic locomotor region (MLR) in decerebrated cats (Guertin et al., 1995; McCrea, 2001). Our data provide evidence that proprioceptive muscle spindle feedback, selectively from the ankle extensor muscles, regulates the speed-dependent amplitude modulation of the distal extensor muscle during walking.

In addition, when the muscle spindles were removed from the TS, the changes in the swing and stance durations and the cycle period during walking at different speeds mimicked the results observed in *Egr3*$^{-/-}$ mice (Figure 4.6B). That is, the swing durations significantly

decreased following muscle spindle removal from the TS with s significant decrease in the stance duration only at 0.2 m/s, leading to a significant decrease in the cycle period (Figure 4.10B). Interestingly, the reduction of the muscle spindle afferents from the QF resulted in a much milder effect on swing duration and the cycle period and no effect on the stance duration (Figure 4.12B). This suggests that muscle spindles from the TS have a more prominent effect on step duration parameters than the muscle spindles from the QF muscles.

Why are the changes in amplitude modulation statistically significant only in BF when all muscle spindles are removed systemically as in *Egr3*$^{-/-}$ mice, but not different when muscle spindles are removed acutely only from a subset of muscles? There could be multiple reasons for this observation. First, when muscle spindles improperly form during development (Oliveira Fernandes & Tourtellotte, 2015; Tourtellotte & Milbrandt, 1998; Tourtellotte, Keller-Peck, Milbrandt, & Kucera, 2001), there may be resultant compensatory changes in BF. Therefore, the acute elimination of muscle spindle feedback from a subset of muscles would have no effect on BF. Second, BF modulation might be controlled by muscle spindle feedback from different muscles that did not receive AAV9 injection in these studies. Third, all extensor muscles could contribute to the speed-dependent modulation of BF activity, and therefore elimination of feedback from only a small number of muscles does not cause a detectable effect. Our current data do not clearly differentiate between these possibilities.

4.4.3 Negative Feedback from Muscle Spindles Controls Amplitude Modulation

Previous studies suggest that positive force feedback signals from the group Ib afferents from the GTOs are the major source of amplitude regulation during walking (Duysens, Clarac, & Cruse, 2000; Gossard, Brownstone, Barajon, & Hultborn, 1994; McCrea, Shefchyk, Stephens, & Pearson, 1995; Pearson & Collins, 1993). In addition, cutaneous afferents have also been shown to be important for the regulation of extensor muscle activity (Duysens & Stein, 1978; Duysens, van Wezel, Prokop, & Berger, 1996). In contrast, how feedback from the muscle spindles might contribute to amplitude modulation has been unclear.

It has been shown that muscle spindle muscle afferents (group Ia and II) from the triceps surae muscles and from vasti muscles (only known for group Ia; group II not known) are active during the early part of stance (Prochazka & Gorassini, 1998; Prochazka, Trend, Hulliger, & Vincent, 1989) when ankle and knee joints flex. In addition, there is an excitatory influence from the muscle spindle afferents from the TS and VL muscle groups on the extensor muscles (Guertin et al., 1995; McCrea et al., 1995), indicating the existence of a negative feedback pathway (Pearson, 2004). Our data provide functional evidence of this negative angular displacement feedback during walking behavior.

4.4.4 Role of Muscle Spindle Feedback During Walking

Locomotion is controlled by a network of interconnected spinal premotor interneurons and sensory feedback from the periphery (McCrea, 2001; McCrea & Rybak, 2008; Pearson, 2004; Rossignol et al., 2006). Previous data and our present data suggest that proprioceptive sensory feedback from the muscle spindles from hindlimb muscle regulates three aspects of a step cycle.

First, it has an important role in the phase transitions. That is, muscle spindle feedback signaling limb extension at the end of stance phase is an important signal to initiate swing phase (Grillner & Rossignol, 1978; Hiebert, Whelan, Prochazka, & Pearson, 1996). Second, muscle spindle feedback is important in the regulation of the precise timing of the activity offset of flexor muscles and therefore important for the precise foot placement at the end of swing phase (Akay et al., 2014). Third, muscle spindle feedback from ankle extensors is important for the regulation of muscle activity strength during stance phase, as our current data suggest. It is well established that ankle joint exerts a brief flexion movement at the beginning of the stance phase that causes the ankle extensor muscles to stretch, activating the stretch-sensitive muscle spindles (Engberg & Lundberg, 1969). It has also been shown that the speed of this yield and the ankle muscle stretch increase with the walking speed (Prilutsky et al., 1994), which would result in higher muscle spindle signaling. The higher muscle spindle signaling would then, in turn, provide stronger excitatory drive to the distal extensor motoneurons to accommodate the speed-dependent amplitude modulation of muscle activity.

CHAPTER 5 CONCLUSIONS

5.1 SUMMARY OF RESULTS

We studied various aspects of locomotion in different mutant mouse models. The lineages used in this thesis were either genetically modified or had their proprioceptive system manipulated with the adeno-associated virus technology. Such an approach enabled us to recreate the following conditions regarding the proprioceptive feedback:

1- Total absence of proprioceptive feedback from group Ia, Ib and II afferents, consequently no input from muscle spindles and GTOs, as studied in the *Pv::cre;Isl2::DTA* mouse line – *Pkill* mice.

Here, the animals in which proprioceptive feedback was completely abolished were not able to perform functional walking or swimming tasks. This was mainly due to the inability to generate an alternated pattern of activation in flexor and extensor muscles. We provided evidence that the onsets of activity of different flexor muscles occurred simultaneously during walking or swimming, and the extensor activities occurred at different stages of the step cycle among individual animals especially during walking. Thus muscle activation in coordinated and patterned fashion requires proprioceptive feedback from both, muscle spindles and GTOs.

The total lack of sensory feedback from group Ia, Ib and II afferents severely compromised the hindlimb movement during locomotion. Especially, the most distal joints (knee and ankle) exhibited inconsistent kinematics recordings while the hip joint showed less disorganized traces. The precision in which the hindlimb landed on the ground at the AEP was also compromised. Our results indicate that the movement of the hind leg is severely disorganized in the absence of proprioceptive feedback from muscle spindles and GTOs.

2- Systemic elimination of proprioceptive feedback from muscle spindles in the *Egr3*$^{-/-}$ mice.

The removal of proprioceptive feedback from muscle spindles showed changes mostly on the swing phase during walking. The duration of the swing phase was shorter without muscle spindle feedback. Joint angles displayed over-flexion, especially in the knee and ankle joints, causing a characteristic high-stepping behavior. These changes in angular joint movements were the outcome of altered activation patterns of flexor muscles. This observation indicate that group Ia/II afferents selectively regulate the swing phase.

Hindlimb foot placement after the swing phase relied on feedback from group Ia/II afferents. The deprivation of muscle spindle proprioceptive feedback not only reduced the accuracy in foot placement during normal gait and skilled walking, but also when the ongoing swing movement was disrupted causing a stumbling corrective reaction (SCR).

The capability to adjust the locomotor output to achieve the demands of faster locomotion speeds was severely compromised in mice lacking proprioceptive feedback from muscle

spindles. Without feedback from muscle spindles, the amplitude modulation in the extensor muscles necessary to reach higher speeds was compromised and mice were unable to walk at faster speeds.

3- Attenuation of proprioceptive feedback from muscle spindles in a specific group of muscles by using mouse genetics (*Pv::cre* mice) and AAV9 virus technology at pre-determined sites.

The manipulation of muscle spindle feedback of a single joint, either hip, knee, or ankle, did not trigger changes in the overall locomotor pattern of the hindlimb. It is likely that the spinal CPG relied on feedback from multiple joints and sources to generate a functional locomotor pattern. However, our data suggested that muscle spindles from a single ankle joint played an important role in controlling the whole cycle period and swing duration of the gait. These findings suggested that muscle spindles from the ankle had a greater influence on the temporal parameters of the step than the muscle spindles from the hip or knee joint muscles. Concerning localized processing of proprioceptive information, our results indicated that muscle spindle feedback from knee extensor muscles do not influence the amplitude modulation required to walk at faster speeds.

5.2 Role of Proprioceptive Feedback in Locomotor Pattern Generation

It is generally accepted that motor programs controlling locomotion emerge from an interneuronal spinal network that function as central pattern generators (CPG) (Brown,

1911; J. C. Eccles et al., 1957; Grillner & Zangger, 1979; Kiehn, 2006). However, since the early 80s two main schools have been proposed that the proprioceptive system influences the motor output of CPGs in different manners (Lundberg, 1981; Grillner, 1981). First, the Lundberg school suggests that proprioceptive afferent feedback interacts with a network of premotor interneurons within the CPG which in turns activate flexor and extensor muscles in an alternating fashion. This model is considered to be aligned with the half-center idea of spinal CPG operation. Under this view, the ablation of proprioceptive feedback would generate a pattern of flexor-extensor alternation solely based on the activity of motoneurons and their reciprocal inhibition as described by Brown (1911), so that all flexor motoneuron (MN) pools controlling a limb would be active during the flexor phases while silencing the extensor MN pools and vice-versa. The second school of thoughts, supported by Grillner's work, argues that each limb is likely to entertain further divisions of CPGs, so that, CPGs subunits may be in place for hip, knee and ankle joints, and the normal pattern of activity arise as a result from broader interaction among these CPGs subunits from different joints (Grillner, 2006). This implies that the normal locomotor pattern would be preserved by the CPG following the abolition of sensory feedback.

Our results corroborate with the hypothesis that proprioceptive feedback is necessary for the establishment of functional locomotor patterns in intact animals (section 2.3.2). Removing proprioceptive feedback from an entire animal did not trigger flexor-extensor alternation. This indicates that the central nervous system, in intact animals, relies on proprioceptive sensory feedback to outline the CPG output engaged in the formation of locomotor patterns.

5.3 Role of Proprioceptive Feedback from Muscle Spindles in Locomotion

The generation of a functional motor output, for example during locomotion, depends on computations by the central nervous system by considering available sensory information (Grillner & El Manira, 2019; McCrea, 2001; McCrea & Rybak, 2008; Pearson, 2004; Rossignol et al., 2006). Our findings suggest that muscle spindle feedback from hindlimb modify three core elements in locomotion.

First, muscle spindle feedback controls the temporal parameters of the swing phase. Our data corroborate with earlier work of Akay et al. (2014) that indicates that group Ia/II feedback control the temporal parameters of the swing phase while the stance duration remains unaltered after the manipulation of muscle spindle feedback. These data merge with previous research (Donelan & Pearson, 2004a; Donelan & Pearson, 2004b; Duysens & Pearson, 1980; Pearson, 2008) and support the view that the stance phase is strongly controlled by the group Ib feedback from the GTOs.

Second, there is a pattern generation aspect that muscle spindle feedback controls the precision of the on- and off-set timing of flexor muscle activities during the swing movement. Furthermore, our results have also shown that the disruption of group Ia/II afferents diminished the accuracy of paw placement at the end of unperturbed swing movement as suggested by Akay et al. (2014) as well as deteriorated the limb target after a stumbling corrective response. Whether or not, the diminished precision of on- and offset timing of flexor muscle activities and the precise foot placement are causally related,

remains unresolved. The data presented in this thesis provide evidence that muscle spindle feedback during locomotion is necessary for the precision of hindlimb movement.

Third, it has been demonstrated in human walking that group Ib feedback from the GTOs, as well as group II afferent feedback from the muscle spindles, play role in amplitude modulation of extensor muscles during stance (Sinkjaer et al, 2000). On the contrary, research conducted on cats suggests that the extensor muscle activity during the stance phase is mainly regulated by the group Ib feedback from the GTOs with no major influence from the muscle spindles (Donelan and Pearson, 2004a and 2004b). Our results indicate that muscle spindle feedback, specifically from ankle extensor muscles, is responsible for the regulation of the activity strength during the stance phase and accommodates the speed-dependent amplitude of muscle activity during locomotion.

5.4 Local vs Global Process of Proprioceptive Feedback Information

How is proprioceptive feedback processed by the central nervous system in order to achieve a desired motor output? We hypothesize two main possibilities for such processing/controlling mechanisms. First, the complex pattern of activation of flexor-extensor muscles in the hindlimb is shaped by the sensory afferents coming from multiple joints (Adrian & John, 2012), and this feedback may be globally processed by a premotor neuronal network (McCrea & Rybak, 2008; Rossignol et al., 2006) that acts as an internal controller responsible for sensorimotor transformations (McCrea, 2001). After processing the feedback information from multiple joints, the motor command is selected and

delivered to execute the desired movement (Figure 5.1). The result of this transformation is the overall functional output required to move multiple joints at the same time.

Figure 5. 1 Diagram illustrating the global processing of proprioceptive feedback in the central nervous system. The information regarding all joints inputs into a neuronal circuitry "internal controller" responsible for sensorimotor transformation. The output from this internal controller regarding the kinetic and kinematic state of the whole limb is then forwarded to the motor command unit and ultimately to the motoneurons.

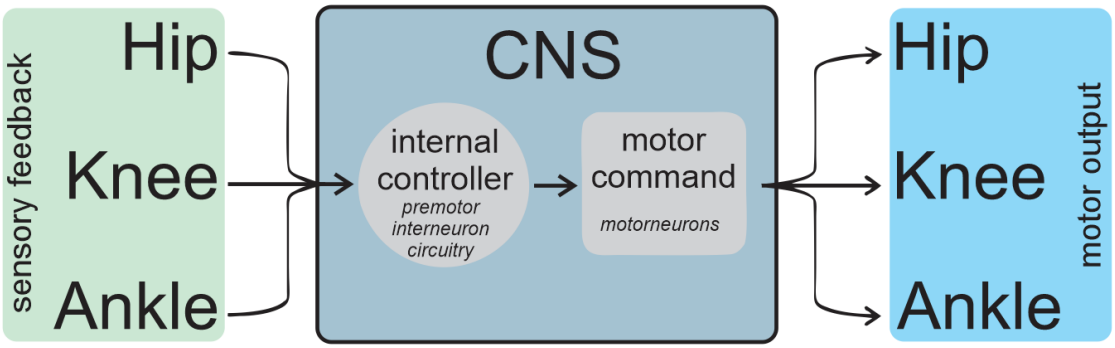

The second possibility is that the CNS may rely on a more localized feedback process from individualized joints to generate coordinated activity of multiple joints (Figure 5.2), where specific motor responses are mirrored based on localized feedback. This kind of joint-specific use of proprioceptive feedback to coordinate motor activity of multiple joints has been demonstrated in stick insect walking system (Akay et al., 2001, 2004, 2007; Akay & Büschges, 2006; Bucher et al., 2003; Büschges et al., 2008; Hess & Büschges, 1997, 1999). However, such a localized joint-specific sensory processing has not been demonstrated in the mammalian locomotor system.

Figure 5. 2 Diagram of local process of proprioceptive feedback into the central nervous system. The information regarding individual joints is delivered to individual motor command units of individual joints. This network could be considered for collection of intra- and inter-joint reflex pathways.

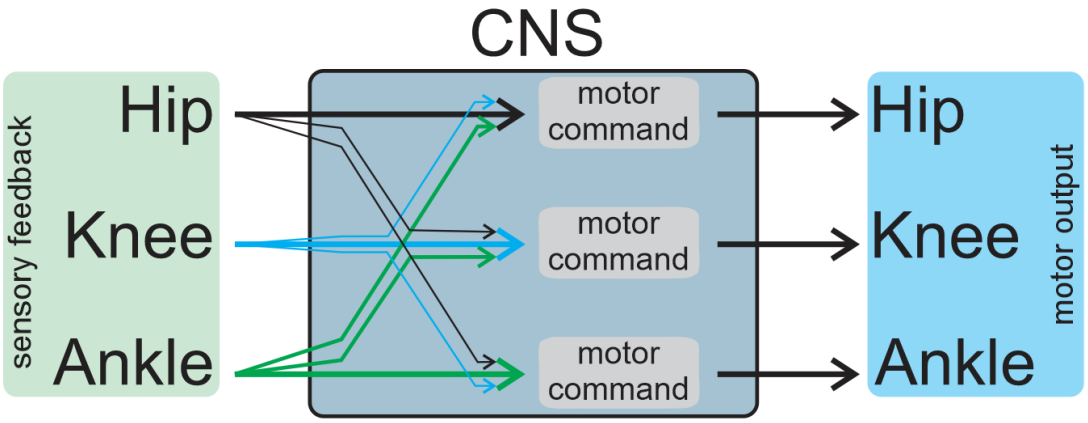

In this thesis, we have shown that removing muscle spindle feedback from the entire animal, but not from individual joints, caused significant changes in the temporal structure of the locomotor pattern. Nevertheless, when we studied the speed-dependent amplitude modulation of the extensor muscles, removing muscle spindle feedback from individual joints caused joint-specific changes. These observations indicate that the pattern formation of the hindlimb (temporal structure of flexor/extensor activity) is likely to be controlled by a general processing mechanism that considers feedback from multiple joints to compute the overall state of the hindlimb and copy this information to generate the appropriate motor command (Figure 5.1). In contrast, amplitude modulation of the motor activity is more likely to be regulated by a localized processing mechanism (Figure 5.2).

5.5 Concluding Remarks and Future Directions

This thesis work provides further evidence that proprioceptive feedback is essential for controlling variable aspects of locomotion. The information carried by the group Ia/II and Ib afferents is used by the spinal cord, either, in localized process that enables modification of muscle activity strength, or in more comprehensive and integrative process where feedback from various sources, together with descending controls, is used to regulate locomotor patterns.

Our results cooperate with the previous body of work that has established the following features of proprioceptive feedback in the mammalian motor system: 1- that proprioceptive feedback is necessary for timing the phase transitions of the gait (Pearson, 2004); 2- that proprioceptive feedback is important for precisely-timing muscle activation (Akay et al 2014); 3- that proprioceptive feedback is important for limb targeting and skilled motor behavior (Azim et al., 2014; Fink et al., 2014) and last; 4- that proprioceptive feedback is an important source to regulate muscular activity strength (Donelan and Pearson, 2004a and 2004b; Sinkjaer et al 2000).

Despite all the developments and insights on the mechanisms that the CNS utilizes to control locomotion, the investigation of how exactly the proprioceptive feedback is incorporated in these neural networks, still open to debate and prolific field for exploration. The ability to genetically manipulate specific neurons in a given neuronal network related to locomotor control, in addition to the studies in which the *in vivo* behavior is recorded as

seen in this thesis, may resolve questions unanswered in the field of sensorimotor transformation and locomotion.

Finally, understanding the mechanisms by which proprioceptive feedback interacts with CPGs to generate locomotor patterns will remain a trending topic for the next several years. Further elaboration on how much proprioceptive feedback from an individual or a particular group of muscles affects the coordinated activity of multiple muscles is needed. Insights from multidisciplinary investigations in which kinematic analysis and modular muscle output in the form of synergies are exposed by mathematical framework may be of key importance for scientists interested in unveiling the obscurities of sensorimotor control of locomotion.

BIBLIOGRAPHY

Adrian, M. H., & John, W. K. (2012). Theoretical Models of Motor Control and Motor Learning. In *Routledge Handbook of Motor Control and Motor Learning*. Routledge. https://doi.org/10.4324/9780203132746.ch1

af Klint, R., Mazzaro, N., Nielsen, J. B., Sinkjaer, T., & Grey, M. J. (2010). Load Rather Than Length Sensitive Feedback Contributes to Soleus Muscle Activity During Human Treadmill Walking. *Journal of Neurophysiology*, *103*(5), 2747–2756. https://doi.org/10.1152/jn.00547.2009

Akay, T. (2014). Long-term measurement of muscle denervation and locomotor behavior in individual wild-type and ALS model mice. *Journal of Neurophysiology*, *111*(3), 694–703. https://doi.org/10.1152/jn.00507.2013

Akay, T., Acharya, H. J., Fouad, K., & Pearson, K. G. (2006). Behavioral and Electromyographic Characterization of Mice Lacking EphA4 Receptors. *Journal of Neurophysiology*, *96*(2), 642–651. https://doi.org/10.1152/jn.00174.2006

Akay, T., Bässler, U., Gerharz, P., & Büschges, A. (2001). The Role of Sensory Signals From the Insect Coxa-Trochanteral Joint in Controlling Motor Activity of the Femur-Tibia Joint. *Journal of Neurophysiology*, *85*(2), 594–604. https://doi.org/10.1152/jn.2001.85.2.594

Akay, T., & Büschges, A. (2006). Load signals assist the generation of movement-dependent reflex reversal in the femur-tibia joint of stick insects. *Journal of Neurophysiology*, *96*(6), 3532–3537. https://doi.org/10.1152/jn.00625.2006

Akay, T., Haehn, S., Schmitz, J., & Büschges, A. (2004). Signals From Load Sensors Underlie Interjoint Coordination During Stepping Movements of the Stick Insect Leg. *Journal of Neurophysiology*, *92*(1), 42–51. https://doi.org/10.1152/jn.01271.2003

Akay, T., Ludwar, B. Ch., Goritz, M. L., Schmitz, J., & Buschges, A. (2007). Segment Specificity of Load Signal Processing Depends on Walking Direction in the Stick Insect Leg Muscle Control System. *Journal of Neuroscience*, *27*(12), 3285–3294. https://doi.org/10.1523/JNEUROSCI.5202-06.2007

Akay, T., Tourtellotte, W. G., Arber, S., & Jessell, T. M. (2014). Degradation of mouse locomotor pattern in the absence of proprioceptive sensory feedback. *Proceedings of the National Academy of Sciences of the United States of America*, *111*(47), 16877–16882. https://doi.org/10.1073/pnas.1419045111

Alvarez, F. J., Jonas, P. C., Sapir, T., Hartley, R., Berrocal, M. C., Geiman, E. J., Todd, A. J., & Goulding, M. (2005). Postnatal phenotype and localization of spinal cord V1 derived interneurons. *The Journal of Comparative Neurology*, *493*(2), 177–192. https://doi.org/10.1002/cne.20711

Azim, E., & Alstermark, B. (2015). Skilled forelimb movements and internal copy motor circuits. *Current Opinion in Neurobiology*, *33*, 16–24. https://doi.org/10.1016/j.conb.2014.12.009

Azim, E., Jiang, J., Alstermark, B., & Jessell, T. M. (2014). Skilled reaching relies on a V2a propriospinal internal copy circuit. *Nature*, *508*(7496), 357–363. https://doi.org/10.1038/nature13021

Bourane, S., Duan, B., Koch, S. C., Dalet, A., Britz, O., Garcia-Campmany, L., Kim, E., Cheng, L., Ghosh, A., Ma, Q., & Goulding, M. (2015). Gate control of mechanical itch by a subpopulation of spinal cord interneurons. *Science*, *350*(6260), 550–554. https://doi.org/10.1126/science.aac8653

Bourane, S., Grossmann, K. S., Britz, O., Dalet, A., Del Barrio, M. G., Stam, F. J., Garcia-Campmany, L., Koch, S., & Goulding, M. (2015). Identification of a Spinal Circuit for Light Touch and Fine Motor Control. *Cell*, *160*(3), 503–515. https://doi.org/10.1016/j.cell.2015.01.011

Brown, T. G. (1911). The Intrinsic Factors in the Act of Progression in the Mammal. *Proceedings of the Royal Society B: Biological Sciences*, *84*(572), 308–319. https://doi.org/10.1098/rspb.1911.0077

Brownstone, R. M., & Wilson, J. M. (2008). Strategies for delineating spinal locomotor rhythm-generating networks and the possible role of Hb9 interneurones in rhythmogenesis. *Brain Research Reviews*, *57*(1), 64–76. https://doi.org/10.1016/j.brainresrev.2007.06.025

Bucher, D., Akay, T., DiCaprio, R. A., & Büschges, A. (2003). Interjoint Coordination in the Stick Insect Leg-Control System: The Role of Positional Signaling. *Journal of Neurophysiology*, *89*(3), 1245–1255. https://doi.org/10.1152/jn.00637.2002

Buford, J. A., & Smith, J. L. (1993). Adaptive control for backward quadrupedal walking. III. Stumbling corrective reactions and cutaneous reflex sensitivity. *Journal of Neurophysiology*, *70*(3), 1102–1114.

Bui, T. V., Akay, T., Loubani, O., Hnasko, T. S., Jessell, T. M., & Brownstone, R. M. (2013). Circuits for Grasping: Spinal dI3 Interneurons Mediate Cutaneous Control of Motor Behavior. *Neuron*, *78*(1), 191–204. https://doi.org/10.1016/j.neuron.2013.02.007

Bui, T. V., Stifani, N., Akay, T., & Brownstone, R. M. (2016). Spinal microcircuits comprising dI3 interneurons are necessary for motor functional recovery following spinal cord transection. *ELife*, *5*. https://doi.org/10.7554/eLife.21715

Büschges, A., Akay, T., Gabriel, J. P., & Schmidt, J. (2008). Organizing network action for locomotion: Insights from studying insect walking. *Brain Research Reviews*, *57*(1), 162–171. https://doi.org/10.1016/j.brainresrev.2007.06.028

Cabelguen, J.-M. (1981). Static and dynamic fusimotor controls in various hindlimb muscles during locomotor activity in the decorticate cat. *Brain Research*, *213*(1), 83–97. https://doi.org/10.1016/0006-8993(81)91249-X

Carp, J. S., Tennissen, A. M., Chen, X. Y., & Wolpaw, J. R. (2006a). Diurnal H-reflex variation in mice. *Experimental Brain Research*, *168*(4), 517–528. https://doi.org/10.1007/s00221-005-0106-y

Carp, J. S., Tennissen, A. M., Chen, X. Y., & Wolpaw, J. R. (2006b). H-reflex operant conditioning in mice. *Journal of Neurophysiology*, *96*(4), 1718–1727. https://doi.org/10.1152/jn.00470.2006

Celio, M. R., & Heizmann, C. W. (1982). Calcium-binding protein parvalbumin is associated with fast contracting muscle fibres. *Nature*, *297*(5866), 504–506.

Charles, J. P., Cappellari, O., Spence, A. J., Hutchinson, J. R., & Wells, D. J. (2016). Musculoskeletal Geometry, Muscle Architecture and Functional Specialisations of the Mouse Hindlimb. *PLOS ONE*, *11*(4), e0147669. https://doi.org/10.1371/journal.pone.0147669

Chen, H.-H., Tourtellotte, W. G., & Frank, E. (2002). Muscle Spindle-Derived Neurotrophin 3 Regulates Synaptic Connectivity between Muscle Sensory and Motor Neurons. *The Journal of Neuroscience*, *22*(9), 3512–3519. https://doi.org/10.1523/JNEUROSCI.22-09-03512.2002

Cruse, H. (1979). The control of the anterior extreme position of the hindleg of a walking insect, Carausius morosus. *Physiological Entomology*, *4*(2), 121–124. https://doi.org/10.1111/j.1365-3032.1979.tb00186.x

Cruse, H., Dean, J., & Suilmann, M. (1984). The contributions of diverse sense organs to the control of leg movement by a walking insect. *Journal of Comparative Physiology A*, *154*(5), 695–705. https://doi.org/10.1007/BF01350223

Cruse, H., Kindermann, T., Schumm, M., Dean, J., & Schmitz, J. (1998). Walknet—A biologically inspired network to control six-legged walking. *Neural Networks*, *11*(7–8), 1435–1447. https://doi.org/10.1016/S0893-6080(98)00067-7

de Nooij, J. C., Doobar, S., & Jessell, T. M. (2013). Etv1 Inactivation Reveals Proprioceptor Subclasses that Reflect the Level of NT3 Expression in Muscle Targets. *Neuron*, *77*(6), 1055–1068. https://doi.org/10.1016/j.neuron.2013.01.015

de Nooij, J. C., Simon, C. M., Simon, A., Doobar, S., Steel, K. P., Banks, R. W., Mentis, G. Z., Bewick, G. S., & Jessell, T. M. (2015). The PDZ-Domain Protein Whirlin Facilitates Mechanosensory Signaling in Mammalian Proprioceptors. *The Journal of Neuroscience*, *35*(7), 3073–3084. https://doi.org/10.1523/JNEUROSCI.3699-14.2015

Dean, J., & Wendler, G. (1983). Stick insect locomotion on a walking wheel: Interleg coordination of leg position. *J. Exp. Biol.*, *103*, 75–94. Scopus.

Delhaye, B. P., Long, K. H., & Bensmaia, S. J. (2018). Neural Basis of Touch and Proprioception in Primate Cortex. In D. M. Pollock (Ed.), *Comprehensive Physiology* (pp. 1575–1602). John Wiley & Sons, Inc. https://doi.org/10.1002/cphy.c170033

Dezhdar, T., Moshourab, R. A., Fründ, I., Lewin, G. R., & Schmuker, M. (2016). A Probabilistic Model for Estimating the Depth and Threshold Temperature of C-fiber Nociceptors. *Scientific Reports*, *5*(1). https://doi.org/10.1038/srep17670

Donelan, J. M., McVea, D. A., & Pearson, K. G. (2009). Force Regulation of Ankle Extensor Muscle Activity in Freely Walking Cats. *Journal of Neurophysiology*, *101*(1), 360–371. https://doi.org/10.1152/jn.90918.2008

Donelan, J. M., & Pearson, K. G. (2004a). Contribution of sensory feedback to ongoing ankle extensor activity during the stance phase of walking. *Canadian Journal of Physiology and Pharmacology*, *82*(8–9), 589–598. https://doi.org/10.1139/y04-043

Donelan, J. M., & Pearson, K. G. (2004b). Contribution of Force Feedback to Ankle Extensor Activity in Decerebrate Walking Cats. *Journal of Neurophysiology*, *92*(4), 2093–2104. https://doi.org/10.1152/jn.00325.2004

Doperalski, A. E., Tester, N. J., Jefferson, S. C., & Howland, D. R. (2011). Altered Obstacle Negotiation after Low Thoracic Hemisection in the Cat. *Journal of Neurotrauma*, *28*(9), 1983–1993. https://doi.org/10.1089/neu.2010.1457

Duysens, J., Clarac, F., & Cruse, H. (2000). Load-Regulating Mechanisms in Gait and Posture: Comparative Aspects. *Physiological Reviews*, *80*(1), 83–133. https://doi.org/10.1152/physrev.2000.80.1.83

Duysens, J., & Pearson, K. G. (1980). Inhibition of flexor burst generation by loading ankle extensor muscles in walking cats. *Brain Research*, *187*(2), 321–332.

Duysens, J., & Stein, R. B. (1978). Reflexes induced by nerve stimulation in walking cats with implanted cuff electrodes. *Experimental Brain Research*, *32*(2). https://doi.org/10.1007/BF00239728

Duysens, J., Trippel, M., Horstmann, G. A., & Dietz, V. (1990). Gating and reversal of reflexes in ankle muscles during human walking. *Experimental Brain Research*, *82*(2), 351–358.

Duysens, J., & Van de Crommert, H. W. A. A. (1998). Neural control of locomotion; Part 1: The central pattern generator from cats to humans. *Gait & Posture*, *7*(2), 131–141. https://doi.org/10.1016/S0966-6362(97)00042-8

Duysens, J., van Wezel, B. M. H., Prokop, T., & Berger, W. (1996). Medial gastrocnemius is more activated than lateral gastrocnemius in sural nerve induced reflexes during human gait. *Brain Research*, *727*(1), 230–232. https://doi.org/10.1016/0006-8993(96)00525-2

Eccles, J. C., Eccles, R. M., & Lundberg, A. (1957). The convergence of monosynaptic excitatory afferents on to many different species of alpha motoneurones. *The Journal of Physiology*, *137*(1), 22–50.

Eccles, R. M., & Lundberg, A. (1958). Integrative pattern of Ia synaptic actions on motoneurones of hip and knee muscles. *The Journal of Physiology*, *144*(2), 271–298.

Ellaway, P., Taylor, A., Durbaba, R., & Rawlinson, S. (2002). Role of the Fusimotor System in Locomotion. In S. C. Gandevia, U. Proske, & D. G. Stuart (Eds.), *Sensorimotor Control of Movement and Posture* (pp. 335–342). Springer US. https://doi.org/10.1007/978-1-4615-0713-0_39

Engberg, I., & Lundberg, A. (1969). An electromyographic analysis of muscular activity in the hindlimb of the cat during unrestrained locomotion. *Acta Physiologica Scandinavica*, *75*(4), 614–630. https://doi.org/10.1111/j.1748-1716.1969.tb04415.x

Ernfors, P., Lee, K.-F., Kucera, J., & Jaenisch, R. (1994). Lack of neurotrophin-3 leads to deficiencies in the peripheral nervous system and loss of limb proprioceptive afferents. *Cell*, *77*(4), 503–512. https://doi.org/10.1016/0092-8674(94)90213-5

Farr, T. D., Liu, L., Colwell, K. L., Whishaw, I. Q., & Metz, G. A. (2006). Bilateral alteration in stepping pattern after unilateral motor cortex injury: A new test strategy for analysis of skilled limb movements in neurological mouse models. *Journal of Neuroscience Methods*, *153*(1), 104–113. https://doi.org/10.1016/j.jneumeth.2005.10.011

Fiander, M. D. J., Stifani, N., Nichols, M., Akay, T., & Robertson, G. S. (2017). Kinematic gait parameters are highly sensitive measures of motor deficits and spinal cord injury in mice subjected to experimental autoimmune encephalomyelitis. *Behavioural Brain Research SreeTestContent1*, *317*, 95–108. https://doi.org/10.1016/j.bbr.2016.09.034

Fink, A. J. P., Croce, K. R., Huang, Z. J., Abbott, L. F., Jessell, T. M., & Azim, E. (2014). Presynaptic inhibition of spinal sensory feedback ensures smooth movement. *Nature*, *509*(7498), 43–48. https://doi.org/10.1038/nature13276

Forssberg, H. (1979). Stumbling corrective reaction: A phase-dependent compensatory reaction during locomotion. *Journal of Neurophysiology*, *42*(4), 936–953.

Forssberg, H., Grillner, S., & Rossignol, S. (1975). Phase dependent reflex reversal during walking in chronic spinal cats. *Brain Research*, *85*(1), 103–107.

Forssberg, H., Grillner, S., & Rossignol, S. (1977). Phasic gain control of reflexes from the dorsum of the paw during spinal locomotion. *Brain Research*, *132*(1), 121–139. https://doi.org/10.1016/0006-8993(77)90710-7

Gossard, J.-P., Brownstone, R. M., Barajon, I., & Hultborn, H. (1994). Transmission in a locomotor-related group Ib pathway from hindlimb extensor muscles in the cat. *Experimental Brain Research*, *98*(2). https://doi.org/10.1007/BF00228410

Goulding, M. (2009). Circuits controlling vertebrate locomotion: Moving in a new direction. *Nature Reviews Neuroscience*, *10*(7), 507–518. https://doi.org/10.1038/nrn2608

Grätsch, S., Büschges, A., & Dubuc, R. (2019). Descending control of locomotor circuits. *Current Opinion in Physiology*, *8*, 94–98. https://doi.org/10.1016/j.cophys.2019.01.007

Grey, M. J., Mazzaro, N., Nielsen, J. B., & Sinkjær, T. (2004). Ankle extensor proprioceptors contribute to the enhancement of the soleus EMG during the stance phase of human walking. *Canadian Journal of Physiology and Pharmacology*, *82*(8–9), 610–616. https://doi.org/10.1139/y04-077

Grey, M. J., Nielsen, J. B., Mazzaro, N., & Sinkjaer, T. (2007). Positive force feedback in human walking: Positive force feedback in human walking. *The Journal of Physiology*, *581*(1), 99–105. https://doi.org/10.1113/jphysiol.2007.130088

Grillner, S. (1981). Control of locomotion in bipeds, tetrapods, and fish. *Handbook of Physiology*, 1179–1236.

Grillner, S. (2003). The motor infrastructure: From ion channels to neuronal networks. *Nature Reviews Neuroscience*, *4*(7), 573–586. https://doi.org/10.1038/nrn1137

Grillner, S. (2006). Biological Pattern Generation: The Cellular and Computational Logic of Networks in Motion. *Neuron*, *52*(5), 751–766. https://doi.org/10.1016/j.neuron.2006.11.008

Grillner, S. (2011). Control of Locomotion in Bipeds, Tetrapods, and Fish. In R. Terjung (Ed.), *Comprehensive Physiology*. John Wiley & Sons, Inc. http://doi.wiley.com/10.1002/cphy.cp010226

Grillner, S., & El Manira, A. (2019). Current Principles of Motor Control, with Special Reference to Vertebrate Locomotion. *Physiological Reviews*. https://doi.org/10.1152/physrev.00015.2019

Grillner, S., & Jessell, T. M. (2009). Measured motion: Searching for simplicity in spinal locomotor networks. *Current Opinion in Neurobiology*, *19*(6), 572–586. https://doi.org/10.1016/j.conb.2009.10.011

Grillner, S., & Rossignol, S. (1978). On the initiation of the swing phase of locomotion in chronic spinal cats. *Brain Research*, *146*(2), 269–277. https://doi.org/10.1016/0006-8993(78)90973-3

Grillner, S., & Zangger, P. (1979). On the central generation of locomotion in the low spinal cat. *Experimental Brain Research*, *34*(2), 241–261.

Grillner, S., & Zangger, P. (1984). The effect of dorsal root transection on the efferent motor pattern in the cat's hindlimb during locomotion. *Acta Physiologica Scandinavica*, *120*(3), 393–405. https://doi.org/10.1111/j.1748-1716.1984.tb07400.x

Gruner, J. A., & Altman, J. (1980). Swimming in the rat: Analysis of locomotor performance in comparison to stepping. *Experimental Brain Research*, *40*(4). https://doi.org/10.1007/BF00236146

Guertin, P., Angel, M. J., Perreault, M. C., & McCrea, D. A. (1995). Ankle extensor group I afferents excite extensors throughout the hindlimb during fictive locomotion in the cat. *The Journal of Physiology*, *487*(1), 197–209. https://doi.org/10.1113/jphysiol.1995.sp020871

Helgren, M. E., Cliffer, K. D., Torrento, K., Cavnor, C., Curtis, R., DiStefano, P. S., Wiegand, S. J., & Lindsay, R. M. (1997). Neurotrophin-3 administration attenuates deficits of pyridoxine-induced large-fiber sensory neuropathy. *The Journal of Neuroscience: The Official Journal of the Society for Neuroscience*, *17*(1), 372–382.

Hess, D., & Büschges, A. (1997). Sensorimotor pathways involved in interjoint reflex action of an insect leg. *Journal of Neurobiology*, *33*(7), 891–913.

Hess, D., & Büschges, A. (1999). Role of Proprioceptive Signals From an Insect Femur-Tibia Joint in Patterning Motoneuronal Activity of an Adjacent Leg Joint. *Journal of Neurophysiology*, *81*(4), 1856–1865. https://doi.org/10.1152/jn.1999.81.4.1856

Hiebert, G. W., & Pearson, K. G. (1999). Contribution of Sensory Feedback to the Generation of Extensor Activity During Walking in the Decerebrate Cat. *Journal of Neurophysiology*, *81*(2), 758–770. https://doi.org/10.1152/jn.1999.81.2.758

Hiebert, G. W., Whelan, P. J., Prochazka, A., & Pearson, K. G. (1996). Contribution of hind limb flexor muscle afferents to the timing of phase transitions in the cat step cycle. *Journal of Neurophysiology*, *75*(3), 1126–1137. https://doi.org/10.1152/jn.1996.75.3.1126

Hilde, K. L., Levine, A. J., Hinckley, C. A., Hayashi, M., Montgomery, J. M., Gullo, M., Driscoll, S. P., Grosschedl, R., Kohwi, Y., Kohwi-Shigematsu, T., & Pfaff, S. L. (2016). Satb2 Is Required for the Development of a Spinal Exteroceptive Microcircuit that Modulates Limb Position. *Neuron*, *91*(4), 763–776. https://doi.org/10.1016/j.neuron.2016.07.014

Hippenmeyer, S., Vrieseling, E., Sigrist, M., Portmann, T., Laengle, C., Ladle, D. R., & Arber, S. (2005). A Developmental Switch in the Response of DRG Neurons to ETS Transcription Factor Signaling. *PLoS Biology*, *3*(5), e159. https://doi.org/10.1371/journal.pbio.0030159

Houk, J., & Henneman, E. (1967). Responses of Golgi tendon organs to active contractions of the soleus muscle of the cat. *Journal of Neurophysiology*, *30*(3), 466–481. https://doi.org/10.1152/jn.1967.30.3.466

Hulliger, M. (1984). The mammalian muscle spindle and its central control. *Reviews of Physiology, Biochemistry and Pharmacology*, *101*, 1–110.

Hutchison, D. L., Roy, R. R., Hodgson, J. A., & Edgerton, V. R. (1989). EMG amplitude relationships between the rat soleus and medial gastrocnemius during various motor tasks. *Brain Research*, *502*(2), 233–244. https://doi.org/10.1016/0006-8993(89)90618-5

Jordan, L. M., Pratt, C. A., & Menzies, J. E. (1979). Locomotion evoked by brain stem stimulation: Occurrence without phasic segmental afferent input. *Brain Research*, *177*(1), 204–207.

Katwal, A. B., Konkalmatt, P. R., Piras, B. A., Hazarika, S., Li, S. S., John Lye, R., Sanders, J. M., Ferrante, E. A., Yan, Z., Annex, B. H., & French, B. A. (2013). Adeno-associated virus serotype 9 efficiently targets ischemic skeletal muscle following systemic delivery. *Gene Therapy*, *20*(9), 930–938. https://doi.org/10.1038/gt.2013.16

Kaya, M. (2003). Coordination of medial gastrocnemius and soleus forces during cat locomotion. *Journal of Experimental Biology*, *206*(20), 3645–3655. https://doi.org/10.1242/jeb.00544

Kiehn, O. (2006). Locomotor Circuits in the Mammalian Spinal Cord. *Annual Review of Neuroscience*, *29*(1), 279–306. https://doi.org/10.1146/annurev.neuro.29.051605.112910

Kiehn, O. (2016). Decoding the organization of spinal circuits that control locomotion. *Nature Reviews Neuroscience*, *17*(4), 224–238. https://doi.org/10.1038/nrn.2016.9

Koch, S. C., Del Barrio, M. G., Dalet, A., Gatto, G., Günther, T., Zhang, J., Seidler, B., Saur, D., Schüle, R., & Goulding, M. (2017). RORβ Spinal Interneurons Gate Sensory Transmission during Locomotion to Secure a Fluid Walking Gait. *Neuron*, *96*(6), 1419-1431.e5. https://doi.org/10.1016/j.neuron.2017.11.011

Laflamme, O. D., & Akay, T. (2018). Excitatory and inhibitory crossed reflex pathways in mice. *Journal of Neurophysiology*, *120*(6), 2897–2907. https://doi.org/10.1152/jn.00450.2018

Lam, T., & Pearson, K. G. (2001). Proprioceptive modulation of hip flexor activity during the swing phase of locomotion in decerebrate cats. *Journal of Neurophysiology*, *86*(3), 1321–1332.

Lam, T., & Pearson, K. G. (2002). The role of proprioceptive feedback in the regulation and adaptation of locomotor activity. *Advances in Experimental Medicine and Biology*, *508*, 343–355.

Lundberg, A. (1981). HALF-CENTRES REVISITED. In J. Szentágothai, M. Palkovits, & J. Hámori (Eds.), *Regulatory Functions of the CNS Principles of Motion and Organization* (pp. 155–167). Pergamon. https://doi.org/10.1016/B978-0-08-026814-9.50025-9

Mayer, W. P., & Akay, T. (2018). Stumbling corrective reaction elicited by mechanical and electrical stimulation of the saphenous nerve in walking mice. *The Journal of Experimental Biology*, jeb.178095. https://doi.org/10.1242/jeb.178095

Mayer, W. P., Murray, A. J., Brenner-Morton, S., Jessell, T. M., Tourtellotte, W. G., & Akay, T. (2018). Role of muscle spindle feedback in regulating muscle activity strength during walking at different speed in mice. *Journal of Neurophysiology*, *120*(5), 2484–2497. https://doi.org/10.1152/jn.00250.2018

Mazzaro, N., Grey, M. J., & Sinkjær, T. (2005). Contribution of Afferent Feedback to the Soleus Muscle Activity During Human Locomotion. *Journal of Neurophysiology*, *93*(1), 167–177. https://doi.org/10.1152/jn.00283.2004

McCrea, D. A. (2001). Spinal circuitry of sensorimotor control of locomotion. *The Journal of Physiology*, *533*(Pt 1), 41–50. https://doi.org/10.1111/j.1469-7793.2001.0041b.x

McCrea, D. A., & Rybak, I. A. (2008). Organization of mammalian locomotor rhythm and pattern generation. *Brain Research Reviews*, *57*(1), 134–146.

McCrea, D. A., Shefchyk, S. J., Stephens, M. J., & Pearson, K. G. (1995). Disynaptic group I excitation of synergist ankle extensor motoneurones during fictive locomotion in the cat. *The Journal of Physiology*, *487*(2), 527–539. https://doi.org/10.1113/jphysiol.1995.sp020897

McVea, D. A., Donelan, J. M., Tachibana, A., & Pearson, K. G. (2005). A role for hip position in initiating the swing-to-stance transition in walking cats. *Journal of Neurophysiology*, *94*(5), 3497–3508. https://doi.org/10.1152/jn.00511.2005

McVea, D. A., & Pearson, K. G. (2007). Long-Lasting, Context-Dependent Modification of Stepping in the Cat After Repeated Stumbling-Corrective Responses. *Journal of Neurophysiology*, *97*(1), 659–669. https://doi.org/10.1152/jn.00921.2006

Metz, G. A., & Whishaw, I. Q. (2002). Cortical and subcortical lesions impair skilled walking in the ladder rung walking test: A new task to evaluate fore- and hindlimb stepping, placing, and co-ordination. *Journal of Neuroscience Methods*, *115*(2), 169–179. https://doi.org/10.1016/S0165-0270(02)00012-2

Oliveira Fernandes, M., & Tourtellotte, W. G. (2015). Egr3-Dependent Muscle Spindle Stretch Receptor Intrafusal Muscle Fiber Differentiation and Fusimotor Innervation Homeostasis. *Journal of Neuroscience*, *35*(14), 5566–5578. https://doi.org/10.1523/JNEUROSCI.0241-15.2015

Pearson, K. G. (2004). Generating the walking gait: Role of sensory feedback. In *Progress in Brain Research* (Vol. 143, pp. 123–129). Elsevier. https://doi.org/10.1016/S0079-6123(03)43012-4

Pearson, K. G. (2008). Role of sensory feedback in the control of stance duration in walking cats. *Brain Research Reviews*, *57*(1), 222–227. https://doi.org/10.1016/j.brainresrev.2007.06.014

Pearson, K. G., Acharya, H., & Fouad, K. (2005). A new electrode configuration for recording electromyographic activity in behaving mice. *Journal of Neuroscience Methods*, *148*(1), 36–42. https://doi.org/10.1016/j.jneumeth.2005.04.006

Pearson, K. G., & Collins, D. F. (1993). Reversal of the influence of group Ib afferents from plantaris on activity in medial gastrocnemius muscle during locomotor activity. *Journal of Neurophysiology*, *70*(3), 1009–1017. https://doi.org/10.1152/jn.1993.70.3.1009

Pearson, K. G., Misiaszek, J. E., & Hulliger, M. (2003). Chemical ablation of sensory afferents in the walking system of the cat abolishes the capacity for functional recovery after peripheral nerve lesions. *Experimental Brain Research*, *150*(1), 50–60. https://doi.org/10.1007/s00221-003-1445-1

Pearson, K. G., & Rossignol, S. (1991). Fictive motor patterns in chronic spinal cats. *Journal of Neurophysiology*, *66*(6), 1874–1887.

Pierotti, D. J., Roy, R. R., Gregor, R. J., & Reggie Edgerton, V. (1989). Electromyographic activity of cat hindlimb flexors and extensors during locomotion at varying speeds and inclines. *Brain Research*, *481*(1), 57–66. https://doi.org/10.1016/0006-8993(89)90485-X

Prilutsky, B. I., Herzog, W., & Allinger, T. L. (1994). Force-sharing between cat soleus and gastrocnemius muscles during walking: Explanations based on electrical activity, properties, and kinematics. *Journal of Biomechanics*, *27*(10), 1223–1235. https://doi.org/10.1016/0021-9290(94)90276-3

Prochazka, A. (2011). *Proprioceptive Feedback and Movement Regulation*. https://doi.org/10.1002/cphy.cp120103

Prochazka, A., & Gorassini, M. (1998). Ensemble firing of muscle afferents recorded during normal locomotion in cats. *The Journal of Physiology*, *507 (Pt 1)*, 293–304.

Prochazka, A., Gosgnach, S., Capaday, C., & Geyer, H. (2017). Neuromuscular Models for Locomotion. In *Bioinspired Legged Locomotion* (pp. 401–453). Elsevier. https://doi.org/10.1016/B978-0-12-803766-9.00008-7

Prochazka, A., Sontag, K.-H., & Wand, P. (1978). Motor reactions to perturbations of gait: Proprioceptive and somesthetic involvement. *Neuroscience Letters*, *7*(1), 35–39. https://doi.org/10.1016/0304-3940(78)90109-X

Prochazka, A., Trend, P., Hulliger, M., & Vincent, S. (1989). Ensemble proprioceptive activity in the cat step cycle: Towards a representative look-up chart. *Progress in Brain Research*, *80*, 61–74; discussion 57-60.

Quevedo, J., Stecina, K., Gosgnach, S., & McCrea, D. A. (2005). Stumbling Corrective Reaction During Fictive Locomotion in the Cat. *Journal of Neurophysiology*, *94*(3), 2045–2052. https://doi.org/10.1152/jn.00175.2005

Quevedo, J., Stecina, K., & McCrea, D. A. (2005). Intracellular Analysis of Reflex Pathways Underlying the Stumbling Corrective Reaction During Fictive Locomotion in the Cat. *Journal of Neurophysiology*, *94*(3), 2053–2062. https://doi.org/10.1152/jn.00176.2005

Radovanović, S., Milićev, M., Perić, S., Basta, I., Kostić, V., & Stević, Z. (2014). Gait in amyotrophic lateral sclerosis: Is gait pattern differently affected in spinal and bulbar onset of the disease during dual task walking? *Amyotrophic Lateral Sclerosis and Frontotemporal Degeneration*, *15*(7–8), 488–493. https://doi.org/10.3109/21678421.2014.918148

Reynolds, R. F., & Day, B. L. (2005). Visual guidance of the human foot during a step. *The Journal of Physiology*, *569*(Pt 2), 677–684. https://doi.org/10.1113/jphysiol.2005.095869

Rizzolatti, G., Cattaneo, L., Fabbri-Destro, M., & Rozzi, S. (2014). Cortical Mechanisms Underlying the Organization of Goal-Directed Actions and Mirror Neuron-Based Action Understanding. *Physiological Reviews*, *94*(2), 655–706. https://doi.org/10.1152/physrev.00009.2013

Romanes, G. J. (1951). The motor cell columns of the lumbo-sacral spinal cord of the cat. *Journal of Comparative Neurology*, *94*(2), 313–363. https://doi.org/10.1002/cne.900940209

Rossignol, S. (2011). Neural Control of Stereotypic Limb Movements. In R. Terjung (Ed.), *Comprehensive Physiology*. John Wiley & Sons, Inc. http://doi.wiley.com/10.1002/cphy.cp120105

Rossignol, S., Dubuc, R., & Gossard, J.-P. (2006). Dynamic Sensorimotor Interactions in Locomotion. *Physiological Reviews*, *86*(1), 89–154. https://doi.org/10.1152/physrev.00028.2005

Roy, R. R., Hutchison, D. L., Pierotti, D. J., Hodgson, J. A., & Edgerton, V. R. (1991). EMG patterns of rat ankle extensors and flexors during treadmill locomotion and swimming. *Journal of Applied Physiology*, *70*(6), 2522–2529. https://doi.org/10.1152/jappl.1991.70.6.2522

Ruffini, A. (1898). On the Minute Anatomy of the Neuromuscular Spindles of the Cat, and on their Physiological Significance. *The Journal of Physiology*, *23*(3), 190-208.3.

Santuz, A., Akay, T., Mayer, W. P., Wells, T. L., Schroll, A., & Arampatzis, A. (2019). Modular organization of murine locomotor pattern in the presence and absence of sensory feedback from muscle spindles. *The Journal of Physiology*. https://doi.org/10.1113/JP277515

Santuz, A., Ekizos, A., Eckardt, N., Kibele, A., & Arampatzis, A. (2018). Challenging human locomotion: Stability and modular organisation in unsteady conditions. *Scientific Reports*, *8*. https://doi.org/10.1038/s41598-018-21018-4

Schillings, A. M., Van Wezel, B. M. H., & Duysens, J. (1996). Mechanically induced stumbling during human treadmill walking. *Journal of Neuroscience Methods*, *67*(1), 11–17. https://doi.org/10.1016/0165-0270(95)00149-2

Sinkjaer, T., Andersen, J. B., Ladouceur, M., Christensen, L. O., & Nielsen, J. B. (2000). Major role for sensory feedback in soleus EMG activity in the stance phase of walking in man. *The Journal of Physiology*, *523 Pt 3*, 817–827.

Smith, J. L., Chung, S. H., & Zernicke, R. F. (1993). Gait-related motor patterns and hindlimb kinetics for the cat trot and gallop. *Experimental Brain Research*, *94*(2). https://doi.org/10.1007/BF00230301

Strata, F., Coq, J.-O., Byl, N., & Merzenich, M. M. (2004). Effects of sensorimotor restriction and anoxia on gait and motor cortex organization: Implications for a rodent model of cerebral palsy. *Neuroscience*, *129*(1), 141–156. https://doi.org/10.1016/j.neuroscience.2004.07.024

Stuart, D. G., & Hultborn, H. (2008). Thomas Graham Brown (1882—1965), Anders Lundberg (1920-), and the neural control of stepping. *Brain Research Reviews*, *59*(1), 74–95. https://doi.org/10.1016/j.brainresrev.2008.06.001

Takeoka, A., Vollenweider, I., Courtine, G., & Arber, S. (2014). Muscle Spindle Feedback Directs Locomotor Recovery and Circuit Reorganization after Spinal Cord Injury. *Cell*, *159*(7), 1626–1639. https://doi.org/10.1016/j.cell.2014.11.019

Taylor, A., Durbaba, R., Ellaway, P. H., & Rawlinson, S. (2006). Static and dynamic γ-motor output to ankle flexor muscles during locomotion in the decerebrate cat. *The Journal of Physiology*, *571*(3), 711–723. https://doi.org/10.1113/jphysiol.2005.101634

Tourtellotte, W. G., Keller-Peck, C., Milbrandt, J., & Kucera, J. (2001). The Transcription Factor Egr3 Modulates Sensory Axon–Myotube Interactions during Muscle Spindle Morphogenesis. *Developmental Biology*, *232*(2), 388–399. https://doi.org/10.1006/dbio.2001.0202

Tourtellotte, W. G., & Milbrandt, J. (1998). Sensory ataxia and muscle spindle agenesis in mice lacking the transcription factor Egr3. *Nature Genetics*, *20*(1), 87–91. https://doi.org/10.1038/1757

Tripodi, M., Stepien, A. E., & Arber, S. (2011). Motor antagonism exposed by spatial segregation and timing of neurogenesis. *Nature*, *479*(7371), 61–66. https://doi.org/10.1038/nature10538

Van Wezel, B. M. H., Ottenhoff, F. A. M., & Duysens, J. (1997). Dynamic Control of Location-Specific Information in Tactile Cutaneous Reflexes from the Foot during Human Walking. *The Journal of Neuroscience*, *17*(10), 3804–3814. https://doi.org/10.1523/JNEUROSCI.17-10-03804.1997

Vincent, J. A., Wieczerzak, K. B., Gabriel, H. M., Nardelli, P., Rich, M. M., & Cope, T. C. (2016). A Novel Path to Chronic Proprioceptive Disability with Oxaliplatin: Distortion of Sensory Encoding. *Neurobiology of Disease*, *95*, 54–65. https://doi.org/10.1016/j.nbd.2016.07.004

Vrieseling, E., & Arber, S. (2006). Target-Induced Transcriptional Control of Dendritic Patterning and Connectivity in Motor Neurons by the ETS Gene Pea3. *Cell*, *127*(7), 1439–1452. https://doi.org/10.1016/j.cell.2006.10.042

Walmsley, B., Hodgson, J. A., & Burke, R. E. (1978). Forces produced by medial gastrocnemius and soleus muscles during locomotion in freely moving cats. *Journal of Neurophysiology*, *41*(5), 1203–1216. https://doi.org/10.1152/jn.1978.41.5.1203

Wand, P., Prochazka, A., & Sontag, K.-H. (1980). Neuromuscular responses to gait perturbations in freely moving cats. *Experimental Brain Research*, *38*(1). https://doi.org/10.1007/BF00237937

Whelan, P. J., Hiebert, G. W., & Pearson, K. G. (1995). Plasticity of the extensor group I pathway controlling the stance to swing transition in the cat. *Journal of Neurophysiology*, *74*(6), 2782–2787. https://doi.org/10.1152/jn.1995.74.6.2782

Woo, S.-H., Lukacs, V., de Nooij, J. C., Zaytseva, D., Criddle, C. R., Francisco, A., Jessell, T. M., Wilkinson, K. A., & Patapoutian, A. (2015). Piezo2 is the principal mechanotransduction channel for proprioception. *Nature Neuroscience*, *18*(12), 1756–1762. https://doi.org/10.1038/nn.4162

Yang, J. F., Stein, R. B., & James, K. B. (1991). Contribution of peripheral afferents to the activation of the soleus muscle during walking in humans. *Experimental Brain Research*, *87*(3). https://doi.org/10.1007/BF00227094

Yang, X., Arber, S., William, C., Li, L., Tanabe, Y., Jessell, T. M., Birchmeier, C., & Burden, S. J. (2001). Patterning of Muscle Acetylcholine Receptor Gene Expression in the Absence of Motor Innervation. *Neuron*, *30*(2), 399–410. https://doi.org/10.1016/S0896-6273(01)00287-2

Zagoraiou, L., Akay, T., Martin, J. F., Brownstone, R. M., Jessell, T. M., & Miles, G. B. (2009). A Cluster of Cholinergic Premotor Interneurons Modulates Mouse Locomotor Activity. *Neuron*, *64*(5), 645–662. https://doi.org/10.1016/j.neuron.2009.10.017

Zehr, E. P., Komiyama, T., & Stein, R. B. (1997). Cutaneous Reflexes During Human Gait: Electromyographic and Kinematic Responses to Electrical Stimulation. *Journal of Neurophysiology*, *77*(6), 3311–3325. https://doi.org/10.1152/jn.1997.77.6.3311

Zhang, Y., Narayan, S., Geiman, E., Lanuza, G. M., Velasquez, T., Shanks, B., Akay, T., Dyck, J., Pearson, K., Gosgnach, S., Fan, C.-M., & Goulding, M. (2008). V3 Spinal Neurons Establish a Robust and Balanced Locomotor Rhythm during Walking. *Neuron*, *60*(1), 84–96. https://doi.org/10.1016/j.neuron.2008.09.027

Zimmermann, K., Hein, A., Hager, U., Kaczmarek, J. S., Turnquist, B. P., Clapham, D. E., & Reeh, P. W. (2009). Phenotyping sensory nerve endings in vitro in the mouse. *Nature Protocols*, *4*(2), 174–196. https://doi.org/10.1038/nprot.2008.223

APPENDIX A COPYRIGHT PERMISSION LETTER

May 28, 2019

Journal of Experimental Biology
The Company of Biologists Limited

Bidder Building
Station Road
Histon
Cambridge
CB24 9LF
UK

I am preparing my Ph.D. thesis for submission to the Faculty of Graduate Studies at Dalhousie University, Halifax, Nova Scotia, Canada. I am seeking your permission to include a manuscript version of the following paper(s) as a chapter in the thesis:

Mayer, W. P., & Akay, T. (2018). Stumbling corrective reaction elicited by mechanical and electrical stimulation of the saphenous nerve in walking mice. The Journal of Experimental Biology, jeb.178095. https://doi.org/10.1242/jeb.178095

Canadian graduate theses are reproduced by the Library and Archives of Canada (formerly National Library of Canada) through a non-exclusive, world-wide license to reproduce, loan, distribute, or sell theses. I am also seeking your permission for the material described above to be reproduced and distributed by the LAC(NLC). Further details about the LAC(NLC) thesis program are available on the LAC(NLC) website (www.nlc-bnc.ca).

Full publication details and a copy of this permission letter will be included in the thesis.

Yours sincerely,

William Paganini Mayer

Permission is granted for:

a) the inclusion of the material described above in your thesis.

b) for the material described above to be included in the copy of your thesis that is sent to the Library and Archives of Canada (formerly National Library of Canada) for reproduction and distribution.

Name: _____ Title: _____

Signature: _____ Date: _____

permissions <permissions@biologists.com>

Wed 2019-05-29 10:33 AM

To:William Mayer <William.Mayer@Dal.Ca>; permissions <permissions@biologists.com>;

Dear William,

Thank you for your request. Permission is granted for a thesis without charge. As a small not-for-profit we cannot sign individual permission letters but most people find this email sufficient.

The acknowledgement is important and should state "reproduced/adapted with permission" and give the source journal name - the acknowledgement should either provide full citation details or refer to the relevant citation in the article reference list - the full citation details should include authors, journal, year, volume, issue and page citation.

Where appearing online or in other electronic media, a link should be provided to the original article (e.g. via DOI).

Journal of Experimental Biology: http://www.biologists.com/journal-of-experimental-biology

We wish you the best of luck with your thesis.

Kind regards

Richard

Richard Grove
Commercial Manager
The Company of Biologists Ltd
Bidder Building, Station Road, Histon, Cambridge, CB24 9LF, UK
T: +44 (0) 1223 632 850 | richard.grove@biologists.com | www.biologists.com

May 28, 2019

Journal of Neurophysiology
The American Physiological Society
6120 Executive Boulevard, Suite #600
Rockville, MD 20852-4906

I am preparing my Ph.D. thesis for submission to the Faculty of Graduate Studies at Dalhousie University, Halifax, Nova Scotia, Canada. I am seeking your permission to include a manuscript version of the following paper(s) as a chapter in the thesis:

Mayer, W. P., Murray, A. J., Brenner-Morton, S., Jessell, T. M., Tourtellotte, W. G., & Akay, T. (2018). Role of muscle spindle feedback in regulating muscle activity strength during walking at different speed in mice. Journal of Neurophysiology, 120(5), 2484–2497. https://doi.org/10.1152/jn.00250.2018

Canadian graduate theses are reproduced by the Library and Archives of Canada (formerly National Library of Canada) through a non-exclusive, world-wide license to reproduce, loan, distribute, or sell theses. I am also seeking your permission for the material described above to be reproduced and distributed by the LAC(NLC). Further details about the LAC(NLC) thesis program are available on the LAC(NLC) website (www.nlc-bnc.ca).

Full publication details and a copy of this permission letter will be included in the thesis.

Yours sincerely,

William Paganini Mayer

Permission is granted for:

a) the inclusion of the material described above in your thesis.

b) for the material described above to be included in the copy of your thesis that is sent to the Library and Archives of Canada (formerly National Library of Canada) for reproduction and distribution.

Name: _____ Title: _____

Signature: _____ Date: _____

APS Permissions <permissions@the-aps.org>

Tue 2019-05-28 5:11 PM

To: William Mayer <William.Mayer@Dal.Ca>;

Dear Dr Mayer,

Authors may reproduce whole published articles in dissertations and post to thesis repositories without charge and without requesting permission. Full citation is required.

Authors may deposit their accepted, peer-reviewed journal manuscripts into an institutional repository providing:

- the APS retains copyright to the article
- a 12-month embargo period from the date of final publication of the article is observed by the institutional repository and the author
- a link to the article published on the APS or publisher-partner website is prominently displayed alongside the article in the institutional repository
- the article is not used for commercial purposes
- self-archived articles posted to repositories are without warranty of any kind

You can find these listed here, https://www.physiology.org/author-info.permissions.

I cannot sign the letter as written as APS will retain the copyright to the article within your thesis.

Please let me know if I can be of further assistance.

Kind Regards,
Stephani

Stephani Rozier
Subscriber Database Specialist/Permissions
w 301.634.7796 f 301.634.7418
6120 Executive Boulevard, Suite 600
Rockville, MD 20852-4911
Visit APS' website. Explore our Journals.

RE: Permission to adapt figures to be published in PhD thesis

PNAS Permissions <PNASPermissions@nas.edu>

Mon 2019-06-03 10:23 AM

To: William Mayer <William.Mayer@Dal.Ca>;

Thank you for your message. Permission is granted for your use of the material as described in your request. Please include a complete citation for the original PNAS article when reusing the material. Because this material published after 2008, a copyright note is not needed. There is no charge for this material, either. Let us know if you have any questions.

Best regards,
Delaney Cruickshank for
Diane Sullenberger
PNAS Executive Editor

From: William Mayer <William.Mayer@Dal.Ca>
Sent: Monday, June 3, 2019 9:00 AM
To: PNAS Permissions <PNASPermissions@nas.edu>
Subject: Permission to adapt figures to be published in PhD thesis

Dear PNS staff,

I am preparing my Ph.D. thesis for submission to the Faculty of Graduate Studies at Dalhousie University, Halifax, Nova Scotia, Canada. I am seeking your permission to include adapted figures from the following paper in a chapter of my thesis:

Akay, T., Tourtellotte, W. G., Arber, S., & Jessell, T. M. (2014). Degradation of mouse locomotor pattern in the absence of proprioceptive sensory feedback. *Proceedings of the National Academy of Sciences of The United States of America*, *111*(47), 16877–16882. https://doi.org/10.1073/pnas.1419045111

I would like to have adapted Figure 2E and Figure S1 from the aforementioned paper. These figures were original drawings of my Ph.D. supervisor Dr. Turgay Akay.

Please find attached in this email the adapted images I am seeking authorization to be reproduced in my thesis.

Please note that Canadian graduate theses are reproduced by the Library and Archives of Canada (formerly National Library of Canada) through a non-exclusive, world-wide license to reproduce, loan, distribute, or sell theses. I am also seeking your permission for the material described above to be reproduced and distributed by the LAC(NLC). Further details about the LAC(NLC) thesis program are available on the LAC(NLC) website (www.nlc-bnc.ca).

Full publication details and a copy of this permission request will be included in the thesis.

Thank you for considering my request.

Yours Sincerely,

William Mayer